Modelling and validating an enhanced transcranial magnetic stimulator for neuroscience and clinical therapies

Karen Wendt

Somerville College

University of Oxford

A thesis submitted for the degree of

Doctor of Philosophy

Trinity 2023

Supervised by Prof. Timothy Denison and Prof. Jacinta O'Shea

Acknowledgements

I am very grateful to all those who have contributed to the completion of this thesis, both directly and indirectly. In particular, I would like to thank the following individuals and organisations who have made this possible:

First of all, I wish to express my deep gratitude to Tim and Jacinta, who I was lucky to have as my two supervisors. Tim, your guidance, mentorship, and patience have been instrumental throughout this journey. Thank you for always finding opportunities for me to not only learn more about brain stimulation but to also gain insight into industry. Your collaborative spirit, your industry lessons and mentorship moments have been an inspiration. Jacinta, your insights, constructive feedback, and encouragement have been invaluable. Your expertise in neuroscience added a vital dimension to my research, guided me through my in-human studies and encouraged me to always disseminate research critically.

Secondly, I am grateful to the Medical Research Council and Magstim who made this DPhil possible through their generous financial support. Thank you to the current and former members of Magstim, for the fruitful discussions and for helping us out with equipment whenever we needed it. You helped drive my research forward and gave me the unique opportunity to gain insights into your company.

Thank you also to the other BNDU members, including Charlie and Hayriye, for letting me pick your brains, for giving me guidance and for being such wonderful humans. I look forward to our paths crossing again.

Dan and Kawsar, it has been an absolute pleasure to work with you on the xTMS and I have learned a lot from both of you.

To all the current and former members of my two labs, the Bioelectronics lab and the TiNSL lab, you have made my time in Oxford such a joy! I'd like to especially thank Majid, for introducing me to everything TMS, for sharing your experience and expertise with me and for always just being a message away, even after leaving Oxford. Verena, thank you for your scientific and social support, your statistics knowledge is significantly better than what mine will ever be. I don't know how I would have run all my testing sessions without always being able to count on all of you and having your heads to test new things on.

It has been an honour to also be adopted into the PiNG family and be part of the wider Neuroplastics research environment. Ioana and Patricia, my fellow

TMS enthusiasts, I have really enjoyed sharing conference experiences, public engagements and all the other TMS-related fun with you.

Oxford would not be the same without the vast social opportunities it offers. I would like to thank my friends from handball, the GTC big band and OxWoCS for helping me strike a balance between DPhil and socials. A special thank you goes to Linde, we shared most of this journey together and you have really made Oxford homely for me. I cannot thank you and Youp enough for your friendship and generosity.

Finally, none of this would have been possible without the support of my family and my partner Aaron. Your unwavering support, encouragement, and understanding sustained me through this crazy endeavour. Miguel, thank you for always encouraging me to go further, to take the leap and to study in the UK. Mum und Papa, danke, dass ihr mir so viele Türen geöffnet habt und immer an mich glaubt. Ich werde euch niemals genug für eure Unterstützung und Zuwendung danken können.

Abstract

Transcranial magnetic stimulation (TMS) is a non-invasive technique for stimulating the nervous system. Conventional TMS devices are limited to a small set of predefined pulse shapes. Recent technological developments in TMS devices using switching circuits have allowed more control over the TMS parameters. Our group has introduced a new TMS device, the programmable TMS (pTMS), which uses pulse-width modulation (PWM) to rapidly switch between voltage levels, allowing the approximation of pulses of arbitrary shape.

In the first part of this thesis, I validated the PWM method by using computational modelling to compare the neuronal response to stimuli generated by the pTMS device and by a conventional transcranial magnetic stimulator. The computational models predicted highly correlated activation thresholds for both stimulator types, showing that the pTMS can approximate existing pulses.

Second, I validated the model and the pTMS by assessing the comparability of the effects of PWM and conventional pulses on motor evoked potentials in a first-in-human validation study. Resting motor thresholds showed a strong correlation between the stimulation pulses, with a consistently lower threshold for the PWM pulses, corroborating the results of the computational model. No significant differences in other motor response measures were found between the pulse types.

Third, I exploited the capabilities of the pTMS device by designing and conducting an in-human study where I investigated a previously unfeasible stimulation pattern, monophasic theta burst stimulation (TBS). Comparing the effects of monophasic TBS with conventional biphasic TBS on corticospinal excitability, the monophasic pulses induced larger plasticity effects than biphasic pulses and than an anatomical control.

Finally, I explored the sources of variability of resting motor thresholds in a large data set collected across TMS clinics, in particular investigating the effects of time of day. The results indicated that the majority of the observed differences in thresholds across the day were due to differences between clinics, highlighting the need to control for and standardise methods across clinics.

In summary, this thesis demonstrates and validates the capabilities of the programmable TMS device, to firstly mimic the stimulation effects of conventional stimulators but importantly to also expand the parameter set to new stimulation protocols with the potential to have stronger effects on the stimulated neurons, and investigates the origins of variance in clinical practice.

Related publications

The background on the programmable transcranial magnetic stimulator in Chapter 1 has been published in the following journal paper:

- Sorkhabi, M. M., Benjaber, M., **Wendt, K.**, West, T., Rogers, D. J., and Denison, T. (2020). "Programmable Transcranial Magnetic Stimulation - A Modulation Approach for the Generation of Controllable Magnetic Stimuli". *IEEE Transactions on Biomedical Engineering* 68.6, pp. 1847-1858. DOI: 10.1109/TBME.2020.3024902

The discussion on physiologically informed stimulation in Chapter 1 has been published in the following journal paper:

- **Wendt, K.**, Denison, T., Foster, G., Krinke, L., Thomson, A., Wilson, S., and Widge, A. S. (2022). "Physiologically informed neuromodulation". *Journal of the Neurological Sciences* 434. DOI: 10.1016/j.jns.2021.120121

Chapter 2 has been published as the following conference paper:

- **Wendt, K.**, Sorkhabi, M. M., O'Shea, J., Cagnan, H., and Denison, T. (2021). "Comparison between the modelled response of primary motor cortex neurons to pulse-width modulated and conventional TMS stimuli". *Annu Int Conf IEEE Eng Med Biol Soc 2021*, pp. 6058–6061. DOI: 10.1109/embc46164.2021.9629605

Chapter 3 has been published as the following journal paper:

- Sorkhabi, M. M.*, **Wendt, K.***, O'Shea, J., and Denison, T. (2022). "Pulse width modulation-based TMS: Primary motor cortex responses compared to conventional monophasic stimuli". *Brain stimulation* 15.4, pp. 980–983, DOI: 10.1016/j.brs.2022.06.013
  *Joint first authors

Chapter 4 has been published as the following journal paper:

- **Wendt, K.**, Sorkhabi, M. M., Stagg, C. J., Fleming, M. K., Denison, T., and O'Shea, J. (2023). "The effect of pulse shape in theta-burst stimulation: Monophasic vs biphasic TMS". *Brain Stimulation* 16.4, pp. 1178–1185, DOI: 10.1016/j.brs.2023.08.001

Chapter 5 has been published in the following letter to the editor:

- **Wendt, K.**, Sorkhabi, M. M., O'Shea, J., Denison, T., and van Rheede, J. (2023). "Influence of time of day on resting motor threshold in clinical TMS practice". *Clinical Neurophysiology* 155, pp. 65–67, DOI: 10.1016/j.clinph.2023.08.017

The background on the xTMS device in Chapter 6 has been published in the following conference paper:

- Ali, K., **Wendt, K.**, Sorkhabi, M. M., Benjaber, M., Denison, T., and Rogers, D. J. (2023). "xTMS: A Pulse Generator for Exploring Transcranial Magnetic Stimulation Therapies". *Conf Proc (IEEE Appl Power Electron Conf Expo) 2023*, pp. 1875–1880. DOI: 10.1109/apec43580.2023.10131554

The below publications have not arisen directly from, but are related to, work presented in this thesis:

- Sorkhabi, M. M., Gingell, F., **Wendt, K.**, Benjaber, M., Ali, K., Rogers, D. J., and Denison, T. (2021). "Design Analysis and Circuit Topology Optimization for Programmable Magnetic Neurostimulator", *Annu Int Conf IEEE Eng Med Biol Soc 2021*, pp. 6384–6389. DOI: 10.1109/EMBC46164.2021.9630915

- Sorkhabi, M. M., **Wendt, K.**, and Denison, T. (2020). "Temporally Interfering TMS: Focal and Dynamic Stimulation Location.", *Annu Int Conf IEEE Eng Med Biol Soc 2020*, pp. 3537–3543. DOI: 10.1109/EMBC44109.2020.9176249

- Sorkhabi, M. M., **Wendt, K.**, Wilson, M. T., and Denison, T. (2021). "Numerical Modeling of Plasticity Induced by Quadri-Pulse Stimulation", *IEEE Access* 9, pp. 26484–26490. DOI: 10.1109/ACCESS.2021.3057829

- Sorkhabi, M. M., **Wendt, K.**, Wilson, M. T., and Denison, T. (2021), "Estimation of the Motor Threshold for Near-Rectangular Stimuli Using the Hodgkin–Huxley Model". *Computational Intelligence and Neuroscience* 2021, DOI: 10.1155/2021/4716161

- Sorkhabi, M. M., **Wendt, K.**, Rogers, D. J., and Denison, T. (2021). "Paralleling insulated-gate bipolar transistors in the H-bridge structure to reduce current stress". *SN Applied Sciences* 3.4, p. 406. DOI: 10.1007/s42452-021-04420-y

- Radyte, E., **Wendt, K.**, Sorkhabi, M. M., O'Shea, J., and Denison, T. (2022). "Relative Comparison of Non-Invasive Brain Stimulation Methods for Modulating Deep Brain Targets." *Annu Int Conf IEEE Eng Med Biol Soc 2022*. pp. 1715–1718. DOI: 10.1109/EMBC48229.2022.9871476

Contents

List of figures

List of abbreviations

AMT . . . . . Active motor threshold

ANOVA . . . . Analysis of variance

AP . . . . . Anterior-posterior (current direction)

CSP . . . . . Cortical silent period

cTBS . . . . . Continuous theta burst stimulation

cTMS . . . . . Controllable transcranial magnetic stimulation

CUREC . . . . Central University Research Ethics Committee

DBS . . . . . Deep brain stimulation

DLPFC . . . . Dorsolateral prefrontal cortex

EEG . . . . . Electroencephalography

ECT . . . . . Electroconvulsive therapy

EMG . . . . . Electromyography

FDA . . . . . U.S. Food and Drug Administration

FDI . . . . . First dorsal interosseous

FEM . . . . . Finite element method

FPGA . . . . . Field-programmable gate array

GABA . . . . . Gamma-aminobutyric acid

GUI . . . . . Graphical user interface

HH . . . . . Hodgkin-Huxley (model)

IAF . . . . . Individual alpha frequency

IGBT . . . . . Isolated-gate bipolar transistors

IO . . . . . Input-output

ISI . . . . . Interstimulus interval

iTBS . . . . . Intermittent theta burst stimulation

LIF . . . . . Leaky integrate-and-fire (model)

LME . . . . . Linear mixed effects (model)

LTD . . . . . Long-term depression

LTP . . . . . Long-term potentiation

MDD . . . . . Major depressive disorder

MEP . . . . . Motor evoked potential

MPC . . . . . Model predictive control

MRI . . . . . Magnetic resonance imaging

MSO . . . . . Maximum stimulator output

MT . . . . . Motor threshold

M1 . . . . . Primary motor cortex

OCD . . . . . Obsessive-compulsive disorder

PA . . . . . Posterior-anterior (current direction)

PWM . . . . . Pulse-width modulation

QPS . . . . . Quadripulse stimulation

pTMS . . . . . Programmable transcranial magnetic stimulation

rmANOVA . . Repeated measures analysis of variance

RMS . . . . . Root mean square

RMT . . . . . Resting motor threshold

rTMS . . . . . Repetitive transcranial magnetic stimulation

TBS . . . . . Theta burst stimulation

tDCS . . . . . Transcranial direct current stimulation

TMS . . . . . Transcranial magnetic stimulation

TOD . . . . . Time of day

VNS . . . . . Vagus nerve stimulation

1 Introduction

Contents

Brain disorders form the most prevalent and disabling disease among non-communicable (chronic) diseases in Europe, with the burden of mental and neurological conditions increasing by up to 20.5% between $1990 - 2017$, mostly due to ageing populations (Raggi et al. 2020). Brain disorders include neurological and psychiatric diseases, many of which are commonly treated by pharmacological interventions. For many people, these treatments are not sufficiently effective or come with major side effects.

Bioelectronic systems offer an alternative and are increasingly used to treat

different neurological and psychiatric disorders. For example, deep brain stimulation (DBS) is used to treat motor symptoms in essential tremor, dystonia and Parkinson's disease (Kocabicak et al. 2015). However, DBS is an invasive treatment requiring brain surgery and is therefore only used in very severe cases. Non-invasive, lower-risk alternatives include transcranial direct current stimulation (tDCS) and transcranial magnetic stimulation (TMS). In tDCS, electrodes are placed on the scalp to inject a low-amplitude direct current into superficial areas of the brain. This can increase or decrease the excitability of the stimulated brain area by shifting the membrane potential of the neurons but does not trigger action potentials (Liebetanz et al. 2002). tDCS has shown promising potential in treating depression (Brunoni et al. 2016) and in stroke rehabilitation (Feng et al. 2013). Transcranial magnetic stimulation can depolarise neurons and induce measurable physiological responses which are commonly used as a diagnostic tool for various neurological disorders. When applying trains of pulses, TMS can cause changes in cortical excitability that outlast the stimulation period (Lefaucheur et al. 2014). TMS is FDA-approved for the treatment of, for example, major depressive disorder and is being investigated as a potential treatment for many other applications (Lefaucheur et al. 2020).

The available stimulation protocols of current TMS devices are limited by the device hardware, only allowing the adjustment of a few parameters such as the amplitude and repetition rate of pulses. For instance, the length and shape of the stimulation pulses are typically determined by the stimulator circuit rather than by the biology of the stimulation targets. Extending the parameter set for TMS promises to increase the selectivity of stimulation and might enable the emergence of novel, more effective stimulation protocols. Recent advances in TMS technology, including the development of a 'programmable TMS' (pTMS) device in our lab, have now enabled a new level of control over these parameters which comprises the main topic of this thesis.

The aim of my DPhil was to help design, refine, model and validate the pTMS. To this end, I consider the parameters of TMS on different time scales, which play important parts in neuromodulation. 1) On the scale of micro- to milliseconds, which

corresponds to individual stimulation pulses, their shape and length, I compare the effects of TMS pulses generated by the programmable TMS with those of a conventional stimulator; 2) On a scale of seconds to minutes, which encompasses stimulation protocols applying trains of pulses, I investigate the effect of pulse shape on corticospinal excitability in a patterned stimulation protocol; And 3) on the scale of hours to days, which covers circadian and diurnal rhythms, I explore the variability in the responses to TMS pulses across the day in a clinical setting. Together, considering these different aspects of pulse design and delivery in neuromodulation may help to improve stimulation effects and reduce response variability.

Over almost 40 years since the introduction of TMS, a large body of TMS research has developed, from the technical specifications and the current understanding of the underlying mechanisms in brain stimulation, to basic neuroscience and clinical investigations. In this Chapter, I will introduce these themes, describe how our programmable TMS device fits into the current state of the art in the TMS device landscape and outline the objectives I aim to address in this thesis.

1.1 Transcranial magnetic stimulation

Transcranial magnetic stimulation, as introduced by Barker et al. in 1985 (Barker et al. 1985), is based on the principles of electromagnetic induction. Conventional devices use an LC resonant circuit, consisting of a large capacitor which is charged to a voltage of up to kilovolts, an inductor which acts as the stimulation coil and a thyristor switch that connects the two (Fig. 1.1 (a)) (Epstein 2008). When the switch is closed, a pulse of electrical current flows through the coil, inducing a rapidly changing magnetic field perpendicular to the coil. This magnetic field passes unimpeded through the skull and generates a primary electric field (E-field) with a magnitude that is proportional to the rate of change of the magnetic field (Epstein 2008). The electric field in turn causes an electric current to flow underneath the coil, in the parallel but opposite direction to the current in the coil (Fig. 1.1 (b)) (Rotenberg et al. 2014).

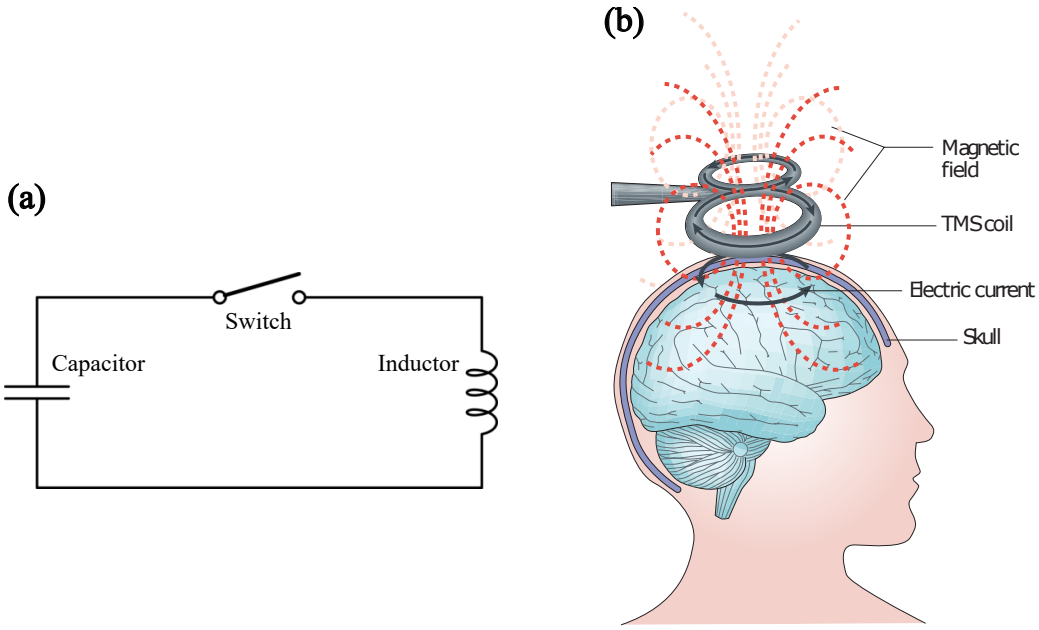

Figure 1.1: **(a)** Simplified circuit diagram of a magnetic stimulator and **(b)** visualisation of magnetic field and electric currents induced by a transcranial magnetic stimulation coil. Reproduced from (Ridding et al. 2007).

At the frequencies used in TMS ($\leq 1MHz$), the electromagnetic field is assumed to behave under the quasi-static approximation (Plonsey et al. 1967) since the size of the conductor (i.e. the head, approx. diameter of 20 cm) is much smaller than the skin depth at these frequencies (approx. 600 cm at $f = 10^5$ Hz) (Heller et al. 1992). Under the quasi-static approximation, propagation, inductive and capacitive effects of the time-varying electromagnetic field can be ignored, although excluding the capacitive effects is less reliable than excluding the other effects (Bossetti et al. 2007). Under the quasi-static assumption, the Biot-Savart Law describes how the magnetic field B is generated by a current applied to the coil:

$$B(r) = \frac{\mu_0}{4\pi} \oint_L \frac{I_{coil} dl \times \hat{r'}}{|r'|^2} \tag{1.1}$$

where μ_0 is the permeability of free space, I_{coil} is the coil current, dl is the line element along the path L of the coil windings, r' is the vector from the line element to the point of interest r and $\hat{r'}$ the corresponding unit vector (Wang et al. 2023). The primary electric field E' generated by electromagnetic induction can be expressed

using the Maxwell-Faraday Equation in differential form:

$$\nabla \times E' = -\frac{\partial B}{\partial t} \tag{1.2}$$

The primary E-field causes charge to accumulate on the conductivity boundaries which generates a secondary E-field E'', depending on the geometry and conductivity of the different tissue types in the head. The secondary E-field is established almost instantaneously and is considered inseparable from the primary E-field in TMS (Wang et al. 2023). It is described by a scalar potential φ:

$$E'' = -\nabla\varphi \tag{1.3}$$

The total E-field E generated by the magnetic field is the sum of the two E-fields and is described as:

$$E = -\frac{\partial A}{\partial t} - \nabla\varphi \tag{1.4}$$

where the curl of the magnetic vector potential A is substituted for the magnetic field according to $\nabla \times A = B$ (Wang et al. 2023).

Under the quasi-static assumption, the E-field generated by the stimulation can be separated into its spatial and temporal components, i.e. the relative spatial distribution is constant and its amplitude scales with the applied temporal waveform (Wang et al. 2023). This assumption of separation is leveraged when simulating the effects of stimulation using computational models.

1.1.1 Spatial component of electric field

The spatial distribution of the electric field is largely determined by the characteristics of the stimulation coil through the spatial integration of $\frac{\partial B}{\partial t}$ according to Equation 1.4. Factors such as the number of turns in the coil windings, the coil shape and the presence of a ferromagnetic coil core affect the spatial component of the stimulation. Common shapes of stimulation coils include circular coils (Fig. 1.2 (a)) and figure-of-eight coils (Fig. 1.2 (c)). The spatial distribution of the electric field generated by TMS can be estimated using numerical models such as the finite

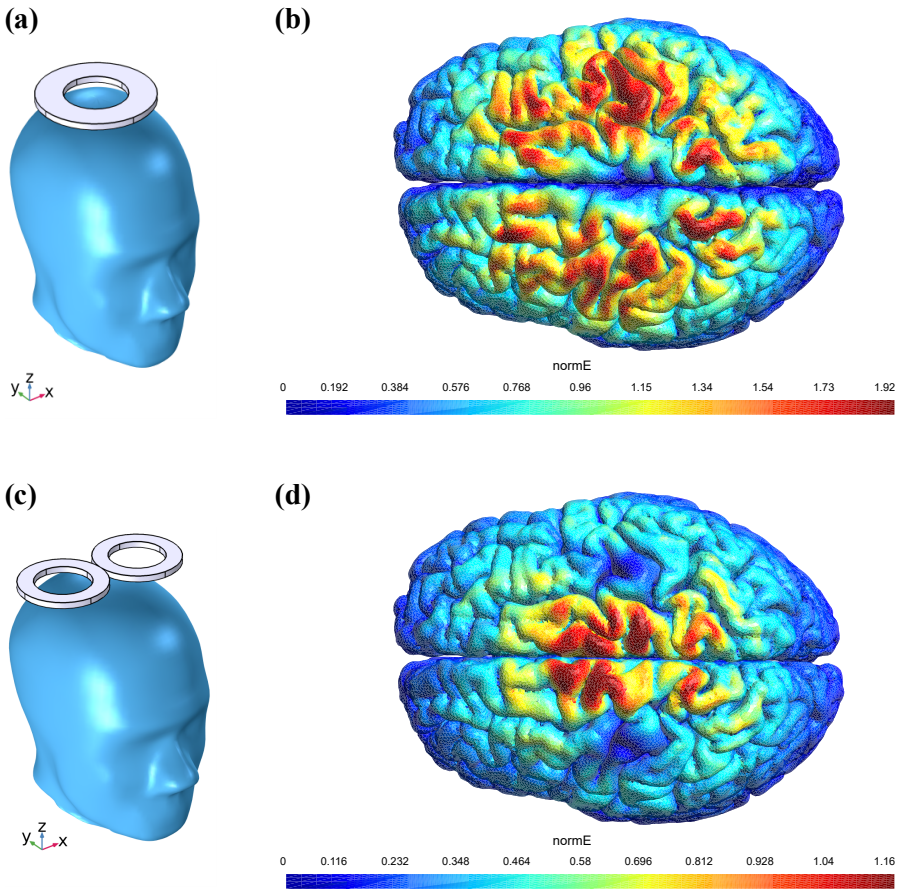

Figure 1.2: Simulation results of electric field distributions of circular and figure-of-eight coils. **(a)** A Magstim 90 mm circular coil and **(c)** a Magstim 70 mm figure-of-eight coil are placed over the vertex of a model head. The spatial distribution of the induced electric field calculated using SimNIBS is shown in **(b)** for the circular coil and **(d)** for the figure-of-eight coil.

element method (FEM) which discretises head models into volumetric elements. Simulation packages such as SimNIBS (Thielscher et al. 2015) take in magnetic resonance (MR) images, segment them into the relevant tissue types, assign them characteristic conductivities and then use the FEM to calculate the electric field. Typical conductivity values for the different tissue types are 0.126 S/m (range: $0.1 - 0.4$ S/m) for white matter, 0.275 S/m (range: $0.1 - 0.6$ S/m) for grey matter, 1.654 S/m (range: $1.2 - 1.8$ S/m) for cerebrospinal fluid, 0.01 S/m (range: $0.003 - 0.04$ S/m) for bone and 0.465 S/m (range: $0.2 - 0.5$ S/m) for the scalp (Wagner et al. 2004) (Saturnino et al. 2019). Using the FEM with the information from the MR images enables a realistic estimate of the spatial distribution of the electric field for individual head models and different stimulation coils and placements. Figure 1.2

(b) shows the electric field strength (i.e. the norm of the E-field vectors) generated by a TMS pulse applied to a circular coil over the vertex of an example brain in SimNIBS. Figure-of-eight coils consist of two circular coils placed side by side, such that the induced electric fields add up at the junction of the two coils. Figure 1.2 (d) shows the electric field strength when applying the same stimulation using a figure-of-eight coil which allows a more focal area to be stimulated.

The primary induced E-field decreases inversely proportionally to the third power of the distance from the coil. This decay is increased by the presence of conductive objects such as the human body (Ilmoniemi et al. 2023), resulting in a rapid decrease of the strength of the electric field with increasing distance from the coil, and thus restricting TMS to the superficial layers of the brain (usually up to $1.5-3.5$ cm deep) (Deng et al. 2013). Coils designed to reach deeper targets include two round coils at an angle, called double cone coils, and more complex winding patterns such as in H coils. However, TMS coils display a depth-focality tradeoff, as coils reaching deeper lead to a wider electrical field spread (Deng et al. 2013).

1.1.2 Temporal component of electric field

The temporal component of the electric field is determined by the circuit of the stimulator and the stimulation coil. In the simplified circuit of a TMS stimulator (Fig. 1.1 (a)), the capacitor is connected to the stimulation coil, which allows the current to flow from the capacitor into the coil, producing a damped cosine stimulus pulse with coil current I_{coil} given by:

$$I_{coil}(t) = \frac{V_{cap0}}{\omega L} \sin(\omega t) \exp(-\alpha t), t \geq 0 \tag{1.5}$$

where V_{cap0} is the initial capacitor voltage, $\alpha = R/2L$ indicates the damping from the circuit series resistance R, $\omega = \sqrt{1/LC - \alpha^2}$ is the damped resonance frequency, L is the inductance of the coil and C is the capacitance of the capacitor (Peterchev et al. 2023). Typical values of C are between $60-200\mu F$ while typical coil inductances range from $10-25\mu H$. The pulse length is determined by the

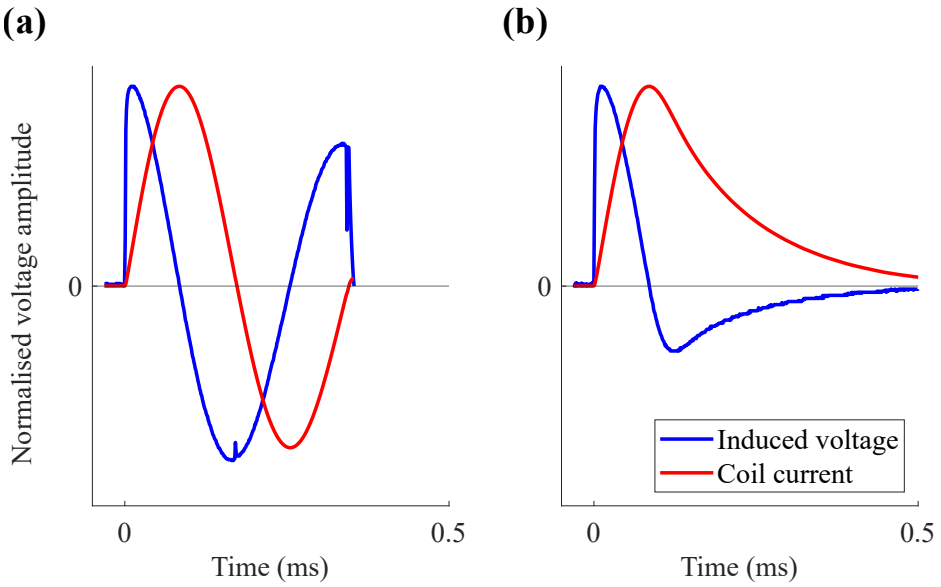

Figure 1.3: Illustration of the basic TMS waveforms. Coil current and induced voltage for **(a)** a biphasic stimulus pulse and **(b)** a monophasic stimulus pulse.

circuit resonance frequency:

$$T \approx 2\pi\sqrt{LC} \tag{1.6}$$

with typical lengths around $200-500\mu s$. The voltage applied to the coil V_{coil} is given by:

$$V_{coil} = L\frac{dI_{coil}}{dt} \tag{1.7}$$

After one cycle, some energy is often lost due to dissipation in the circuit, but up to 64% of the energy can be recovered and partially recharge the capacitor (Peterchev et al. 2023). Turning the switch off after one period generates a biphasic waveform (Fig. 1.3 (a)), while slowly dissipating the current through a resistor after the initial quarter of the pulse generates a monophasic waveform (Fig. 1.3 (b)) (Epstein 2008). The biphasic pulse has two phases that can depolarise neurons, while the monophasic pulse only has one, as indicated by the shaded areas. The induced E-field follows the same damped cosine shape as the voltage across the stimulation coil.

The tunable stimulation parameters for an individual stimulator are commonly limited to the amplitude (percentage of the maximum stimulator output power), the number of pulses and the repetition rate (stimulation frequency) of the pulses. However, other parameters such as the pulse shape, the pulse width and the direction

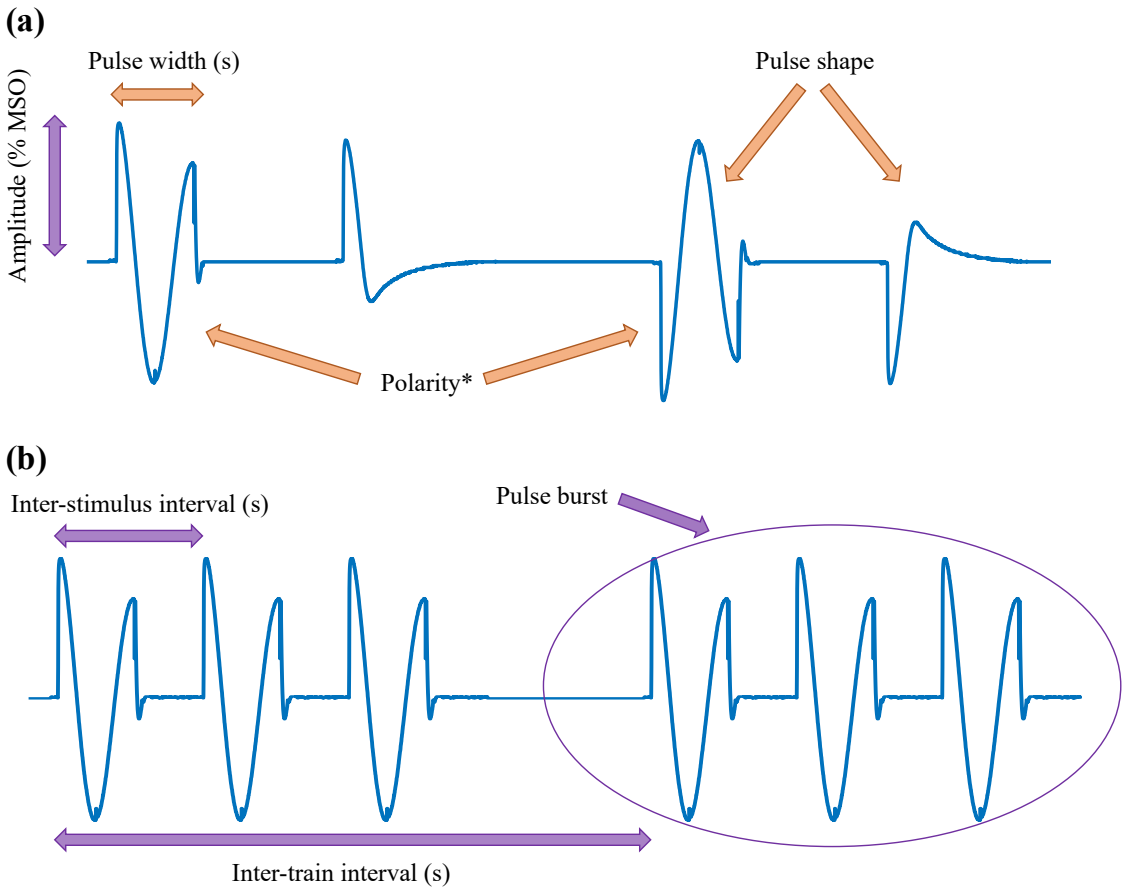

Figure 1.4: TMS parameters of interest for **(a)** individual stimulation pulses and **(b)** pulse trains. Purple arrows indicate parameters adjustable in conventional stimulators and orange ones indicate parameters of interest that are not commonly adjustable. MSO: Maximum stimulator output
*The polarity can be changed mechanically in any stimulator by changing the orientation of the coil on the head, however, changing the polarity in software without movement of the coil is desirable to ensure consistent targeting.

of the induced current in the brain (polarity) are important stimulation parameters (D'Ostilio et al. 2016). Fig. 1.4 visualises possible stimulation parameters of interest in a pulse train with purple indicating parameters adjustable in conventional stimulators and orange indicating parameters of interest that are not commonly adjustable.

1.1.3 Neural activation

Neuronal membranes separate the inside from the outside of the neuron, with each side having different concentrations of ions such as sodium and potassium. The membrane acts as an electrical insulator, stopping ions from freely flowing in and

out, and contains proteins that act as ion gates. The difference in electrical potential between the inside and outside of the cell is called the membrane potential. The E-fields that are applied to neurons during the stimulation polarise the neuronal membranes which can lead to neural activation. The stimulation effects can be described on different levels using a group of mathematical models. The simplest model, the leaky integrate-and-fire (LIF) model (Gerstner et al. 2014), assumes the neural membrane to be a passive, isopotential cell and is useful to describe the subthreshold behaviour of the membrane. The Hodgkin-Huxley (HH) model (Hodgkin et al. 1952), on the other hand, takes into account different ion channels inside the membrane which lead to the non-linear behaviour of the neurons, including the generation of action potentials. Finally, the cable equation helps to describe how the current flows along the neurons spatially (Ermentrout et al. 2010). While these models only provide an approximation of the neuronal dynamics, together, they can help us estimate, understand and predict the effect of TMS on the neurons.

1.1.3.1 Passive, linear model of an isopotential cell

A simple description of the evolution of the membrane potential is given by the leaky integrate-and-fire model. Considering only the subthreshold dynamics of the model, the membrane potential of a passive, isopotential cell is described using the electrical equivalent circuit shown in Figure 1.5 (a): The cell membrane is described as a capacitor, which is charged by an incoming current, in parallel with a resistor, representing the current slowly leaking across the membrane (Gerstner et al. 2014). According to the law of current conservation and Ohm's law, the applied current $I(t)$ is split into the two branches of the circuit and given by:

$$I(t) = I_R + I_C = \frac{u(t) - u_{rest}}{R} + C\frac{du}{dt} \tag{1.8}$$

where I_R and I_C are the currents across the resistor and capacitor, respectively, $u(t)$ is the membrane potential as a function of time, u_{rest} is the resting potential of the membrane, R is the membrane resistance and C is the membrane capacitance

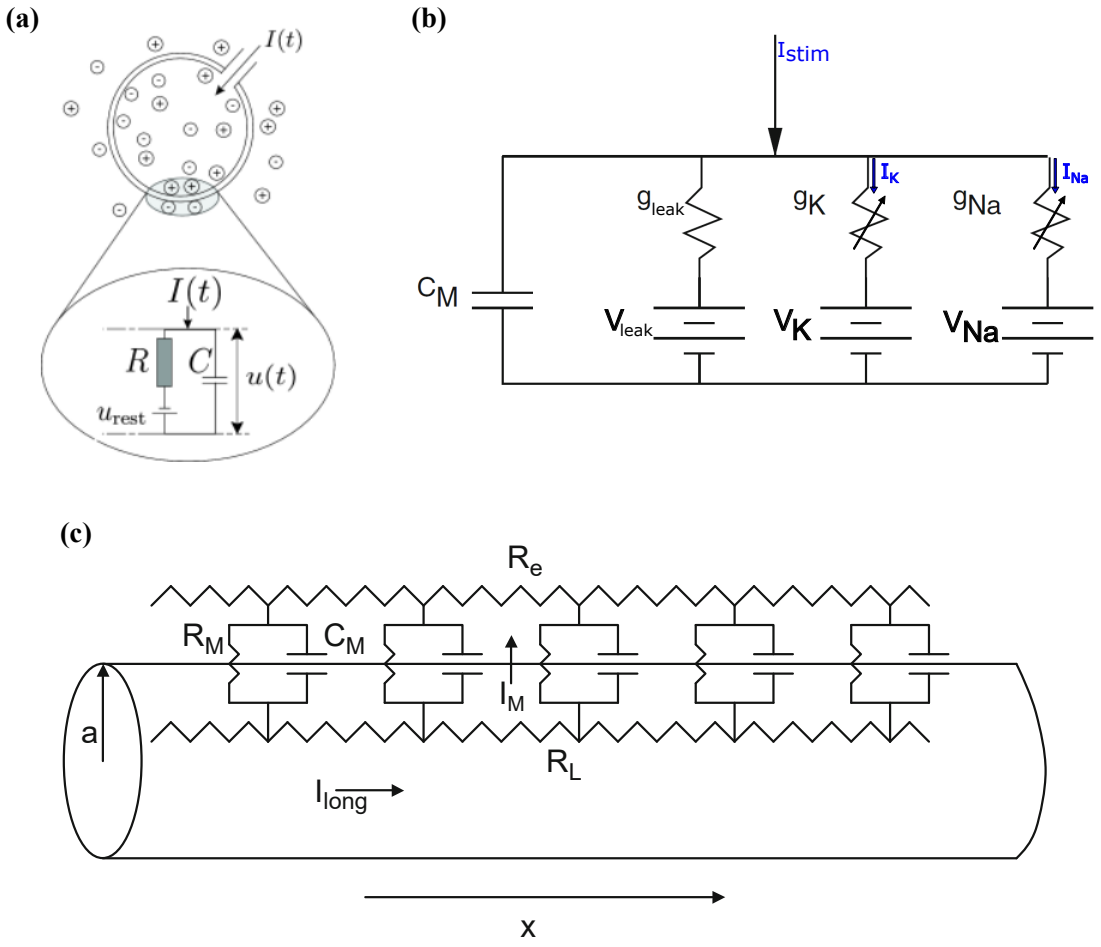

Figure 1.5: Equivalent circuits underlying the computational models of the neuronal membrane potential. **(a)** In the integrate-and-fire model, the cell membrane is modelled as a capacitor in parallel with a resistor which is in series with a battery representing the resting membrane potential. **(b)** In the Hodgkin-Huxley model, the flow of the potassium, sodium and leak currents through ion channels is modelled as the current flowing through parallel branches of an equivalent circuit. The resistors representing the ion channel conductivity of the sodium and potassium ion channels are nonlinear and voltage and time-dependent. **(c)** The equivalent circuit underlying the cable equation describes the current flow both through the membrane and along it in the x-direction. (a) was reproduced from (Gerstner et al. 2014), (c) was reproduced from (Ermentrout et al. 2010).

(Gerstner et al. 2014). Multiplying this by R and substituting the membrane time constant $\tau_m = RC$ yields the equation of a passive low-pass filter:

$$\tau_m \frac{du}{dt} = -[u(t) - u_{rest}] + RI(t) \tag{1.9}$$

1.1.3.2 Non-linear model of an isopotential cell

However, neuronal dynamics are in fact non-linear and include the generation of action potentials. The Hodgkin-Huxley model (Hodgkin et al. 1952) captures this non-linear behaviour and is widely used in computational neuroscience. Similar to the passive model, the HH model describes a neuron's axon using an equivalent circuit, in which the cell membrane's charge-storing capabilities are represented as a capacitor, but it models different types of ion channels in parallel branches (Fig. 1.5 (b)). Each ion channel is described as a conductor, some of which are voltage- and time-dependent, and the concentration gradients of the ions are modelled as DC sources. The electrical behaviour is then characterised by a set of differential equations which describe how the ion currents pass through the channels in the membrane and how action potentials are initiated, using the following membrane equation (Hodgkin et al. 1952):

$$C_m \frac{dV_m}{dt} = -g_{leak}(V_m - V_{leak}) - I_{Na} - I_K - I_{stim} \tag{1.10}$$

where C_m is the specific capacitance of the membrane, V_m is the membrane potential and I_{stim} is the stimulation pulse. g_{leak} represents the resting membrane conductance and V_{leak} its reversal potential. The remaining currents capture the nonlinear behaviour which is observed when a neuron fires. I_{Na} and I_K are the sodium and potassium currents, respectively, whose conductances change with time and voltage, allowing the generation of action potentials (Hodgkin et al. 1952). I_{stim} can be derived from the electric field induced in the brain during TMS (which is proportional to the coil voltage) using Ohm's law.

The original HH model was developed from experimental work on the giant axon of the squid, where the electrical properties rely mainly on sodium and potassium ions. Other groups (e.g. (Pospischil et al. 2008)) have adapted this model and fit it to experimental data from different mammalian in vivo and in vitro preparations (such as rat, ferret, cat and guinea-pig cortices), which include further ionic currents and firing behaviours. Additionally, HH-type channels are used in more complex, morphologically-realistic neuron models such as in the Blue Brain Project (Markram

et al. 2015) which were reconstructed from the somatosensory cortex of rats. These models were further adapted to match the biophysical and geometric properties of human cortical neurons (Aberra et al. 2018).

1.1.3.3 The cable equation

In contrast to the previous models' assumption of isopotentiality, the neuronal membrane potential differs along its three-dimensional structure. The different parts of the neuron can be represented as one-dimensional cylinders (or cables), where the current flows along the cylinder inside the cell and radially through the membrane. Dividing the cylinder into small compartments, it can be represented as the electrical equivalent circuit shown in Fig. 1.5 (c) (Ermentrout et al. 2010). The current across the membrane is again represented as a capacitor and resistor in parallel (as in Equation 1.8). According to Kirchhoff's current law, the current flowing out of each compartment equals the currents flowing into it from adjacent compartments. The equivalent circuit is described by the cable equation which calculates the membrane potential V_m from current flow both through the membrane and along it in the x-direction:

$$\tau_m \frac{\partial V_m}{\partial t} = \lambda^2 \frac{\partial^2 \varphi_e}{\partial x^2} + \lambda^2 \frac{\partial^2 V_m}{\partial x^2} - V_m \tag{1.11}$$

where φ_e is the extra-cellular potential due to the applied E-field, $\tau_m = C_m R_m$ is the membrane time constant and $\lambda = \sqrt{aR_m/2R_l}$ is the length constant with a being the radius of the cylinder, R_m being the specific membrane resistance and R_l being the intra-cellular resistance (Wang et al. 2023).

The term $\lambda^2 \frac{\partial^2 \varphi_e}{\partial x^2}$ is called the activating function which describes the influence the applied E-field has on the excitation of the neuron. For magnetic stimulation, the activating function includes both the primary and secondary components of the applied electric field described in Equation 1.4 (Nagarajan et al. 1996).

For myelinated axons, the cable equation and activation function are more complex since their axial resistance is not uniform (Wang et al. 2023). However,

computational models showed that the effective length constant of myelinated axons would be much longer, leading to stronger activation (Wang et al. 2018).

1.1.3.4 Sites of activation

TMS most likely activates neuronal axons rather than somas as indicated by measurements of the minimum intensity and duration of a stimulus to evoke a motor evoked potential (MEP). Together, these measurements allow the calculation of the rheobase (the minimum current amplitude of infinite duration needed for depolarisation), and the strength-duration time constant (or chronaxie, i.e. the minimum time required for a current with an amplitude twice as large as the rheobase to initiate an action potential) (Siebner et al. 2022). A cell soma has a much longer time constant and higher excitation threshold than axons (Siebner et al. 2022). Further, the myelination of axons causes them to experience much stronger polarisation as the applied E-field restricts axial current across the membrane to the unmyelinated part of the axon at small nodes. Additionally, myelinated axons are much smaller than somas, leading to lower stimulation thresholds (Wang et al. 2023).

At the scale of cortical neurons, the electric field generated in TMS has a negligible spatial gradient and is therefore commonly treated as quasi-uniform. In this scenario, electric field gradients are only strong enough to stimulate axons at geometric discontinuities such as terminations, bifurcations and bends. The generalised activation function takes into account these changes in geometry by considering the individual parameters of each compartment n (Rattay 1998):

$$f_n = \left[\frac{\varphi_{e,n-1} - \varphi_{e,n}}{R_{n-1}/2 + R_n/2} + \frac{\varphi_{e,n+1} - \varphi_{e,n}}{R_{n+1}/2 + R_n/2} + ... \right] / C_{m,n} \tag{1.12}$$

Here, the depolarisation is driven by the gradient provided by the physical neurons instead of the gradient of the E-field. Thus, the area with the lowest activation thresholds in the hand knob region of the primary motor cortex has been shown to be the gyral crown and lip, where the E-field amplitude is highest and the spatial change in neural processes is largest (Aberra et al. 2020), although the electric field direction is also important for neuronal recruitment. In particular,

stimulation is likely to occur when e.g. axon terminals are aligned to the local electric field direction (Siebner et al. 2022).

However, TMS does not only stimulate individual neurons, especially at supra-threshold intensities. In fact, each TMS pulse can induce a complex pattern of neuronal activity (Siebner et al. 2022). Electrodes implanted into the epidural space can record descending volleys, a series of waves of activity that travel down the corticospinal tract and are separated from one another by an inter-peak interval of about 1.5 ms (Di Lazzaro et al. 2014). The first wave, called the D-wave, is thought to originate from direct activation of the axons of corticospinal neurons in the subcortical white matter. The later waves, called the I-waves, are thought to stem from indirect, trans-synaptic activation of the same neurons and are numbered in order of appearance as I1, I2, etc. At low intensities, TMS usually evokes I1-waves, at medium intensity later I-waves and only at high intensities D-waves (Di Lazzaro et al. 2014). However, the exact composition of the descending volleys in TMS also depends on the direction of the induced current in the brain.

1.1.4 TMS protocols

So far, I explained how TMS generates an electric field and how this field can excite neurons through the activating function. In this section, I describe how common stimulation protocols leverage this excitation and affect the targeted brain areas. These protocols make TMS a valuable tool for basic investigations of the nervous system as well as for therapeutic applications, including for the treatment of disorders such as major depression, obsessive-compulsive disorder and addiction (Lefaucheur et al. 2020).

TMS pulses can be applied as single pulses, paired pulses or repeated as trains of pulses. Repetitive protocols are used to alter cortical excitability, while single and paired-pulse protocols are commonly used to probe the nervous system both in research and clinical settings, giving an insight into a patient's neurophysiology. For this, motor responses called motor evoked potentials can be elicited by stimulating the hand area of the primary motor cortex with TMS and recording a muscle response

of the contralateral hand using surface electrodes through electromyography (EMG) (Fig. 1.6). The peak-to-peak amplitude of the MEPs is used as a quantification of the effect TMS has on the nervous system and the threshold to induce them is used as a reference for many treatment protocols and investigations. TMS is also commonly applied to the visual cortex in the occipital lobe, which can cause participants to see a flash of light (a phosphene) or experience a blind spot (a scotoma) depending on the stimulation parameters (Kammer 1999). Already in the 1980's, applying magnetic stimulation to the visual cortex has been shown to allow the induction of 'virtual lesions' when applied between $80 - 100$ ms after presentation of alphabetic characters, stopping participants from correctly identifying them (Amassian et al. 1989). Other examples of using TMS in basic neuroscience include the stimulation of the occipital cortex to probe its involvement in face processing (Pitcher et al. 2007) or of the dorsolateral prefrontal cortex to investigate its role in perceptual decision making (Philiastides et al. 2011). TMS is also used as a potential measure of consciousness by assessing the complexity of the neural response to it using electroencephalography (Casali et al. 2013). In this thesis, and thus in this section, I will mainly focus on the stimulation of the primary motor cortex since it allows an immediate objective quantification of stimulation effects via motor evoked potentials, which results in its common use to test new stimulation protocols.

1.1.4.1 Motor thresholds

The most commonly used thresholds are the resting motor threshold (RMT) and the active motor threshold (AMT). The RMT is usually defined as the minimum intensity required to evoke an MEP of at least $50\mu V$ peak-to-peak amplitude in 5 out of 10 consecutive trials while the target muscle is at rest (Rossini et al. 1994). This method is based on the relative frequency of the evoked MEPs while other methods, such as the adaptive method (Awiszus 2003), instead estimate the probability to evoke an MEP. The AMT is often estimated as the lowest intensity required to evoke an MEP of at least $200\mu V$ in 5 out of 10 consecutive trials during contraction of the target muscle at 10 or 20% of the individual's maximum strength (Groppa

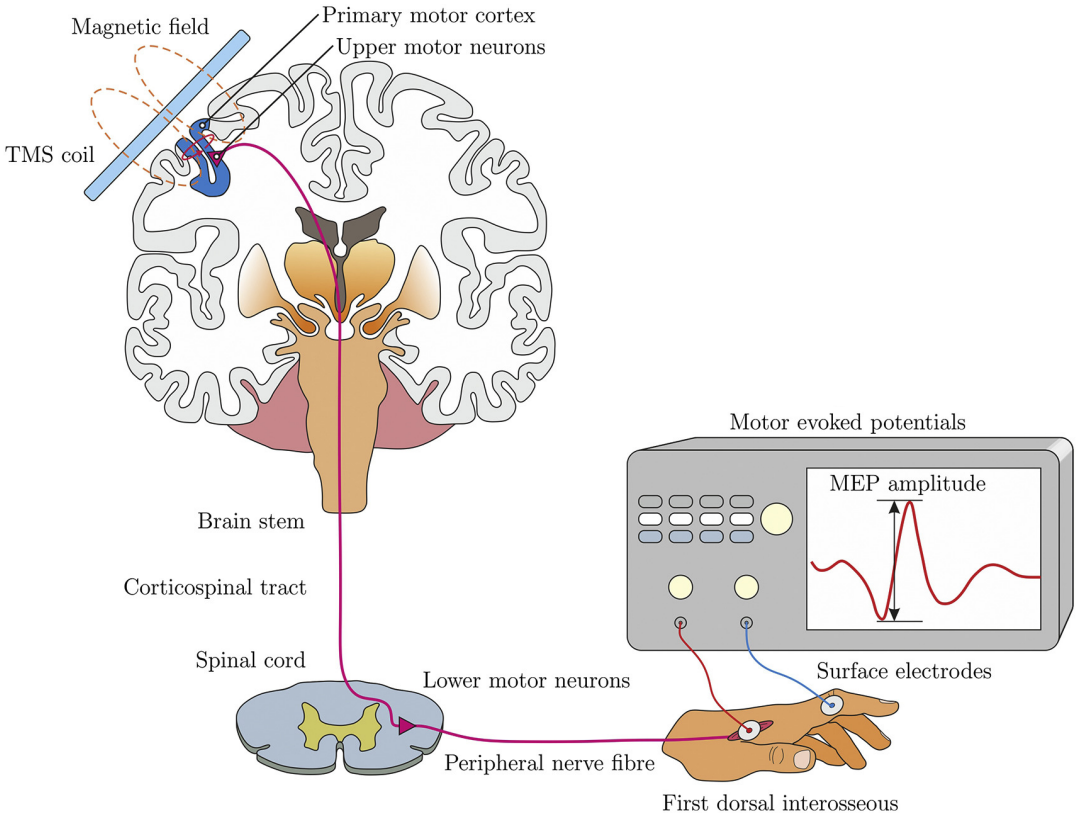

Figure 1.6: Schematic overview of the setup to elicit motor evoked potentials. The TMS coil is held above the hand representation in the primary motor cortex. A stimulation pulse travels through the spinal cord to the hand muscles which elicits a twitch measured by electrodes attached to the first dorsal interosseous. The muscle movement is recorded and displayed on a screen. Adapted from (Weise et al. 2020)

et al. 2012). Threshold levels depend on the direction of the induced current flow in the brain, with lower thresholds for current flow in the posterior-anterior (PA) direction for monophasic pulses (Sommer et al. 2006).

1.1.4.2 Single-pulse measures

The size of the motor evoked potentials is influenced by external factors such as the stimulation intensity, the stimulation waveform, the coil and the coil position (Farzan 2014). Yet, even with these factors kept constant, MEPs show a large variability from one stimulus to the next and across experimental sessions (Kiers et al. 1993) (see Section 1.1.8 for a discussion of relevant factors). Therefore, to obtain reliable MEP measurements, $10 - 15$ pulses are usually recorded and then averaged. To quantify the relationship between the stimulus intensity and the amplitude of the MEPs, a

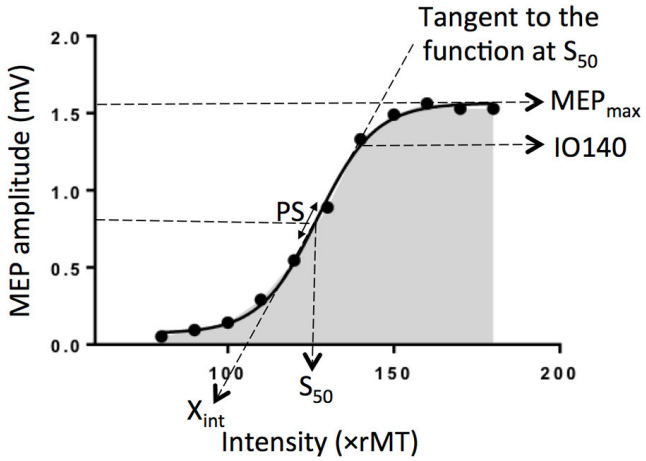

Figure 1.7: An example input-output curve is fitted by a sigmoid function with its characteristic flat line at zero, a linear increase between $120 - 140\%$ of the resting motor threshold and the plateau at the maximum MEP amplitude MEP_{max}. IO140 indicates the MEP amplitude recorded at 140% of the resting motor threshold, PS indicates the peak slope of the curve, S_{50} is the stimulus intensity needed to obtain 50% of MEP_{max} and X_{int} is the X intercept of the tangent to the sigmoid at S_{50}. Reproduced from (Kemlin et al. 2019).

recruitment curve, also called the stimulus-response or input-output (IO) curve, is obtained by measuring the MEP peak-to-peak amplitude across a range of intensities (Fig. 1.7). At low intensities, where no MEPs are elicited, the curve is a flat line at zero. When the stimulation intensity increases and reaches the motor threshold, the MEP amplitude increases, with a linear increase between $120 - 140\%$ of the RMT, until it reaches a plateau where the MEP amplitude does not increase further (Rossini et al. 2015). During the linear increase, the higher the stimulation intensity is, the higher the number of corticospinal fibres that are recruited. The relationship between the stimulus intensity and the amplitude of the MEPs can be modelled by a Boltzmann sigmoid function (Devanne et al. 1997). The curve parameters such as the slope and the plateau value differ between people and target muscles. Clinically, the recruitment curve is used in diseases that affect the pyramidal tract fibres such as stroke or amyotrophic lateral sclerosis (Rossini et al. 2015).

Immediately after an MEP is elicited by a TMS pulse during tonic contraction of the contralateral hand muscle, the background EMG activity is suppressed for up to $100 - 300$ ms (Rossini et al. 2015). This is referred to as the cortical silent period (CSP) and has been suggested to be mediated by gamma-aminobutyric

acid (GABA) type B receptors as concluded from pharmacological studies such as (Siebner et al. 1998). The duration of the CSP varies with stimulus intensity, and a CSP stimulus intensity-duration curve, similar to the recruitment curve, can be obtained by recording the silent period for a range of intensities (Groppa et al. 2012).

1.1.4.3 Repetitive TMS protocols

Applying TMS in a repetitive protocol can induce changes in corticospinal excitability that outlast the stimulation duration. The exact timing and the number of stimuli applied determine whether a protocol tends to increase or decrease excitability (Fitzgerald et al. 2006). Repetitive protocols are commonly applied to the primary motor cortex and their effects are measured using MEPs, by comparing MEP amplitudes before and after the protocol, since this gives an immediate objective readout. The results in the motor cortex have also led to investigations of therapeutic effects such as in the treatment of depression where repetitive (r)TMS is applied to a different area of the cortex (Lefaucheur et al. 2014) (see Section 1.1.6). Fig. 1.8 gives an overview of commonly used rTMS protocols.

Conventional rTMS

The left column of Fig. 1.8 shows the conventional rTMS protocols. Applying pulses at a fixed frequency of 1 Hz for several minutes, called low-frequency repetitive TMS, has been shown to induce inhibitory after-effects (for example (Sommer et al. 2002)), while high-frequency rTMS ($\geq$ 1 Hz) tends to induce facilitatory after-effects (for example (Pascual-Leone et al. 1994)). Protocols with frequencies of 5 Hz or more are usually applied as short periods of stimulation, interleaved with periods of no stimulation, to stay within safety limits determined by the international safety consensus (Rossi et al. 2009).

Theta burst stimulation (TBS)

The right column in Fig. 1.8 shows more complex patterned protocols. The most commonly used one is theta burst stimulation (TBS), where a triplet of pulses at 50 Hz is repeated at a frequency of 5 Hz (Huang et al. 2005). This stimulation pattern

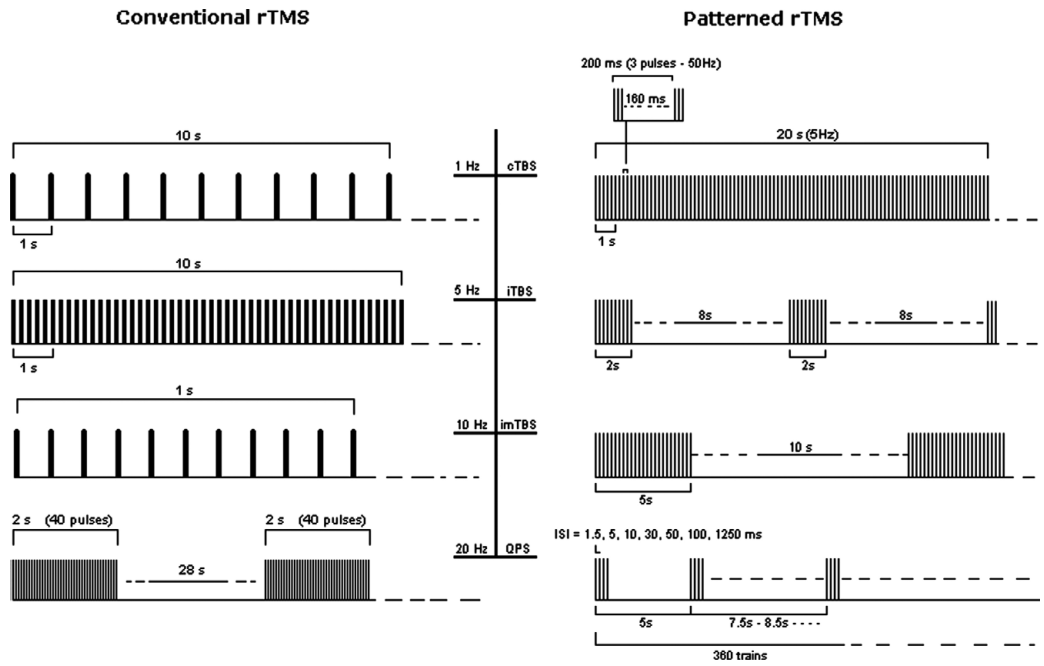

Figure 1.8: Overview of repetitive TMS protocols. The left panel shows examples of the conventional rTMS protocols. From top to bottom: rTMS patterns applied at 1 Hz, at 5 Hz, at 10 Hz and at 20 Hz. The right panel shows patterned TMS protocols. From top to bottom: continuous theta burst stimulation (cTBS), intermittent theta burst stimulation (iTBS), intermediate theta burst stimulation (imTBS) and quadripulse stimulations (QPS). Reproduced from (Rossi et al. 2009)

aims to imitate the firing of pyramidal cells in the hippocampus of behaving rats (Larson et al. 1989) which have been shown to cause an increase in the strength of connections through long-term potentiation (LTP) in studies using electrical stimulation on rodent brain slices (Larson et al. 1986) (Hess et al. 1996). Mimicking this with TMS, in intermittent theta burst stimulation the 50Hz-triplets are applied for 2 s followed by an 8 s break and then repeated again, increasing corticospinal excitability (Huang et al. 2005). Conversely, applying the same triplets continuously for 20 s as in continuous TBS has been shown to decrease corticospinal excitability (Huang et al. 2005). The increase and decrease in excitability have been hypothesised to arise from a mixture of excitatory and inhibitory effects and have been attributed to calcium-dependent plasticity. A model by Huang and colleagues describes three stages (Huang et al. 2011): In the first stage, a single 50 Hz burst is assumed to increase the postsynaptic Ca^{2+} influx through voltage-gated calcium channels, followed by an exponential decay in Ca^{2+} ions. In the second stage, iTBS would

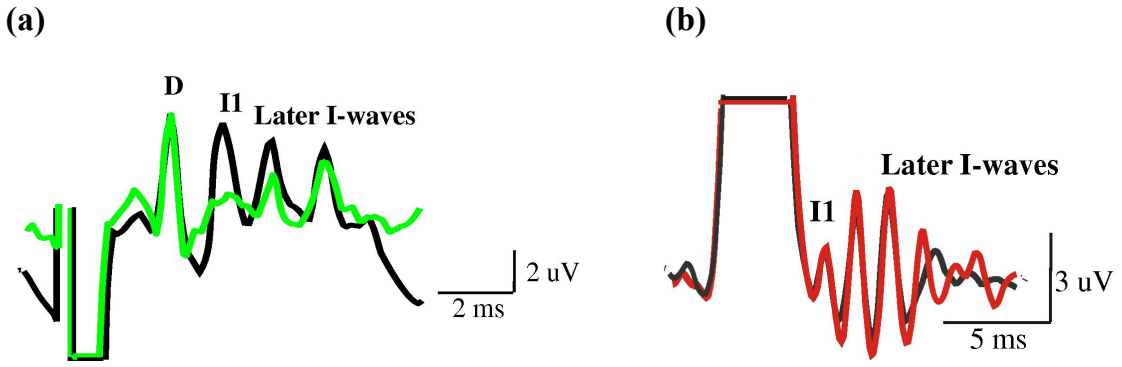

Figure 1.9: Effect of theta burst stimulation on corticospinal descending volleys. **(a)** After cTBS (green), the amplitude of the I1 wave is suppressed compared to baseline recordings (black). The D-wave and later I-waves are not affected. **(b)** After iTBS (red), the amplitude of the late I-waves is increased compared to baseline recordings (black). The I1 wave is not affected. For each trace, $10 - 25$ responses are averaged. Adapted from Figures 5 and 9 in (Di Lazzaro et al. 2010).

trigger the production of a facilitatory type of protein kinase through a rapid increase in Ca^{2+} ions. In cTBS, the bursts are repeated continuously leading to the accumulation of Ca^{2+} ions which would trigger an inhibitory type of protein kinase (Huang et al. 2011). The sum of the inhibitory and excitatory protein kinases at the end of this stage would then determine the after-effects through processes such as phosphorylation or dephosphorylation of AMPA receptor proteins in the third stage, leading to long-term potentiation and long-term depression (Huang et al. 2011). Additionally, GABA-ergic interneurons have been identified as playing a key role in promoting long-term plasticity through disinhibition of pyramidal neurons (Suppa et al. 2022).

Recordings of corticospinal descending volleys from epidural electrodes showed that cTBS suppresses the I1 wave, without affecting the later I-waves and the D-wave, while iTBS enhances late I-waves but does not affect the amplitude of the I1 wave (Fig. 1.9) (Di Lazzaro et al. 2010). This leads to the hypothesis that iTBS and cTBS affect different populations of neurons (Suppa et al. 2016).

However, the effects of TBS suffer from large inter- and intra-individual variability (Schilberg et al. 2017) (Boucher et al. 2021), some of which may be due to age and genetic factors (Jannati et al. 2017) (Jannati et al. 2019) (see Section 1.1.8 for a detailed discussion). Additionally, factors such as muscle contraction before the

application of the TBS protocol have been shown to influence the effects of TBS (Gentner et al. 2008) (Goldsworthy et al. 2012). An increasing body of literature is investigating possible modifications of the original TBS protocols to increase plasticity effects. Increasing the number of pulses per burst from 3 up to 6 pulses in iTBS has been shown to trigger a significantly larger increase in corticospinal excitability in rodent motor cortices (Meng et al. 2022). A study investigating different stimulation intervals between repeated iTBS trains suggests this can affect the direction of the plasticity effects (Tse et al. 2018), while another study aiming to optimise the 8 second interval of iTBS found significant differences in plasticity effects when increasing and decreasing this interval (Abboud Chalhoub et al. 2020). Furthermore, increasing the total number of pulses applied during the protocol from 600 up to 3600 pulses has been shown to reverse the effect of the protocols in some studies, with prolonged cTBS of 1200 pulses leading to facilitatory effects (McCalley et al. 2021) and prolonged iTBS of 1200 pulses leading to inhibitory effects (Gamboa et al. 2010). This reversal of effects has been hypothesised to be due to the first half of the applied pulses having a 'priming' effect on the second half (Gamboa et al. 2010). However, other studies did not replicate this reversal (Hsu et al. 2011).

Quadripulse stimulation (QPS)

Another patterned protocol is quadripulse stimulation (QPS), where four pulses separated by $1.5 - 1250$ ms are repeated every 5 s (Hamada et al. 2008) (bottom right in Fig. 1.8). This protocol was built on the idea of increasing the plasticity effects of monophasic paired-pulse rTMS by increasing the number of pulses per train from two to four (Hamada et al. 2007). The inter-stimulus interval of 1.5 ms, which corresponds to the I-wave periodicity, has then been increased to up to 1250 ms (Hamada et al. 2008) which leads to facilitatory or inhibitory after-effects depending on the interval. To generate this protocol, four Magstim 200^2 stimulators are connected to combine the output through one stimulation coil with a specially designed combining module (Hamada et al. 2008) (Fig. 1.10). The combination of several stimulators is necessary since the smaller inter-stimulus

Figure 1.10: Quadripulse stimulation setup. Four Magstim 200^2 stimulators are connected to combine the output through one stimulation coil with a specially designed combining module. Reproduced from (Matsumoto et al. 2020)

.

intervals could not be generated by conventional individual monophasic stimulators and the inter-train interval of 5 s has not been shortened due to the time needed to recharge the capacitors within the individual devices (Hamada et al. 2008). The technical challenges of implementing the QPS protocol highlight that the currently used patterns in TMS are limited by the available stimulators and may therefore not be optimal from a neuroscience perspective.

1.1.5 Effect of pulse shape

In conventional stimulators, transcranial magnetic stimulation is limited to either monophasic or biphasic waveforms. When monophasic pulses are applied to induce currents in the posterior-anterior direction in the brain, the motor thresholds have been shown to be lower than in the anterior-posterior direction (Sommer et al. 2006) with early studies using epidural recordings in human participants showing that pulses with these current directions likely activate different sites or different neuron populations, in particular at low intensities (Di Lazzaro et al. 2001b). For biphasic pulses, the second half of the pulse is thought to more effectively depolarise neurons than the first, with lower thresholds when this phase is applied in the posterior-anterior direction (Sommer et al. 2006) (Aberra et al. 2020). This second phase has been shown to recruit descending volleys, similar to posterior-anterior monophasic

pulses, however, cortical activation patterns depend on relative thresholds and intensities of the different pulse phases (Di Lazzaro et al. 2001a).

When generating monophasic pulses, conventional stimulators do not recover the pulse energy effectively, which limits the repeatability of the pulses to low frequencies since the capacitors of the stimulator cannot be recharged quickly enough. Consequently, high-frequency protocols such as TBS are only possible with biphasic waveforms unless several monophasic stimulators are combined, as done in QPS. However, monophasic pulses are thought to more selectively recruit cortical neurons, which could lead to less contamination from different circuits (Huang et al. 2017) and result in more strongly modulated cortical excitability than biphasic pulses in repetitive TMS protocols (Rossini et al. 2015). For instance, monophasic pulses lead to stronger after-effects than biphasic pulses in 1 Hz rTMS (Taylor et al. 2007), additionally lasting longer in 10 Hz rTMS (Arai et al. 2007). Similarly, a study comparing the after-effects of monophasic and biphasic QPS found that monophasic QPS induced stronger and longer-lasting after-effects compared with biphasic QPS (Nakamura et al. 2016). Therefore, enabling the generation of high-frequency monophasic protocols may enable more effective stimulation.

1.1.6 Mapping TMS parameters to therapeutic applications

TMS has been increasingly used in clinical practice over the last 15 years. In many therapeutic applications, TMS is applied to areas outside the motor cortex. However, to determine the stimulation intensity, pulses are usually first applied to the muscle representation of the abductor pollicis brevis or the first dorsal interosseous in the primary motor cortex to measure the motor threshold. Once the threshold is established, the coil is moved to the treatment location to apply the stimulation protocol at an intensity relative to the threshold.

The first approval by the US Food and Drug Administration (FDA) was obtained for major depressive disorder (MDD) in 2008, where 10 Hz rTMS is applied to the left dorsolateral prefrontal cortex (DLPFC) at 120% of the motor threshold for 4 s, followed by a 26 s break, repeated for 75 trains per session. In total, 3000 pulses

are applied over 37.5 min per session, five days a week for $4-6$ weeks (Perera et al. 2016). The DLPFC has been identified as a stimulation target by physiological studies showing decreased metabolism in the left DLPFC and increased metabolism in the right DLPFC in depression, as well as due to its synaptic connections to the limbic system involved in mood regulation (Lefaucheur et al. 2014). This led to the hypothesis that high-frequency stimulation inducing neural excitation in the left DLPFC or conversely, low-frequency stimulation inducing neural inhibition in the right DLPFC could normalise the activity in these brain areas and therefore lead to a reduction in depressive symptoms. A large, multi-site, randomised, sham-controlled trial demonstrated the efficacy of 10 Hz rTMS applied to the left DLPFC (O'Reardon et al. 2007) and led to the FDA approval. Low-frequency rTMS applied to the right DLPFC has also shown antidepressant effects but with lower statistical power than high-frequency rTMS applied to the left DLPFC (Lefaucheur et al. 2020) and has not been FDA-cleared yet (Cotovio et al. 2023). Since 2008, TMS has been approved for cortical mapping (2009), the treatment of migraines with aura (2013), obsessive-compulsive disorder (2017), smoking cessation (2020) and anxious depression (2021) (Cohen et al. 2022).

Intermittent TBS offers the opportunity to decrease the duration of the treatment protocol from 37.5 min to only 3 minutes, allowing clinics to treat more patients in one day than when using rTMS (Blumberger et al. 2018). In 2018, a randomised, multi-centre, clinical trial led to FDA-clearance of iTBS for the treatment of depression by demonstrating the non-inferiority of iTBS compared to 10 Hz rTMS. The trial showed responder and remission rates of 49% and 32%, respectively, following iTBS treatment, compared to 47% and 27% following rTMS treatment (Blumberger et al. 2018). In comparison, a previous meta-analysis found rTMS with frequencies of $5-20$ Hz led to response and remission rates of 29.3% and 18.6%, respectively (Berlim et al. 2014). In 2022, a further acceleration of the treatment using iTBS in depression was FDA-approved: the Stanford Neuromodulation Therapy (SNT). This protocol aims to improve the treatment in three ways: 1) have ten sessions per day, spaced at 50 minute intervals due to studies showing

that this interval has a cumulative effect on synaptic strengthening, 2) applying 1800 instead of the usual 600 pulses per session, i.e. increasing the overall pulse dose of stimulation, and 3) increasing the precision in targeting the left DLPFC by finding the area most anti-correlated with the subgenual anterior cingulate cortex circuit, a site that has been shown to lead to better clinical efficacy in depression treatment (Fox et al. 2012) (Cole et al. 2020). Following 5 days of treatment, a randomised, sham-controlled trial of 29 participants reported a response rate of 69% and a remission rate of 46% four weeks after the last treatment day (Cole et al. 2022). As discussed in Section 1.1.4.3, ongoing research aims to refine stimulation protocols to improve stimulation effects by creating different pulse shapes and patterns. Alternative neuromodulation therapies in treatment-resistant depression include the FDA-approved use of electroconvulsive therapy (ECT) and vagus nerve stimulation (VNS), and an investigational treatment of deep brain stimulation targeting the subgenual cingulate region (Mayberg et al. 2005). However, ECT, VNS and DBS require anaesthesia and ECT carries the risk of cognitive side effects such as amnesia whereas TMS offers low-risk treatment with few side-effects.

1.1.7 Common side effects of TMS

Compared to ECT, VNS and DBS, transcranial magnetic stimulation has few adverse effects, with the most common ones being transient headaches or discomfort. Table 1.1 summarises potential side effects during TMS for the stimulation protocols used in this thesis. To reduce the risk of side effects, particularly of seizure induction, TMS participants are screened for contraindications to TMS and the stimulation is applied within established safety guidelines (Rossi et al. 2009).

1.1.8 Variability in TMS

Motor evoked potentials show a large variability from one stimulus to the next and across experimental sessions. The origin of the stimulus-to-stimulus variability is not fully understood but physiological mechanisms such as the number of motor neurons in the spinal cord recruited by a stimulus and firing more than once as well

Table 1.1: Potential TMS side effects. Summarised from (Rossi et al. 2009).

Side effect	**Single-pulse TMS**	**Theta burst**
Seizure induction	Rare	Possible
Syncope (fainting due to a decrease in blood flow to the brain)	Possible (not caused by the brain stimulation)	Possible
Transient headache, discomfort under the coil, neck pain, toothache, prickling sensation	Possible	Possible
Transient hearing changes	Possible	Not reported
Transient cognitive/ neuropsychological changes	Not reported	Transient impairment of working memory

as the synchronisation of motor neuron discharges are thought to contribute to it (Roesler et al. 2008). Recent papers from the 'Big TMS collaboration' examined potential sources of inter-individual variability in neural responses to TMS with the aim of improving its utility and reliability as an experimental and clinical tool. From data pooled across 35 studies, Corp et al. identified TMS machine and with it pulse waveform, neuronavigation use, age, target muscle and M1 hemisphere as possible sources of this variability (Corp et al. 2021). Other participant-specific factors such as sex and genotypes (e.g. (Cheeran et al. 2008)) have been suggested to impact the individual response to TMS. Furthermore, when investigating factors driving iTBS responses, baseline MEP amplitude, age, target muscle, and time of day significantly predicted induced plasticity effects (Corp et al. 2020). Psychological factors such as the attentional focus of subjects have also been shown to influence plasticity effects (Conte et al. 2007). Further important intra-individual factors include the duration of time awake, the circadian rhythm, the menstrual cycle and hormonal levels (Ridding et al. 2010) (Farzan 2014). Indeed, cortical excitability has been shown to be influenced by various factors that vary systematically with time of day, such as time awake (Huber et al. 2013), circadian phase (Ly et al. 2016), and cortisol levels (Milani et al. 2010).

1.1.9 Addressing variability

One consideration in the context of variability is that TMS and other neuromodulation techniques are commonly used in 'open-loop', i.e. the stimulation parameters are set by the operator to achieve a target outcome, defined as the reference, and the actuator, in this case the stimulator, applies the stimulation to the nervous system. However, to decrease the variability observed in stimulation responses between and within individuals, additional information should be used to inform stimulation as illustrated in Fig. 1.11. Ideally, neuromodulation would be applied in a closed-loop, where the variable of interest is directly measured and controlled. However, due to the complexity of the brain and how neuromodulation affects it, current approaches are unable to achieve that but instead enable 'state-informed' stimulation, where the stimulation is informed by some potentially interesting markers of the 'brain state'. To account for time-based rhythms such as circadian and multi-day rhythms, these factors should be taken into account when choosing the stimulation target values and the control policy of the stimulation. On a smaller time scale, an adaptive feedback pathway could be used to take into account the instantaneous physiological state of the nervous system. This could be monitored through sensors such as electroencephalography (EEG) or EMG which can help to identify biomarkers and feed the information to a classifier which could then provide extra information for the control policy to stimulate the brain at potentially more optimal time points or physiological states.

To address the stimulus-to-stimulus and intra-individual variability, examples of possible biomarkers to guide the timing of the pulse delivery include the phase and power of specific neuronal oscillatory activity. Targeting these brain rhythms more optimally with rTMS could decrease the variability in TMS responses. For instance, in the motor cortex, studies combining TMS with EEG have found that the phase of the mu ($8-13$ Hz) and beta ($14-30$ Hz) oscillations modulate corticospinal excitation. Larger MEP amplitudes have been observed when stimulating at the trough of the mu oscillation compared to the mu peak, representing higher and lower excitability states, respectively (C. Zrenner et al. 2018). The opposite pattern

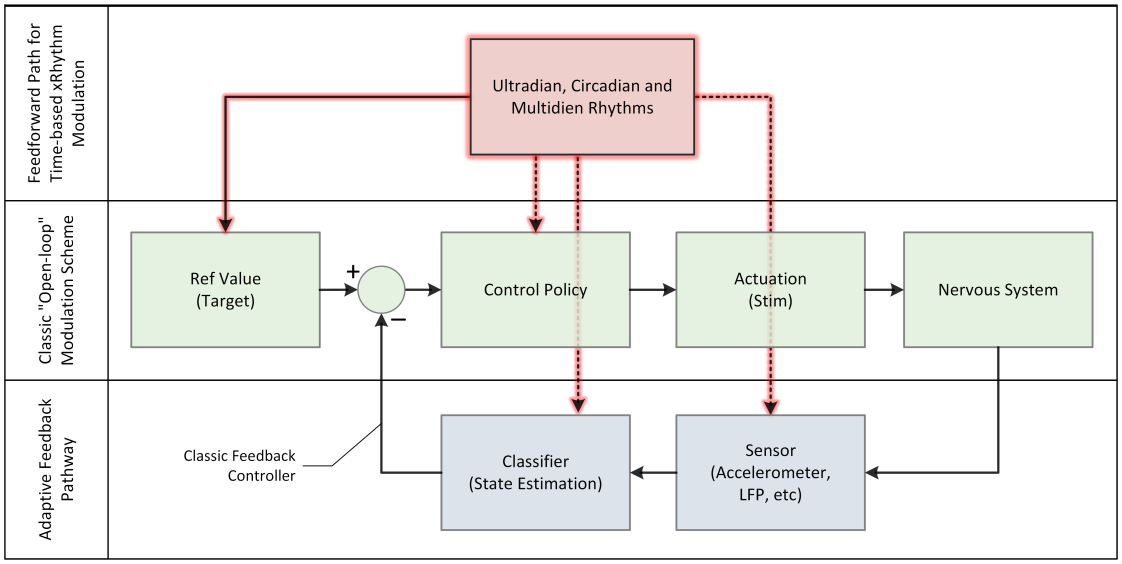

Figure 1.11: Control loops of neuromodulation. Neuromodulation can be applied in open-loop, closed-loop and using feed-forward pathways. Reproduced from (Wendt et al. 2022)

has been found for the phase-dependence in the beta frequency band (Wischnewski et al. 2022). A study translating these methods to the DLPFC has shown that rTMS synchronised to the alpha oscillations in the DLPFC can reduce resting-state alpha activity in this area, which is generally increased in major depressive disorder (B. Zrenner et al. 2020).

To address the inter-individual variability, another aspect may be personalising the stimulation according to the dominant frequencies of individual brains. In clinical settings, TMS is delivered almost exclusively in 10 Hz or TBS paradigms (Lefaucheur et al. 2020). Individual patients, however, show variation in the peak frequencies of endogenous brain rhythms, a “brain fingerprint” that remains stable over time (Grandy et al. 2013) (Kondacs et al. 1999). There is theoretical and empirical evidence that neuromodulation interacts with these rhythms, in a frequency-dependent manner (Thut et al. 2017) (Schmidt et al. 2014). Thus, treatment outcomes might be improved by taking these endogenous frequency variations into account. For instance, the individual alpha frequency (IAF) is an EEG measurement commonly recorded in psychiatric research. Tuning rTMS to this frequency has been hypothesised to increase its effectiveness (Leuchter et al.

2013). This has been demonstrated in schizophrenia patients, where stimulation at the IAF produced a greater therapeutic effect on negative symptoms (Jin et al. 2006) and on both positive symptoms and depressive symptoms (Jin et al. 2012) than sham or other set frequencies. In depression, a correlation between the IAF and the response to rTMS has been suggested in some studies (Arns et al. 2012) but failed to be replicated in others (Krepel et al. 2018). Another study in depression patients showed that the proximity of the IAF to the stimulation frequency of 10 Hz, rather than the value of the IAF itself, was associated with a better treatment response after rTMS applied to the left DLPFC (Corlier et al. 2019). However, it should be noted that if the IAF is part of the pathological state of the patient, stimulation at this frequency might not be optimal as this could reinforce rather than restore the pathological state.

Together, these examples illustrate the ongoing research into finding optimal stimulation parameters to treat various disorders and to decrease outcome variability. Increasing control over the stimulation parameters may increase the opportunities to identify effective protocols and personalise treatments.

1.2 Current state of the art of TMS devices

An ideal TMS device would have full flexibility in generating stimulation pulses and patterns without the hardware constraints of conventional devices. Expanding the parameter set promises to increase the selectivity when targeting specific neural populations (D'Ostilio et al. 2016) and might enable the emergence of novel, more effective stimulation protocols. Specifically, full control over pulse shapes and widths, higher stimulation rates independent of pulse shape and the possibility to generate variable patterns are desirable. Additionally, the ideal device would enable software control of the direction of the induced current in the brain (polarity) and have enough output power to stimulate individuals with high motor thresholds.

To date, a number of new stimulator designs have been introduced with the aim of increasing stimulation control, most prominently a series of devices with controllable pulse width called cTMS (Peterchev et al. 2008)(Peterchev et al. 2011)

(Peterchev et al. 2014). These devices moved away from the conventional stimulator design in which the pulse characteristics are determined by the circuit resonance. In the first cTMS design, the thyristor switch in conventional TMS devices was replaced with an isolated-gate bipolar transistor (IGBT), allowing control of the duration of the pulse. Further developments led to the latest generation of the device which consists of two half-bridge circuits using four IGBTs and two energy-storage capacitors (Fig. 1.12 (a)). This design allows the generation of four different voltage levels (Peterchev et al. 2014). Combining these voltage levels enables the generation of monophasic and biphasic near-rectangular stimuli of adjustable ratios between the first and the second pulse phases (Fig. 1.12 (b)). Additionally, it allows a number of different pulse widths and smaller interpulse intervals than conventional devices.

However, the cTMS device is still limited to a set number of pulse shapes and widths and does not allow the generation of sinusoidal pulse shapes. Furthermore, pulse waveforms need to be balanced in their phases according to specific device requirements and pulse losses need to be split between the two capacitors to prevent a net energy transfer from the capacitor C_1 to C_2 which would restrict the repetition frequency (Peterchev et al. 2023). Despite these restrictions, the cTMS architecture offers a new range of pulses which studies have leveraged to investigate the characteristics of the membrane dynamics, e.g. by generating strength-duration curves (D'Ostilio et al. 2016) (Halawa et al. 2019), and to further explore the effect of pulse shape on neuronal populations (Sommer et al. 2018). Moreover, studies have investigated the influence of pulse width on the aftereffects of a 1 Hz rTMS train (Halawa et al. 2019), which has not been possible with conventional stimulators.

Another device, called flexTMS, was introduced with the aim to increase the flexibility of TMS (Gattinger et al. 2012). It uses an H-bridge structure with four IGBTs (Fig. 1.12 (c)) which can switch the current on and off but otherwise relies on the resonance period of the circuit given by the capacitor and the coil. This allows some control over the pulse generation, yet the pulse width is still restricted by the resonance of the circuit and the small capacitor used in the design causes large voltage decays over the pulse period (Sorkhabi et al. 2020).

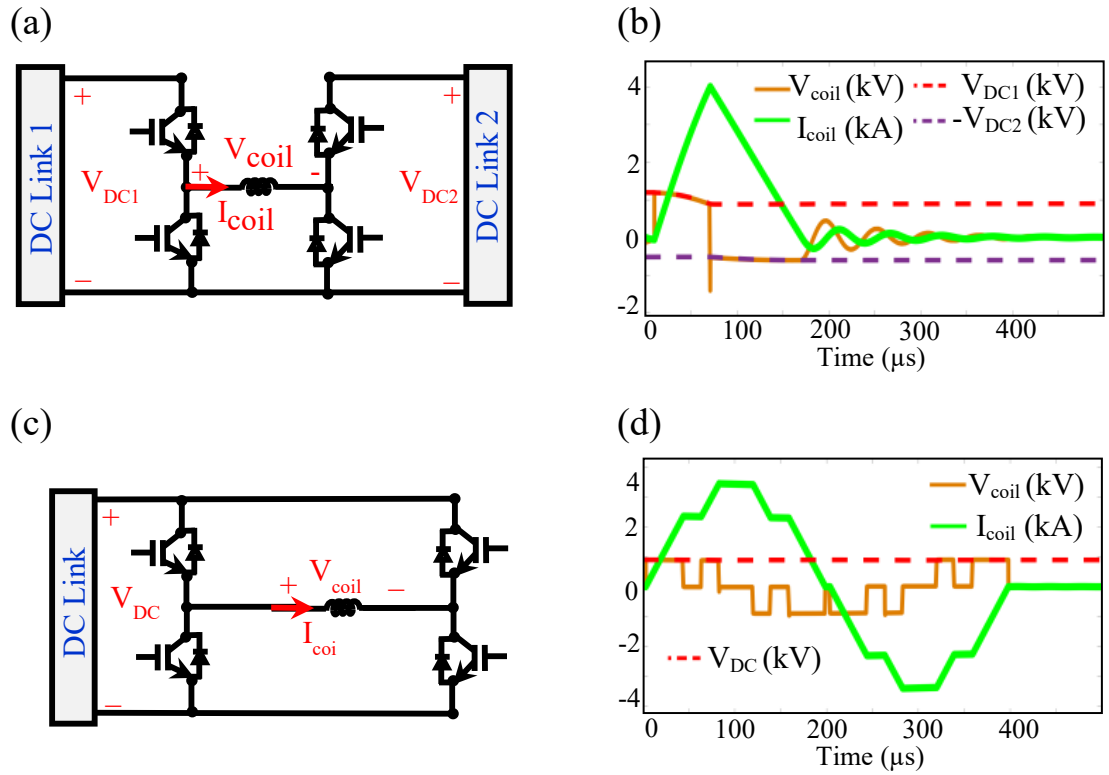

Figure 1.12: H-bridge inverters used in novel TMS devices and their typical pulse characteristics. Key elements of **(a)** the cTMS3 circuit using two half-bridges connected to two separate DC power supplies and **(c)** the flexTMS and pTMS circuits, consisting of an H-bridge connected to a single DC power supply. The flexTMS and pTMS devices differ in the components used in the DC link and in their mode of operation. **(b)** The cTMS3 device generates monophasic and biphasic near-rectangular pulses. **(d)** The pTMS generates pulse width-modulated pulses which can approximate monophasic, biphasic or polyphasic sinusoidal pulses. The coil voltage V_{coil} is shown in brown, the coil current I_{coil} is shown in green and the DC-link voltages are shown in red and purple. Adapted from Table II in (Sorkhabi et al. 2020).

More recently, the focus of stimulator design shifted to combining multiple modules to increase the flexibility of stimulators. These prototypes combine for example ten cascaded H-bridge modules which can generate a larger range of pulses, including very brief pulses (around $8\mu s$) which are much quieter than longer pulses (Zeng et al. 2022). Another design utilises silicon-carbide semiconductors which enable faster switching frequencies (Li et al. 2022), allowing closer approximation of reference pulses and fast repetition rates. However, the cost of silicon-carbide transistors is much higher than silicon IGBTs and the combination of many modules results in large devices, several times the size of conventional stimulators, making

them impracticable to move and store in most laboratories.

Another focus in TMS design is on increasing control over the spatial parameters of the electric field. The multi-locus TMS uses multiple H-bridge-based channels to electronically shift the electric field via a set of large overlapping coils (Koponen et al. 2018) (Nieminen et al. 2022). However, while this device greatly increases spatial specificity, it was optimised to generate near-rectangular single pulses and can be used e.g. for motor mapping, rather than for repetitive protocols.

1.2.1 Programmable TMS (pTMS)

Our group has recently introduced a new TMS device, called the programmable TMS (pTMS), which also uses a fully-symmetrical H-bridge structure (Fig. 1.12 (c)) (Sorkhabi et al. 2020). Compared to the flexTMS, the pTMS uses a large capacitor which reduces the voltage decay and therefore allows the generation of larger pulse widths. Additionally, it does not operate at the resonant frequency but is controlled by a technique called pulse-width modulation (PWM) in which the IGBTs are rapidly switched on and off to create pulses with varying widths , enabling the generation of rectangular, sinusoidal and arbitrary pulse shapes (Fig. 1.12 (d)).

Fig. 1.13 (a) shows a diagram of the pTMS device. On the hardware side, a step-up transformer increases the AC voltage from the mains up to 1 kV, the rectifier converts the voltage to DC which is then stored in the DC capacitors. The software then operates a set of inverters to generate the desired stimulation pulses. On the software side, the reference pulses can be designed in Simulink (MATLAB, The MathWorks, Inc.) and uploaded to the MicroLabBox controller using dSPACE (dSPACE GmbH, Germany) which controls the switching of the IGBTs. Fig. 1.13 (b) shows the final pTMS device prototype which I used in Chapters 2 - 4. To be able to use the pTMS for my in-human research studies, we applied for ethical approval at the Central University Research Ethics Committee, after electrical safety testing according to the medical electrical equipment standard IEC $60601-1$. For the safety of the operators and participants, additional risk mitigations were

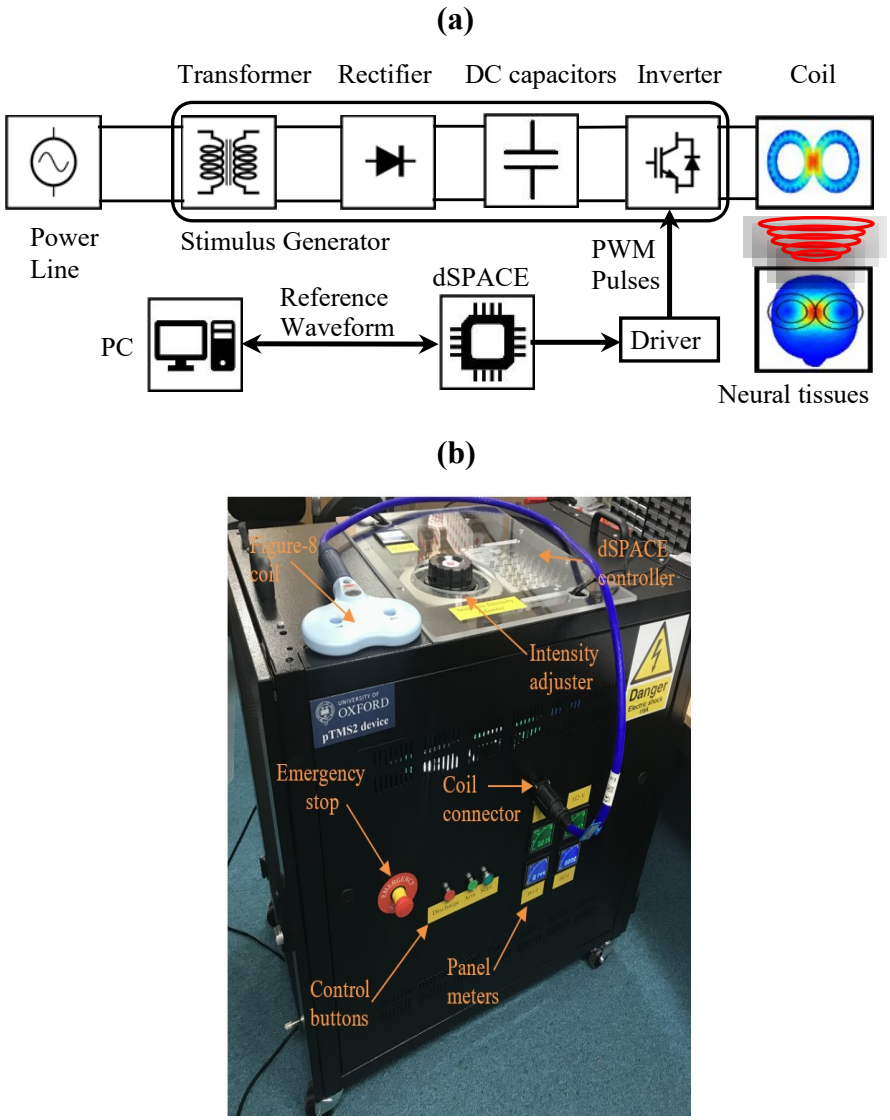

Figure 1.13: Overview of the programmable TMS device. **(a)** Schematic diagram of the pTMS device and how it interfaces with neural tissue. Reproduced from (Sorkhabi et al. 2020). **(b)** Photo of the pTMS device connected to a figure-of-8 stimulation coil. The device was built by Majid Memarian Sorkhabi, a post-doctoral researcher in our lab. Reproduced from (Sorkhabi et al. 2021) ©2021 IEEE

implemented, including magnetic door locks which only open when power is turned off and automatic power-off when the doors are open.

1.2.1.1 Device operation

Depending on the state of the IGBTs, the path the current takes is determined by the different modes of operation of the inverter as shown in Fig. 1.14 (a). In the powering mode (I and V), the DC capacitor is connected to the coil and the

energy stored in the capacitor is transferred to the coil. In the regeneration mode (IV and VIII), the energy flows back from the coil to the capacitor. In each case, the sign of the voltage across the coil depends on the direction of the current flow. In the zero-operation mode (II, III, VI and VII), the IGBTs are switched such that the coil is disconnected from the capacitor. This means that almost no voltage is applied across the coil, keeping the current flowing through it approximately constant (Sorkhabi et al. 2020). As shown in Fig. 1.14 (b), switching rapidly between these modes of operation generates a coil voltage that approximates a predefined reference waveform. To determine the switching sequence, the desired reference signal (V_{Rf}) is phase shifted by 180° to generate $-V_{Rf}$. Together, the signals are compared to a triangular carrier signal (V_C) with a frequency several times that of the reference signal frequency (15 kHz in this example) (Sorkhabi et al. 2020). This enables the generation of any arbitrary waveform, not limiting the TMS pulses to cosine-shaped or rectangular waveforms. In the first generation of the device (pTMS1), the H-bridge allows the generation of three different output voltage levels (0, $-V_{DC}$ and $+V_{DC}$). Cascading two H-bridges as in the second generation (pTMS2) increases the possible different voltage levels to five (0, $-V_{DC}$, $-2V_{DC}$, $+V_{DC}$ and $+2V_{DC}$). This improves the waveform approximation and increases the maximum stimulator output power but it also increases the complexity and size of the device. In this thesis, I used the pTMS2 device with five voltage levels, since five levels (compared to three or seven voltage levels) provided an optimal trade-off between pulse approximation accuracy, output power and complexity (Sorkhabi et al. 2021). Thus from here forth, pTMS refers to the second-generation pTMS device with two H-bridges and five different voltage levels.

1.2.1.2 Stimulation pulses

The pTMS device can generate approximations of conventional monophasic and biphasic TMS pulses, as well as rectangular, polyphasic and other arbitrary pulse shapes. The frequency of the individual pulse can be 2 - 5 kHz and the maximum pulse repetition rate up to 1 kHz, although at high frequencies the pulses will

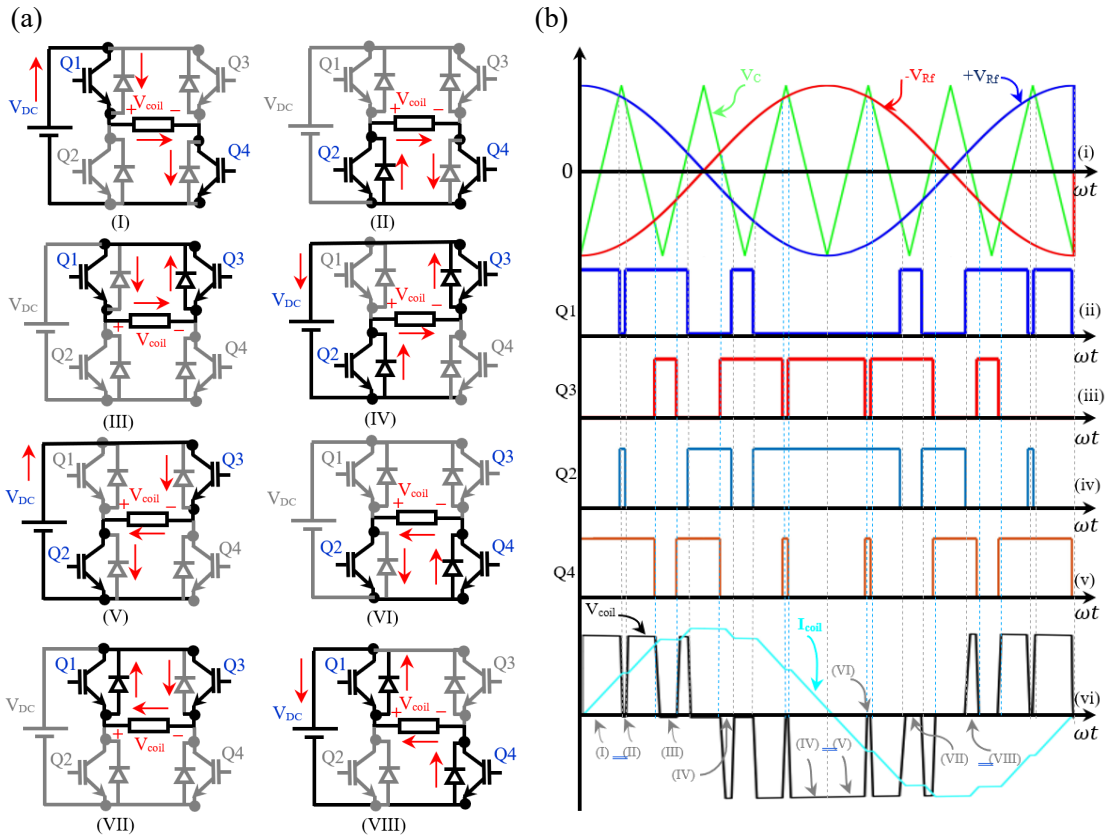

Figure 1.14: Modes of operation and switching states in pTMS circuit. **(a)** The modes of operation of the pTMS device shown in the equivalent circuit of the H-bridge inverter. In the powering mode (I and V), the energy stored on the DC capacitor is transferred to the coil, in the regeneration mode (IV and VIII), the energy is transferred back from the coil to the DC capacitor and in the zero-operation mode (II, III, VI and VII), the capacitor and the coil are not connected. **(b)** The switching patterns of the IGBTs to approximate a cosine-shaped reference waveform. (i) A triangular carrier waveform (V_C) is compared with the reference waveform (V_{Rf}) that will be approximated. (ii-vi) The switching patterns of the four IGBTs to generate the coil voltage that approximates the reference waveform. (vi) The coil voltage generated by switching the IGBTs and the resulting coil current. Adapted from Fig. 3 and 4 in (Sorkhabi et al. 2020)

show a voltage decay when operated at high intensities and the temperature of the stimulation coil will exceed safe temperatures (usually set to 40°C to ensure a safe temperature at the surface of the coil which is in contact with the skin). To demonstrate this flexibility, Fig. 1.15 shows recordings of a set of pulses generated by the pTMS device. (a-d) show biphasic sinusoidal pulses of different pulse widths, (e-h) show monophasic pulses of different pulse widths, (i-j) show rectangular pulses and (k) shows a polyphasic pulse by concatenating two biphasic pulses and (l) by concatenating two monophasic pulses. In summary, the pTMS can approximate the

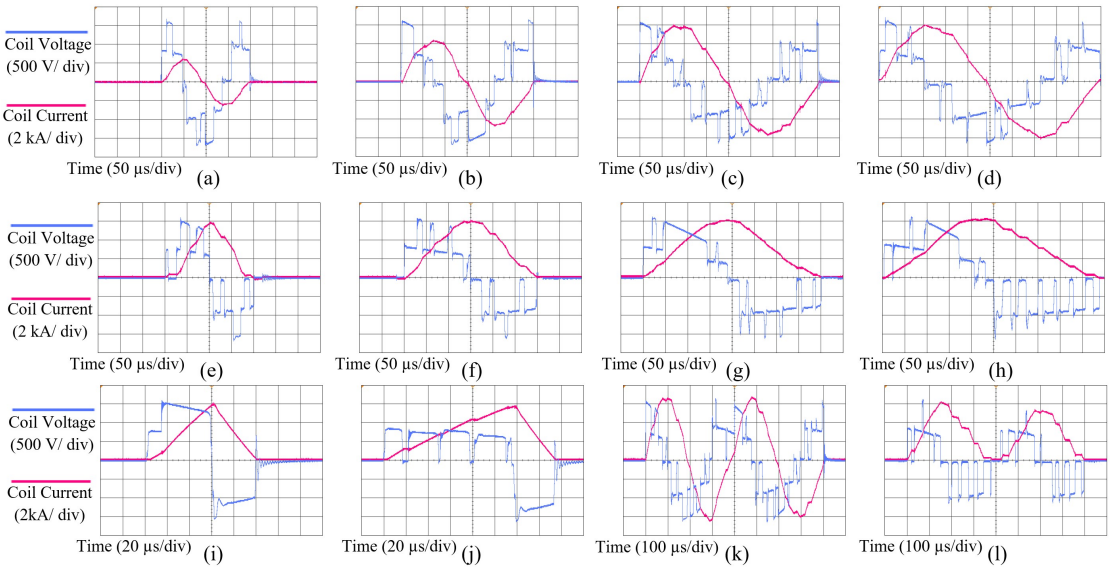

Figure 1.15: Recordings of pTMS pulses. **(a)** - **(d)** show biphasic sinusoidal pulses with frequencies of **(a)** 5 kHz, **(b)** 3.3 kHz, **(c)** 2.5 kHz and **(d)** 2 kHz. **(e)** - **(h)** show monophasic pulses with frequencies of **(e)** 5 kHz, **(f)** 3.3 kHz, **(g)** 2.5 kHz and **(h)** 2 kHz. **(i)** and **(j)** show rectangular pulses and **(k)** and **(l)** show polyphasic pulses by concatenating two biphasic and two monophasic pulses, respectively. For each pulse, the coil voltage is shown in blue and the coil current is shown in red. Recordings are courtesy of Majid Memarian Sorkhabi, (c), (g) and (k) have been published in (Sorkhabi et al. 2021). ©2021 IEEE

stimulation pulses and protocols achievable by currently available devices (including QPS which previously required the combination of four devices) while adding further flexibility. Additionally, to change the direction of the current induced in the brain, conventional stimulators require the coil orientation to be changed manually. For the pTMS, the current direction can be changed by inverting the reference waveform without needing any manual adjustments. Further, the output power of the current pTMS prototype was designed to match the output of the Magstim Rapid^2 stimulator, with a maximum pulse amplitude of 1600 V compared to 1650 V. This is lower than the stimulation amplitude of some single-pulse stimulators, such as the Magstim 200^2, which achieve amplitudes of up to 2800 V. In future generations of the pTMS device, the maximum output intensity can be increased by cascading additional H-bridges.

1.2.1.3 Critical assumption

The rectangular TMS pulses produced by PWM have a high-frequency content ($>$ 10 kHz) which resonance-based stimuli do not have to the same extent. The use of PWM to generate TMS stimuli is based on the assumption that the neurons effectively act as a low-pass filter (Hutcheon et al. 2000), as described in Equation 1.9 from the leaky integrate-and-fire model, and therefore only follow the approximated waveform instead of the fast switching between voltage levels (Sorkhabi et al. 2020).

1.3 Research objectives

This thesis aims to help design, model and validate the programmable transcranial magnetic stimulation device with an extended parameter set. The research objectives can be split into three aims:

1. Validation of pTMS synthesis approach: First, to ensure that the newly developed TMS device can affect the brain similarly to existing devices, equivalence between the TMS devices will be tested. This is particularly important due to the increased high-frequency components in the stimulation pulses of the pTMS. In Chapter 2, I use computational modelling to compare the neural response to stimuli generated by the pTMS device and by a conventional transcranial magnetic stimulator. Following this, in Chapter 3, the pTMS and computational model will be validated in humans. For this, I designed a validation protocol incorporating TMS measures in healthy volunteers, obtained ethical approval for a study incorporating the protocol and conducted the study.

2. Parameter expansion: After the conclusion of the validation of the pTMS device, the aim of Chapter 4 is to generate a novel repetitive pulse pattern with the goal of improving an existing protocol used in the treatment of depression. For this, I designed and conducted another study applying both stimulation protocols to healthy participants and comparing their plasticity effects.

3. Variability investigation: Finally, to address the variability observed in TMS treatment outcomes, in Chapter 5, I investigate the sources of variability of resting motor thresholds in a data set from 60 TMS clinics across the US.

Together, the outcome of the thesis is a validated TMS device, which helped inform and guide the design of the next-generation device, the xTMS, which is now licensed by Magstim and deployed to lead users.

2

Computational validation of the programmable TMS

Contents

The work presented in this chapter has been published in the following peer-reviewed conference paper:

***Wendt, K.**, Sorkhabi, M. M., O'Shea, J., Cagnan, H., and Denison, T. (2021). "Comparison between the modelled response of primary motor cortex neurons to pulse-width modulated and conventional TMS stimuli". Annu Int Conf IEEE Eng Med Biol Soc 2021, pp. 6058–6061.*

2.1 Introduction

The stimulation pulses generated using pulse-width modulation include high-frequency components due to the fast switching between voltage levels. For the pTMS device with two H-bridges, the carrier frequency for the PWM is $f = 8$ kHz, which locates the main switching frequency harmonic at $2 * N_{modules} * f = 32$ kHz (Sorkhabi et al. 2022). Conventional, resonance-based TMS stimuli do not have such prominent high-frequency components (Fig. 2.1). When using PWM to approximate the waveforms of conventional TMS devices, the effects of these need to be compared to ensure the stimulation acts as expected. For the effects to be equivalent from the perspective of the neurons, the key assumption is that neurons cannot follow the high frequency of switching and effectively filter out the high-frequency harmonics (Hutcheon et al. 2000). This would then result in an equivalent effect of the PWM pulses on neurons as compared to conventional TMS pulses. As a first step, computational modelling is a useful tool to visualise and assess these neuronal effects of brain stimulation.

A commonly used, quick estimate of how a TMS pulse interacts with a neuron is the leaky integrate-and-fire model, which describes how the membrane voltage changes as a result of the stimulation. Considering only the subthreshold dynamics, the model describes the cell membrane as a capacitor, which is charged by an incoming current, and a resistor, representing the current slowly leaking across it as described in Chapter 1.1.3 (Gerstner et al. 2014).

However, while this simple linear model is useful as a first examination of the effects of different TMS pulses, it is a strong simplification of neuronal membrane behaviour and does not capture the nonlinear behaviour observed in the nervous system or any spatial characteristics of the neurons. To take these aspects into account, non-linear models of the ion channels and the morphology of the neurons need to be considered. The Blue Brain Project (Markram et al. 2015) experimentally characterised different neuron types in the rat neocortex and constructed multi-compartmental models with Hodgkin-Huxley-type ion channels which capture the morphology of different neurons. Aberra et al. published a computational model

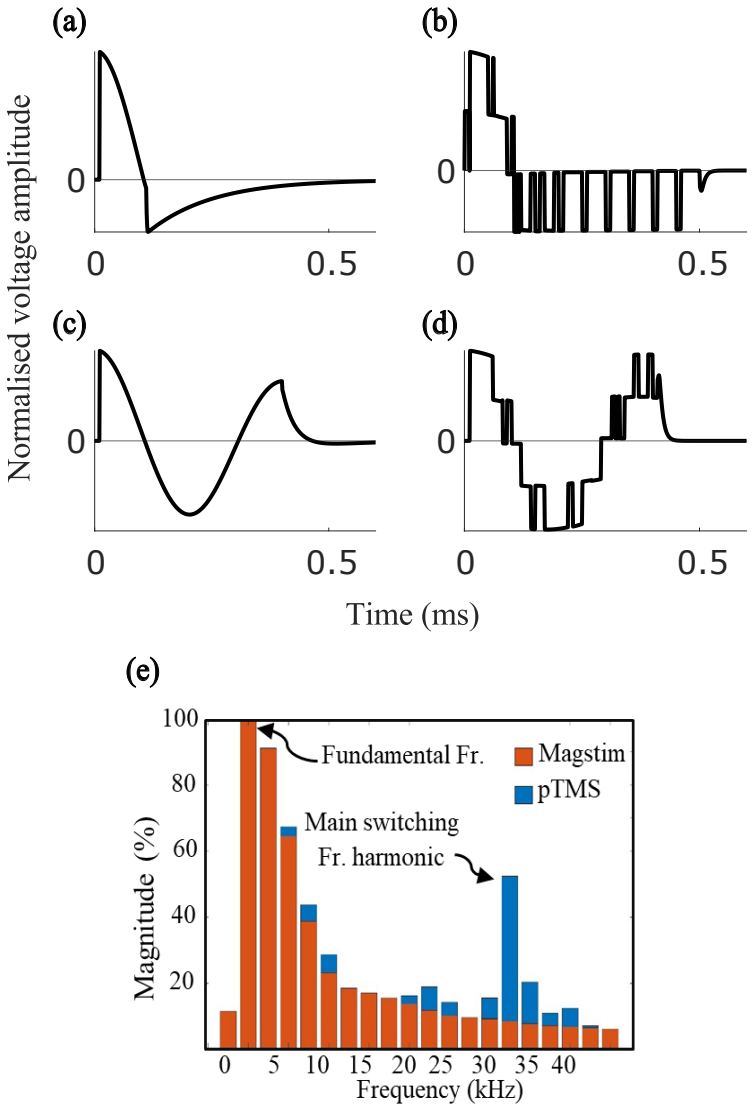

Figure 2.1: Simulated waveforms from **(a)** the monophasic Magstim 200 and **(b)** its pulse-width modulated equivalent, **(c)** the biphasic Magstim Rapid^2 and **(d)** its pulse-width modulated equivalent using the five-level pTMS architecture. **(e)** The frequency spectra of the monophasic Magstim and pTMS voltage waveforms showing the additional harmonic components present in the PWM-equivalent pulse. The largest harmonic is observed at 32 kHz and is about 50% of the fundamental harmonic. Since the Magstim pulse is also not a pure sinusoid but a damped sinusoidal pulse, it also has high high-frequency components, although these reach only about 10% of the fundamental frequency at 32 kHz. The y-axis represents the percentage of the fundamental frequency. Reproduced from (Sorkhabi et al. 2022).

which adapted a subset of the model neurons from the Blue Brain Project to the biophysical and geometric properties of adult, human cortical neurons (Aberra et al. 2018). They then combined these morphologically-realistic models of cortical neurons with a FEM model of a human head to quantify the neural response to

TMS (Aberra et al. 2020). The resulting computational model considers both the spatial and temporal components of the electric field induced by a TMS pulse. Using this more detailed model allows the estimation of the activation threshold of cortical neurons in response to different TMS pulses.

Thus, in the first step of validating the pTMS pulses, the leaky integrate-and-fire, as well as the computational model by Aberra et al. (Aberra et al. 2020), were utilised to compare the neural response to magnetic stimuli generated using PWM and conventional magnetic stimulators. In Chapter 3, the results of these computational models will be validated in-human by comparing the effect these different pulses have on the motor cortex of healthy volunteers.

2.2 Methods

2.2.1 Simulated stimulation pulses

The temporal component of the electric fields used in the models was simulated in Simulink in MATLAB (R2019a & R2020a, The MathWorks, Inc.) with $1\mu s$ time steps. The circuits of two commonly used stimulators, the Magstim 200 and the Magstim Rapid^2 (Magstim Company Ltd, UK), and their PWM equivalents using the 5-level pTMS architecture, were modelled using the Powergui block set in Simulink. The resulting electric field waveforms are shown in Fig. 2.1.

2.2.2 Leaky integrate-and-fire model

Considering only the subthreshold dynamics of a cell membrane, the membrane potential can be estimated according to the equation of the passive membrane (Equation 1.9). Thus, when an electric field waveform $E(t)$ is applied to a region of the cortex, the change in membrane potential ΔV_m of a neuron in a specific spatial coordinate, is proportional to:

$$\Delta V_m \sim \alpha E(t) * h(t) \tag{2.1}$$

where $*$ denotes the temporal convolution (Deng et al. 2011), α is a scaling factor that depends on the characteristics of the specific neuron (Jezernik et al. 2010)

and $h(t)$ is the impulse response defined as:

$$h(t) = \frac{1}{\tau_m} e^{\frac{-t}{\tau_m}} u(t) \tag{2.2}$$

where $u(t)$ is the Heaviside step function and τ_m is the membrane time constant (Deng et al. 2011). Assuming that TMS preferentially stimulates axons, the membrane time constant τ_m is usually approximated to be around $150\mu s$ (Barker et al. 1991) (Peterchev et al. 2008), which corresponds to a filter cut-off frequency of approximately 1 kHz according to the relation $f_c = \frac{1}{2\pi\tau_m}$. The main switching frequency of the pTMS at 32 kHz is therefore expected to be reduced significantly by the filtering mechanism, while the carrier frequency at 8 kHz will be reduced less since it is closer to the cut-off frequency. However, as shown in Fig. 2.1 (e), frequencies around 8 kHz are also present in the conventional pulse waveform. The axonal time constant can be considered the worst-case scenario with regards to the low-pass filtering since cellular excitation is described by a time constant of an order of magnitude larger (Gerstner et al. 2014). A larger time constant would filter the signal more strongly, which would remove more of this high-frequency content, making the effect of the PWM stimuli more similar to the conventional low-frequency stimuli.

2.2.3 Morphologically-realistic computational model

The computational model combining the morphologically-realistic models of cortical neurons with a finite element method model of a human head to quantify the neural response to TMS is freely available on GitHub (Aberra 2019) and has been described in detail in (Aberra et al. 2020). The model is based on the assumption that the quasi-static approximation may be used to calculate potentials generated by neural stimulation as described in Chapter 1.1. Thus, the electric field induced by TMS can be separated into its spatial and temporal components, where the amplitude of the electric field scales instantaneously with the temporal waveform of the stimulator (Wang et al. 2023).

Fig. 2.2 gives a schematic overview of how the model was used in this chapter. The spatial component of the electric field was computed (see Section 2.2.3.2) and

the region of interest around the motor hand knob in the primary motor cortex was extracted. Model neurons were placed into the region of interest (see Section 2.2.3.1) and the cable equation (Equation 1.11 using the membrane time constant, see Section 1.1.3.3) was used to couple the E-field to the neurons. However, as the primary component of the induced electric field is non-conservative and can thus not be expressed as a scalar potential, a potential-like extracellular variable called a quasipotential (Wang et al. 2018) was computed at the compartment centres of each neuron (Aberra et al. 2020). The quasipotentials were then applied to the neuron compartments as extracellular potentials in the NEURON simulation environment (Hines et al. 1997). The spatial distribution was subsequently scaled uniformly over time by the temporal component of the electric field according to the simulated waveform (see Section 2.2.3.3). The membrane potentials were calculated with the backward Euler method (time step: $dt = 5\mu s$) after equilibrating to steady state. A neuron was considered activated if the membrane potential of at least three of its compartments crossed 0 mV with a positive slope. To find the activation threshold of a neuron, a binary search algorithm was used to scale the coil current's rate of change at the pulse onset to find the minimum intensity needed to activate the neuron (Aberra et al. 2020). Finally, the activation thresholds were displayed across a 2D cross-section of the pre-central crown.

Comparing the resulting model thresholds for different pulse shapes and current directions in (Aberra et al. 2020), showed that the relative thresholds correspond well with experimentally measured motor thresholds, although absolute threshold values are higher. Since the aim of this study was to compare relative thresholds across waveforms, the offset in absolute values is unlikely to impact the conclusions drawn.

2.2.3.1 Model neurons

Aberra et al. adapted multi-compartment models of the neuron types found in the cortical layers 1-6 from the Blue Brain Project (Markram et al. 2015) to match the properties of human neurons using Hodgkin-Huxley-type models of the membrane dynamics (Equation 1.10). They then created five clones of each cell type by

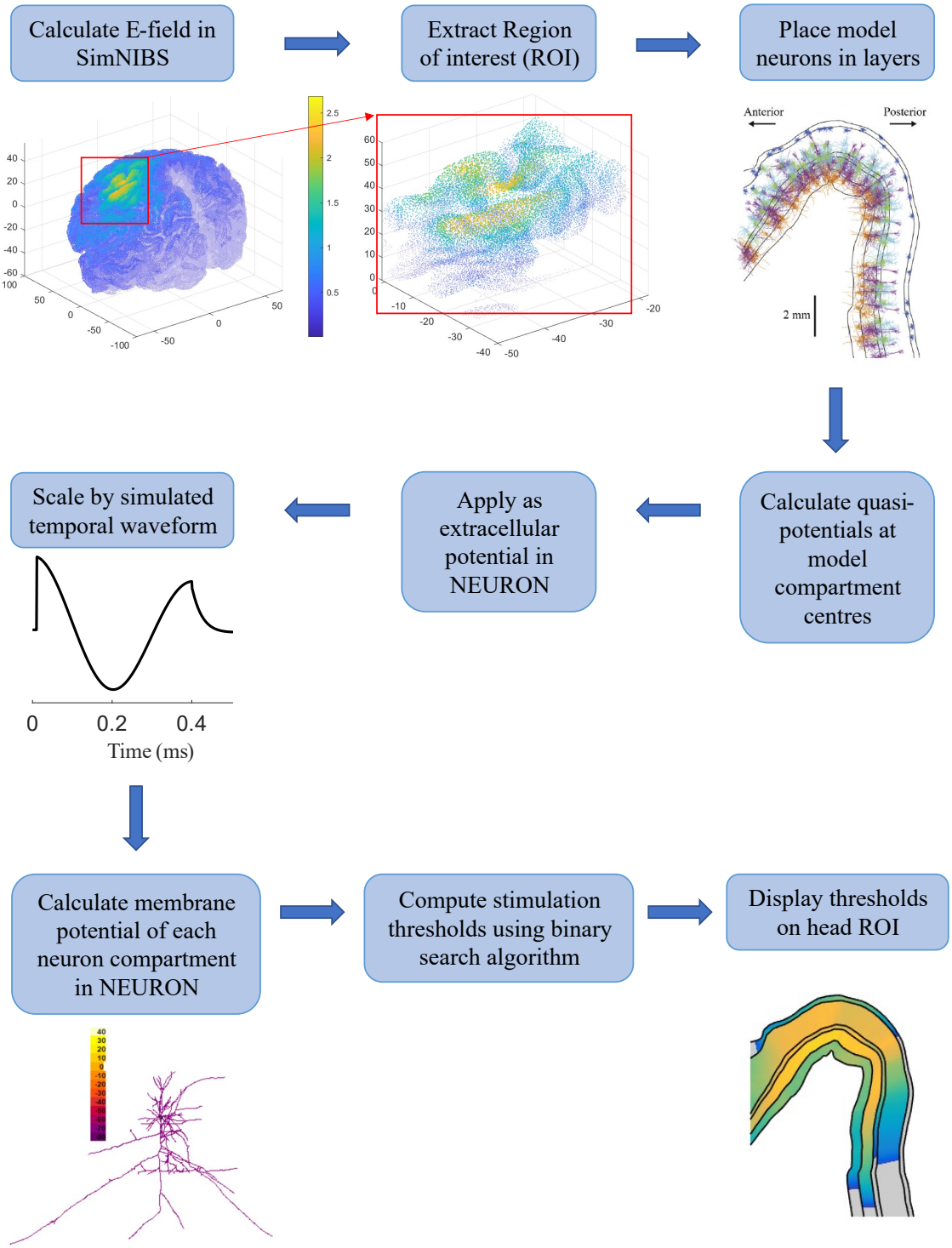

Figure 2.2: Flowchart summarising the workflow of the morphologically-realistic computational model from (Aberra 2019). Figures from (Aberra et al. 2020).

varying their morphologies stochastically to represent the diversity within each cell type (Aberra et al. 2018). The region of interest around the motor hand knob

was populated with 3000 neurons of each type. For this, the cell body of each neuron clone was centred within a surface element of its respective layer, aligning its somatodendritic axis with the element normal, and rotated randomly around its somatodendritic axis. Additional rotations could be included for each neuron model as demonstrated in (Aberra et al. 2020), however, to reduce the computational time, only one orientation was included here. From the results presented in (Aberra et al. 2020), the impact of this simplification could be estimated as changing the median thresholds of the different neuron models on average by less than 1%.

2.2.3.2 Spatial component of electric field

The spatial component of the electric field was calculated on the example data set of a healthy subject in SimNIBS (Thielscher et al. 2015) as in (Aberra et al. 2020), using Equation 1.4 with conductivity values of the different tissue types as described in Section 1.1.1. Uncertainties in these values on the electric field were estimated to only have a small influence on the spatial pattern of the electric field, with a larger effect on the magnitude of the electric field. The main influence is likely from the white matter and grey matter conductivities, causing an uncertainty in the electric field magnitude of less than 5% in the gyral crown and about $20 - 25\%$ in the sulcal walls (Saturnino et al. 2019).

To compare the different stimulus waveforms, the electric field distribution of the Magstim 70 mm figure-of-8 coil (Magstim Company Ltd, UK), when positioned over the hand knob representation of the left primary motor cortex and oriented at 45° to the midline, was used for all simulations. The coil-to-scalp distance was set to 2 mm and the coil current's rate of change to $1 A/\mu s$. The primary induced current direction was set to posterior-anterior (PA) for monophasic waveforms and to anterior-posterior (AP) for biphasic waveforms according to experimental data showing lower motor thresholds in the hand muscle for these directions (Aberra et al. 2020) (Sommer et al. 2006).

2.2.3.3 Temporal component of electric field

The temporal waveforms in Fig. 2.1 were down-sampled with 5μs time steps and the amplitude was normalised by their peak voltage. They were then inserted into the model to scale the spatial distribution of the electric field over time.

2.2.4 Data analysis

To compare the effects of different stimulation waveforms in the morphologically-realistic model, all parameters, including the spatial distribution of the electric field, were kept constant, while the temporal component of the electric field was varied according to the specific device, pulse waveform and current direction. The data analysis was conducted using the functions available in the GitHub repository of the computational model (Aberra 2019). This includes an estimation of the cortical region that represents the first dorsal interosseous muscle in the right hand and the visualisation of a 2D cross-section of the crown of the pre-central gyrus. Using this, the median thresholds for each waveform and current direction were compared across each cortical layer. Additionally, linear regression was used to quantify the relationship between the activation thresholds for each device for the same waveform type and current direction and correlations between the Magstim pulses and their PWM equivalents were computed.

2.3 Results

Fig. 2.3 shows the expected change in membrane potential for the different waveforms as estimated using the leaky integrate-and-fire model. The stimuli generated by the Magstim devices elicit a smooth change in membrane potential, while the pTMS stimuli elicit a response that approximates this, albeit not perfectly (Fig. 2.3 (c) and (d)).

The morphologically-realistic model was used to investigate if the deviations in membrane potential between the PWM and conventional waveforms affect the stimulation thresholds when taking into account the non-linear behaviour

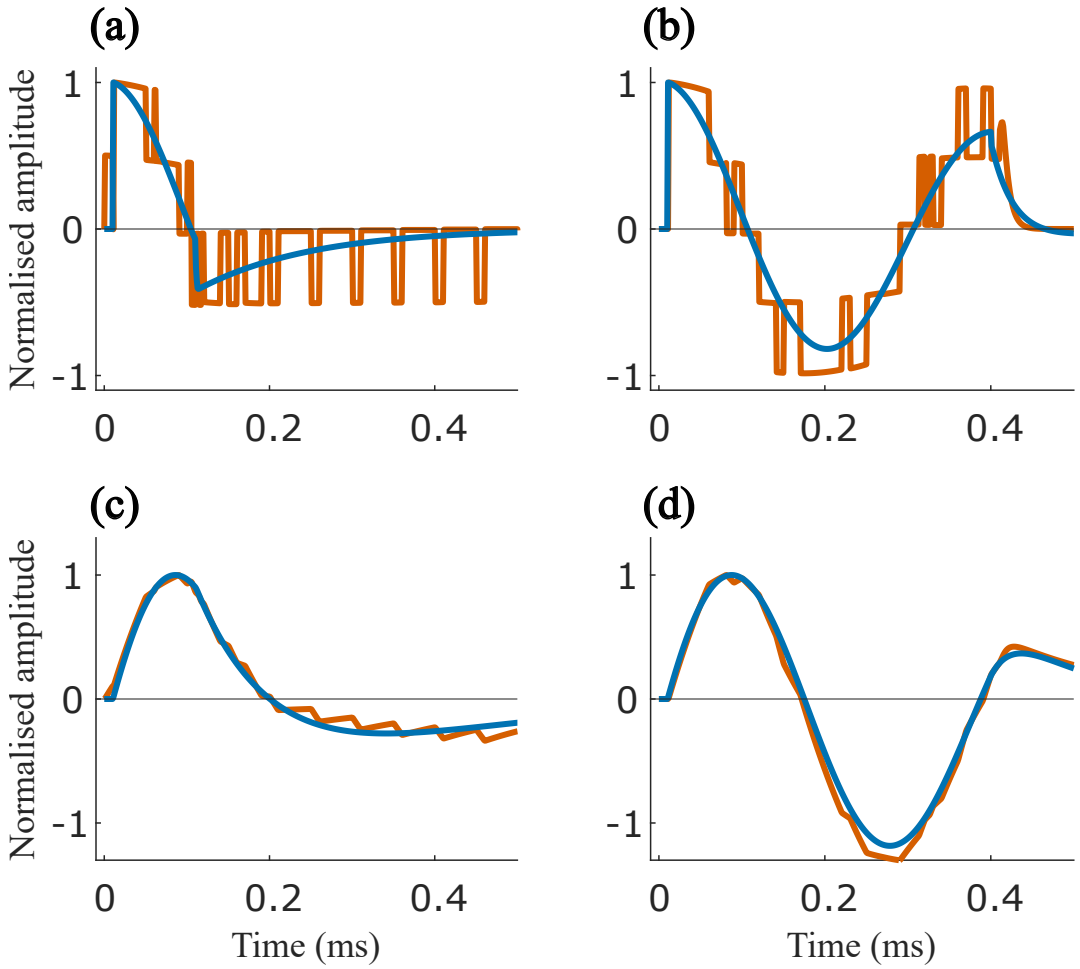

Figure 2.3: The TMS pulse shapes and membrane potential estimated by the leaky integrate-and-fire model. The simulated TMS pulses as generated by **(a)** a Magstim 200 and **(b)** a Magstim Rapid^2 are shown in blue with their PWM approximations from the programmable TMS shown in orange. The expected change in membrane voltage of a neuron is shown when **(c)** the monophasic and **(d)** the biphasic pulses are applied.

observed in neurons as well as the spatial component of the induced electric field. Fig. 2.4 (a) i-iv displays the median excitation thresholds for waveforms generated by conventional Magstim stimulators across the 2D cross-section of the pre-central crown for monophasic PA and AP stimulation and biphasic AP and PA stimulation, respectively. Fig. 2.4 (b) i-iv shows the median thresholds for the corresponding pulse-width modulated pulses generated by the pTMS device. The thresholds from the two devices differed from $7.6 - 87 A/\mu s$, which corresponds to $8.6 - 14.6\%$ for different neurons (Fig. 2.4 (c)), with the thresholds for the monophasic stimuli differing uniformly across all neurons in the different layers

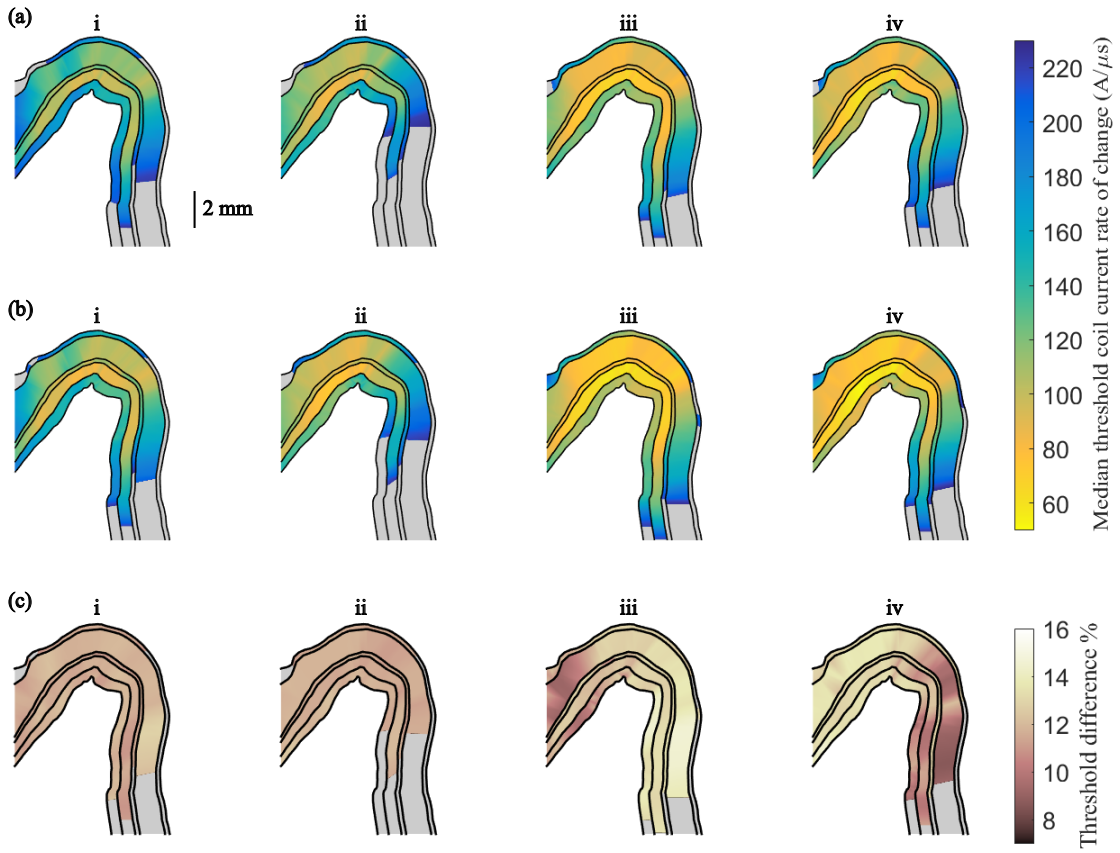

Figure 2.4: The median thresholds of the change in coil current for the six cortical layers are shown on a 2D cross-section of the crown of the pre-central gyrus on a plane parallel to the stimulation coil orientation. **(a)** shows the thresholds for the pulse waveforms from the Magstim devices for i. monophasic stimulation in the PA direction, ii. monophasic stimulation in the AP direction, iii. biphasic stimulation in the AP direction and iv. biphasic stimulation in the PA direction. **(b)** shows the thresholds for 5-level pulse-width modulated approximations of each of the pulses in (a). The thresholds are given in $A/\mu s$ and thresholds above $230A/\mu s$ are displayed in grey. **(c)** shows the percent difference in median thresholds between the conventional and pulse-width modulated pulses.

(standard deviation $< 0.5\%$).

To investigate the individual cortical layers in more detail, Fig. 2.5 shows the activation thresholds of each layer within the cortical area approximating the hand muscle representation for each stimulus waveform and current direction. Each boxplot includes the data from the five neuron clones within the relevant layer with the outliers excluded. Overall, the activation thresholds for biphasic stimuli (Fig. 2.5 (b)) were lower than for monophasic stimuli (Fig. 2.5 (a)). Additionally, monophasic stimuli had lower thresholds when applied in the posterior-anterior current direction, while biphasic stimuli had lower thresholds when their initial

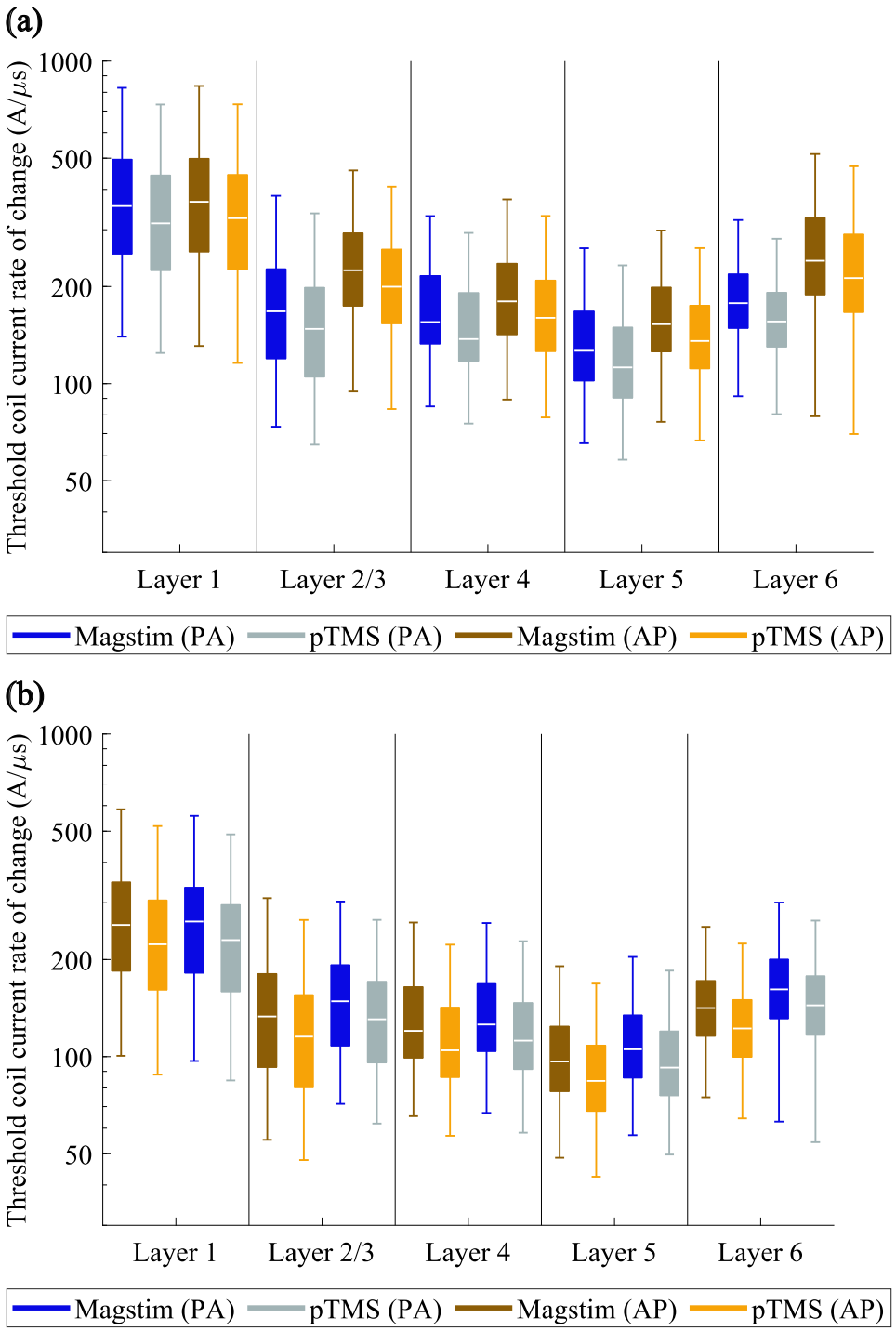

Figure 2.5: Comparison of modelled neural activation thresholds within the cortical area representing the hand muscle. The modelled thresholds for the conventional TMS devices and the programmable TMS are shown in log scale for **(a)** monophasic stimuli and for **(b)** biphasic stimuli for the posterior-anterior (PA) and anterior-posterior (AP) direction of the primary current in each layer. Each boxplot includes the data from five clones with the outliers removed.

current direction was in the anterior-posterior direction.

To quantify the relationship between the thresholds for the different stimulation devices, Fig. 2.6 shows the threshold of each neuron in the hand muscle representation for Magstim pulses (abscissa) and pTMS pulses (ordinate) for monophasic (i-ii) and biphasic pulses (iii-iv). Linear regression revealed a strong correlation ($r^2 > 0.998, p < 0.001$) between the thresholds of the two stimulation devices for all waveforms and current directions. The slopes of the lines of best fit were between 0.883 and 0.891. This analysis was repeated for the entire neuron population used in the model, which showed an equally strong correlation. Additionally, thresholds were estimated from the leaky integrate-and-fire model for monophasic PA pulses and biphasic AP and PA pulses (not monophasic AP pulses since the negative phase of the monophasic pulses is not expected to contribute to neuron activation). Fig. 2.6 shows that these threshold estimates approximated the linear regression lines from the morphologically realistic models closely with a membrane time constant of $150\mu s$. Using the upper estimate of the membrane time constant (around $300\mu s$ (Siebner et al. 2022)) results in a maximum change in the relative thresholds between Magstim and pTMS pulses of 4% compared to the lower limit of $150\mu s$.

2.4 Discussion

This chapter directly compares the modelled effects of TMS on cortical neurons using PWM versus conventional TMS using damped cosine pulses. The results indicate that the PWM pulses approximate the neural activation by conventional pulses very closely. The uniform difference observed in the activation thresholds and the slope of the linear regression lines suggest that the energy required to stimulate a desired neuron population is lower for the PWM pulses than for the Magstim pulses used here. In particular, for the monophasic stimuli, the thresholds differed uniformly across all neurons in the different layers. This suggests that decreasing the stimulation intensity of the programmable TMS device by around 11% should achieve an equivalent neural response to the Magstim 200. The difference in thresholds for the biphasic pulses was less uniform, which may partially be due to the balancing between the positive and negative phases of the pulses. Before

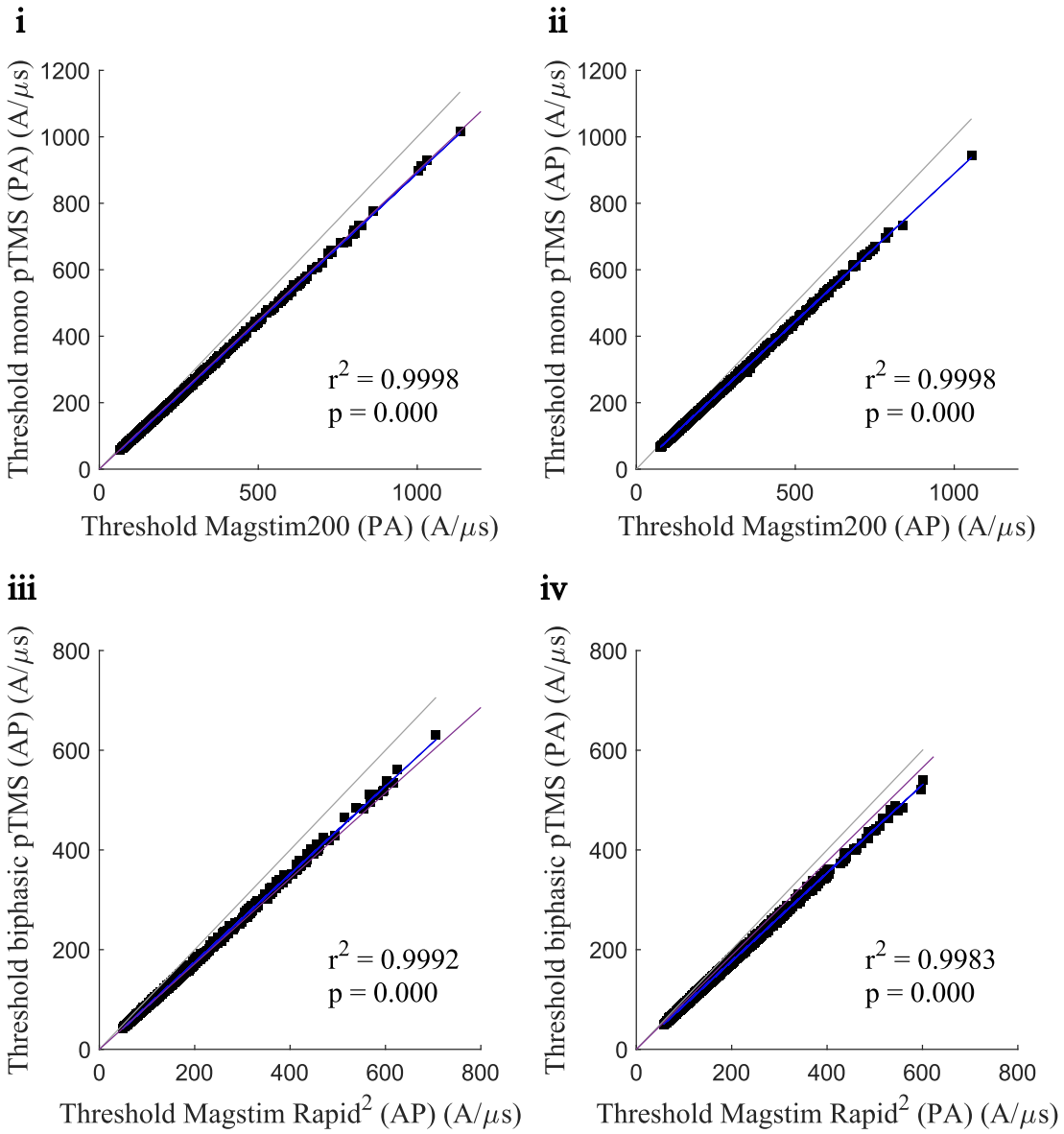

Figure 2.6: Correlation between the threshold coil current rate of change for Magstim pulses and their pulse-width modulated equivalents. The thresholds for the pTMS pulses are plotted against the thresholds for their Magstim references for **i.** the monophasic stimuli in the posterior-anterior direction, **ii.** the monophasic stimuli in the anterior-posterior direction, **iii.** the biphasic stimuli in the anterior-posterior direction and **iv.** the biphasic stimuli in the posterior-anterior direction. The linear regression is displayed in blue and the threshold estimate from the LIF model in purple for each waveform and current direction.

being used in the model, the pulses were normalised by their peak voltages, however, for the biphasic pulses this did not result in a perfectly matched amplitude in the second phase of the pulse. Alternatively, the waveforms of the different stimulators could for example be normalised by the area under the curve.

Furthermore, the activation thresholds for different waveforms depend on the coil orientation. The results showed that the monophasic stimuli had lower thresholds when applied in the posterior-anterior current direction, while biphasic stimuli had lower thresholds when their initial current direction was in the anterior-posterior direction, due to their dominant second phase. This agrees with the results of previous computational and experimental studies of the motor threshold using the MagPro stimulators and coils (Aberra et al. 2020) (Sommer et al. 2006).

2.5 Limitations

In this chapter, stimulation pulses generated by resonance-based and PWM-based architectures were compared under ideal conditions. The head model, the stimulation coil, as well as all other parameters within the model, were kept constant while the temporal waveform was varied. It should be noted that variables other than the shape of the waveform have a large impact on the neural response to stimulation. For instance, the type of stimulation coil heavily influences the spatial distribution of the induced electric field (Deng et al. 2013). Even two coils of the same type but from different manufacturers may have different properties which must be considered when comparing the effects of different stimulus waveforms. In practice, any differences shown here between the threshold effects are likely to be obscured by the inherent variability of TMS effects. Furthermore, while this study only looks at one example brain from the SimNIBS database, the effects of TMS may vary between individuals, and this analysis should be validated using head models of different individuals. Additionally, the models used in this chapter focussed on the electrophysiology of individual neurons and did not consider the effects of the stimulation pulses on non-neuronal elements such as glial cells, mechanical changes in neurons such as membrane deformation during depolarisation or any interaction between neurons. Thus, further investigations into these aspects are required to fully understand any differences between PWM and conventional pulses.

2.6 Conclusions and contributions

In this chapter, computational modelling was used to evaluate pulse-width modulated TMS pulses, establish trade-offs with conventional pulses and guide the stimulator design. For this, morphological neural models integrated with transcranially induced electric fields were used to directly compare the neural response to PWM TMS versus conventional TMS pulses. For both monophasic and biphasic stimulus waveforms, the effects of the different pulse types were shown to be highly correlated. This demonstrates that PWM pulses can approximate the conventional resonance-based pulses well, even though the introduced switching frequencies are only expected to be partially removed by the low-frequency filtering of the neurons. This suggests that the pulse synthesis of the pTMS device is sufficient with existing device components, although an increase in the switching frequency e.g. with silicon-carbide semiconductors may improve this further. The validation of these results under practical conditions, by measuring the motor response of human participants in the next chapter, is essential to pave the way to explore new stimulation parameters and patterns using the pTMS architecture in the future.

3

In-human validation of the model and programmable TMS

Contents

The work presented in this chapter has been published in the following journal paper:

Sorkhabi, M. M., **Wendt, K.***, O'Shea, J., and Denison, T. (2022). "Pulse width modulation-based TMS: Primary motor cortex responses compared to conventional monophasic stimuli.", Brain Stimulation 15.4, pp. 980–983*

*Joint first authors

3.1 Introduction

The modelling study in the previous chapter showed that the stimulation thresholds of pulse-width modulated TMS pulses were highly correlated with the thresholds of conventional pulses. Following these results, the next step was to validate the model and the pTMS device by comparing stimulation effects in a study with healthy human participants. For this, I used the pTMS to approximate conventional single-pulse monophasic TMS and assessed the comparability of the effects of both pulse forms on different physiological measures using motor evoked potentials.

The resting motor threshold and the MEP latency are both measures derived from single-pulse TMS that can be used to compare the effects of different pulse shapes. Biphasic pulses have been shown to have a lower motor threshold and a shorter MEP latency than monophasic pulses (Kammer et al. 2001) (Sommer et al. 2006) while smaller pulse widths tend to have higher RMTs and longer latencies (Halawa et al. 2019). The direction of the current induced in the brain is another factor affecting the motor response (D'Ostilio et al. 2016), where the more effective direction of current flow has been shown to be opposite for monophasic and biphasic stimulation (Di Lazzaro et al. 2001a) (Sommer et al. 2006). Additionally, the peak-to-peak amplitude of the MEPs in response to a single TMS pulse can be used to measure excitability. However, as MEPs are very variable, a more reliable measure is given by the input-output curve which measures the amplitude of the MEPs over a range of stimulus intensities. When fitting a sigmoid curve to the MEP amplitude measurements, the slope of the input-output curve can be used to compare different stimulation pulses across a range of individualised excitability levels (D'Ostilio et al. 2016).

The aim of this study was to acquire physiological data to establish cross-validation of the findings from the previous modelling Chapter 2 in humans.

3.2 Methods

3.2.1 TMS devices

In this study, a commercial Magstim 200 and the pTMS device were used to generate single pulses. The monophasic pulse generated by the Magstim 200 was approximated using the pTMS device as previously shown in Fig. 2.1(a) and (b). Both devices were connected to the same 70 mm figure-of-eight coil (Magstim Co., P/N 9925e00). The positive peak coil voltage of the pTMS device was compared with the Magstim device to calibrate the stimulation intensity between the two devices and all intensities are reported relative to the maximum stimulator output of the Magstim 200.

3.2.2 Participants

Twelve healthy participants (mean age: 28.6 years, range: $22-37$ years; 4 male) were recruited to participate in the study which was approved by the Central University Research Ethics Committee (CUREC), University of Oxford (R75180/RE002). The sample size was chosen to match the first-in-human studies using the cTMS device, such as in (Peterchev et al. 2014) (D'Ostilio et al. 2016). All participants were right-handed as assessed by the Edinburgh Handedness Inventory (Oldfield 1971), an inclusion criterion in order to avoid variance caused by hemispheric differences between left- and right-handers. Further, participants were included if they were healthy, between the ages of 18 and 45 years and fluent in English. Exclusion criteria were developed based on international safety guidelines (Rossi et al. 2021) and consisted of any current significant medical condition, including epilepsy, multiple sclerosis or migraines, any previous or current psychiatric illness, intake of any medication except the contraceptive pill, pregnancy or breastfeeding, or any other contraindication to TMS such as a family history of epilepsy or a metallic implant (see Appendix A.2 and A.3 for detailed inclusion and exclusion criteria). After reading the study information, having their questions answered, and passing the safety screening, participants gave written informed consent.

3.2.3 Protocol

Fig. 3.1 (a) shows an overview of the data collection during the visit (see Appendix A.1.1 for the step-by-step protocol). For each participant, conventional and PWM stimuli were applied using the Magstim stimulator and pTMS devices, respectively, in counterbalanced order. The participants were seated in a chair with their arms resting on a pillow on top of a table in front of them. The coil was held by the operator, positioned over the left primary motor cortex and oriented at 45° to the midline with the handle pointing posteriorly (Fig. 3.1 (b)). At the beginning of each session, the motor hotspot was determined with the Magstim stimulator, defined as the optimal scalp position where MEPs could be elicited in the right first dorsal interosseous (FDI) muscle. To find the motor hotspot, the pulse timing and delivery were controlled by the experimenter using the foot pedal. Then, to confirm the hotspot, and to also measure the RMT and the IO curve, the pulses were applied automatically via scripts in Signal version 7.01 (Magstim device) and Control desk (pTMS device) software at varying inter-pulse intervals between 4.25 to 6 seconds.

Electromyography

Electromyography was recorded from the FDI of the right hand by positioning disposable neonatal ECG electrodes in a belly-tendon montage (see Fig. 1.6), with the ground electrode over the ulnar styloid process. The EMG signals were recorded using a D440 Isolated Amplifier (Digitimer, Welwyn Garden City, UK), a Micro1401 (Cambridge Electronic Design, Cambridge, UK), a Digitimer HumBug Noise Eliminator and Signal version 7.01 (Cambridge Electronic Design), with a 16-bit resolution at a 10 kHz sampling rate, an amplifier gain of 1000 and a $10-1000$ Hz filter. The HumBug Noise Eliminator attenuates the unwanted 50 Hz line noise by subtracting a replica of the measured noise from the input signal without filtering.

Neuronavigation

A Brainsight neuronavigation system (Rogue Research Inc., Montreal, Canada) was used to track the position and orientation of the coil to maintain consistent

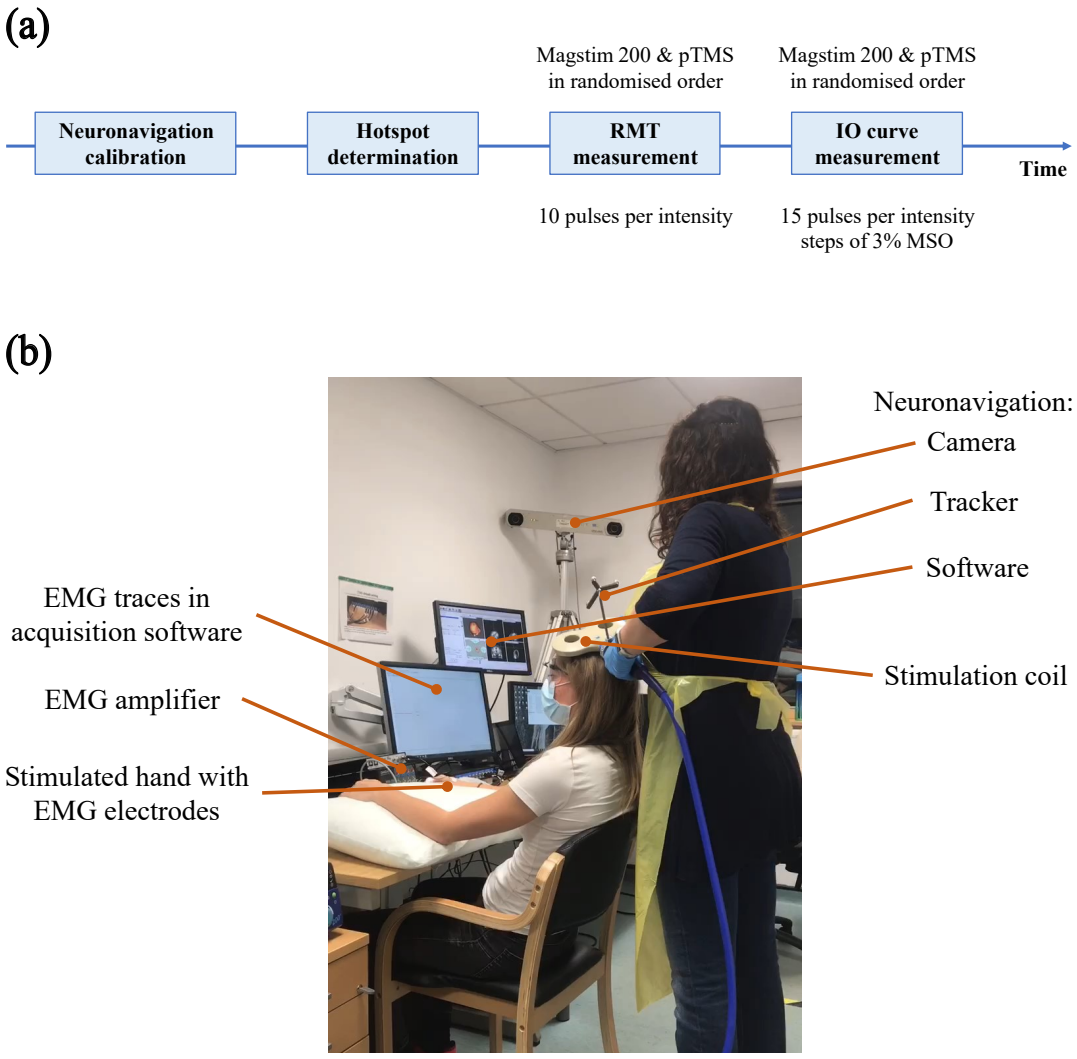

Figure 3.1: Overview of study design and setup. **(a)** Overview of the workflow during the study visit. First, the neuronavigation was set up and calibrated to the participant's head. Next, the hotspot was determined and the resting motor threshold measured for each device in randomised order, counterbalanced across participants. Finally, input-output (IO) curves were measured for each device in randomised order by applying 15 pulses per intensity and increasing the intensity in steps of 3% of the maximum stimulator output (MSO). Panel **(b)** shows the physical setup in the lab, including the electromyography (EMG), the neuronavigation and the positioning of the TMS coil.

placement. Neuronavigation (also called frameless stereotaxy or image-guided TMS) utilises an optical camera to track three reflective spheres attached to the participant's head and the stimulation coil in real time (Fig. 3.1 (b)). It then references the location of these spheres to an average head model which is scaled to the size of the participant's head using landmarks which are identified during the setup. Individual participants' MRI data can be loaded into the software to

guide the stimulation, however, this study targeted the motor cortex which is easily identifiable by eliciting a twitch in the target muscle, thus it was sufficient to use the average head model. The location of the motor hotspot was saved in the software which helped the operator to stay on target throughout the session and therefore reduces errors through coil movement.

Resting motor threshold

To determine the RMT, 10 pulses were applied at each intensity and the EMG traces were inspected visually in real time. The stimulator outputs were adjusted manually to determine the minimum intensity required to evoke an MEP of ≥ 50 µV peak-to-peak amplitude in 5 out of 10 consecutive trials.

Input-output curves

For the IO curve, 15 MEPs at each intensity up to the maximum voltage achievable by the pTMS device were measured. The stimulation intensities can be delivered in randomised, increasing or decreasing orders, the choice of which may affect the resulting IO curve (Möller et al. 2009). Similar to other recent work (Sommer et al. 2018), TMS stimuli were applied in increasing order from low to high intensities in steps of 3% of the maximum stimulator output of the Magstim 200. This fixed order of stimulation, rather than randomised intensities, was chosen to compare the devices because the intensity of the pTMS device needs to be adjusted manually. The coil was lifted from the participants' heads during 1-min rest blocks between each set of stimuli, introduced because breaks longer than 20 seconds between stimulation blocks have been shown to minimise hysteresis effects (Pearce et al. 2013) (Möller et al. 2009).

MEP measurements below 0.02 mV were set to 0.02 mV, as this was the lowest amplitude that was distinguishable from EMG signal noise. The data were log-transformed, similar to (D'Ostilio et al. 2016), to normalise the MEP amplitude distribution (Pasqualetti et al. 2011). The `curve_fit` function in the `scipy` package in `Python`, which employs a non-linear least-squares curve fitting approach, was

used to fit a Boltzmann sigmoid to the data for each participant for each device. The Boltzmann equation is given by:

$$y = \frac{y_{high} - y_{low}}{1 + \exp\left(\frac{V_{midpoint} - V_{pulse}}{K}\right)} + y_{low} \tag{3.1}$$

where y is the log-transformed peak-to-peak MEP amplitude, V_{pulse} is the TMS pulse amplitude as a percentage of the maximum stimulator output, y_{low} is the lowest MEP amplitude considered, y_{high} is the maximum MEP amplitude value, $V_{midpoint}$ is the stimulus intensity where the MEP amplitude is halfway between y_{low} and y_{high} and K is the slope parameter (Möller et al. 2009). y_{low} was set to $log_{10}(0.02)$ to constrain the minimum of the curve to the lowest amplitude distinguishable from noise for all curves. The inverse of the slope parameter K was used to compare the maximal steepness of the curves at $V_{midpoint}$ (Devanne et al. 1997) since previous studies reported that the stimulus shape affects the slope of the IO curve at the midpoint (Sommer et al. 2018) (D'Ostilio et al. 2016). For two of the participants, who had a high threshold, the plateau value for the IO curves could not be reached. These participants were therefore excluded and the IO curve analysis was conducted for the remaining 10 participants.

MEP Latencies

The EMG recordings for the input-output curves were also used to calculate the MEP onset latencies, defined as the time point after the TMS artefact where the EMG signals surpass $0.035mV$. This threshold allowed consistent detection as verified by visual inspection and resulted in comparable latencies as in previous studies (D'Ostilio et al. 2016). Since latencies vary with MEP amplitude (Vallence et al. 2023), latencies were measured separately for MEPs with peak-to-peak amplitudes of $500\mu V \pm 20\%$ and $1mV \pm 20\%$. The latencies were then averaged for each participant and TMS device.

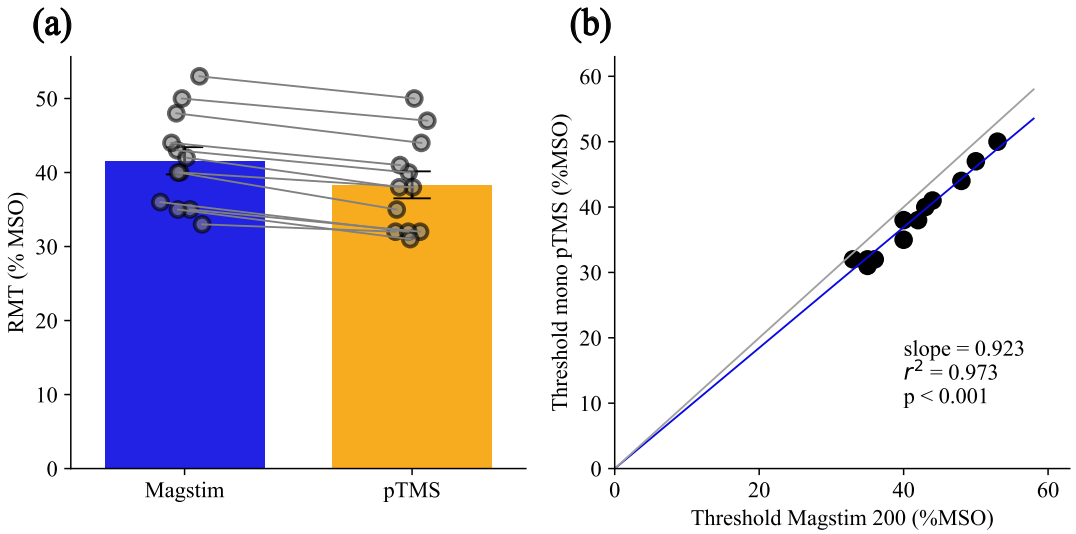

Figure 3.2: Comparison of resting motor thresholds between the pTMS and Magstim devices. **(a)** The thresholds for the Magstim pulse (in blue) were consistently higher than the thresholds for its pulse-width modulated equivalent pTMS pulse (in orange) across participants. The bars and whiskers show mean and standard error, respectively, with individual data points overlaid in grey. **(b)** The thresholds for the pTMS pulse are plotted against the thresholds for the Magstim pulse. The linear regression is displayed in blue and a line with a slope of 1 in grey for comparison. MSO: Maximum stimulator output

3.2.4 Statistical analysis

Resting motor thresholds, input-output curve slopes and latencies were compared using paired t-tests with a significance level of 0.05. Since significant differences between the RMTs of the two devices were found, linear regression was additionally used to compare the resting motor thresholds for each device and their correlation was computed.

3.3 Results

3.3.1 Motor thresholds

The RMTs, expressed as a percentage of the equivalent Magstim maximum stimulator output, were $41.58 \pm 6.10\%$ (mean $\pm$ standard deviation) for the Magstim pulse and $38.33 \pm 6.05\%$ for pTMS stimuli (Fig. 3.2 (a)). The RMTs differed significantly between devices ($t(11) = 10.67, p < 0.001$). Notably, for all participants, the RMT for PWM pulses was approximately 3% MSO lower than for the monophasic Magstim pulses. Linear regression showed a strong correlation between the thresholds of

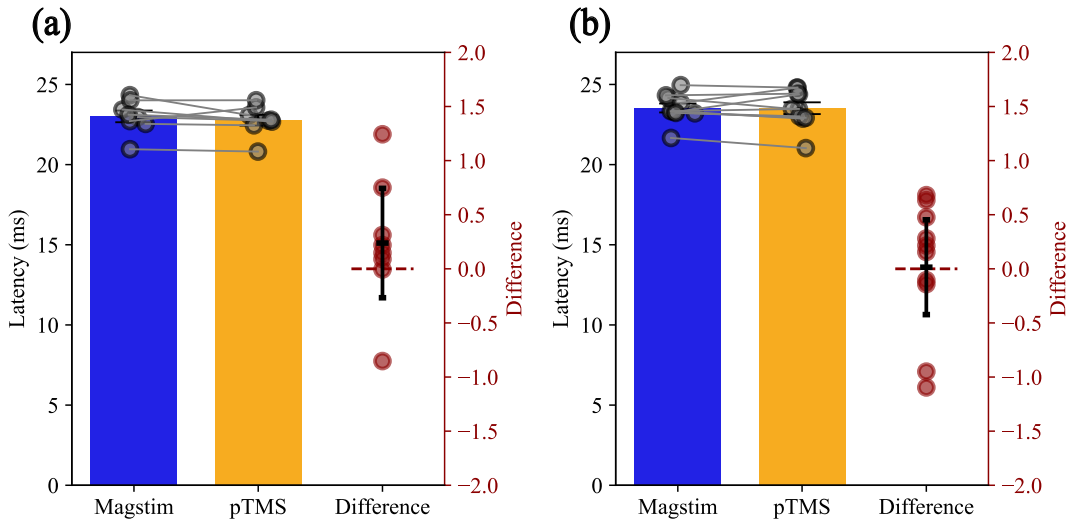

Figure 3.3: Comparison of MEP onset latencies. Average MEP latencies were calculated for **(a)** $1m$V and **(b)** 500μV peak-to-peak MEP amplitudes. The bars and whiskers show mean and standard error, respectively, with individual data points overlaid in grey. The difference between the latencies of the pulses from the pTMS and Magstim device are shown in red for each participant with the group mean and 95% confidence interval overlaid in black.

the two devices ($r^2 = 0.973, p < 0.001$) with a slope of the line of best fit of 0.977 (Fig. 3.2 (b)), which is consistent with the trend suggested by the modelling results in Chapter 2.

3.3.2 MEP latencies

The mean and individual MEP latencies are shown in Fig. 3.3 (a) for MEPs with peak-to-peak amplitudes of $1m$V ±20% and (b) for MEPs with amplitudes of 500μV ±20%. In each plot, the blue bar represents the mean latency for the Magstim pulses, while the orange bar represents the mean latency for the pTMS pulses. The latencies did not differ significantly between the devices for $1m$V MEPs ($t(7) = 1.114, p = 0.302$), or for 500μV MEPs ($t(9) = 0.077, p = 0.941$).

Additionally, the difference between the latencies of the two devices was inspected, which is shown on the right of each plot in Fig. 3.3. In line with the non-significant result from the t-tests, the difference between the latencies was small with a mean difference and standard deviation interval of 0.238 ms ±0.604 ms for the $1m$V MEP latencies and 0.015 ms ±0.612 ms for the 500μV MEP latencies.

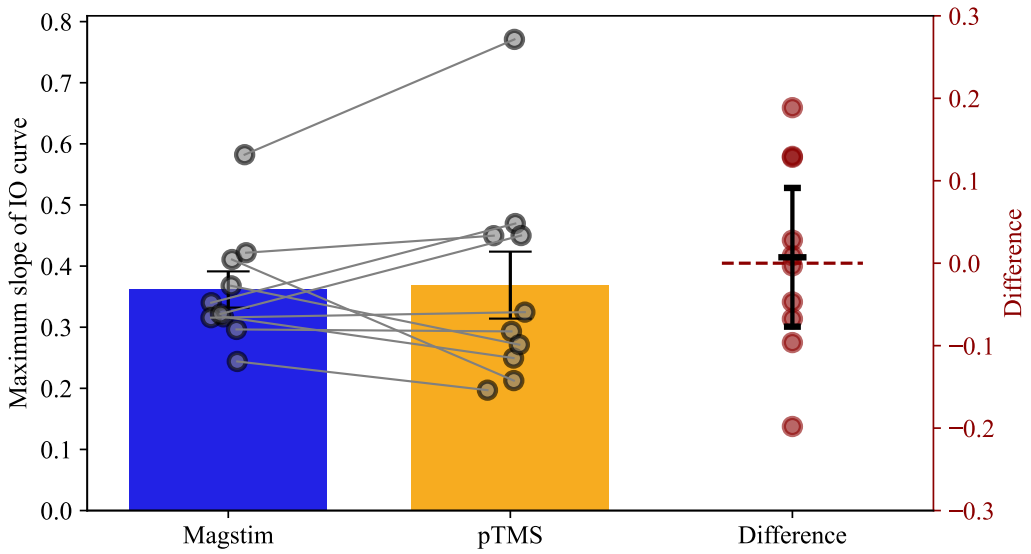

Figure 3.4: Comparison of input-output curve slopes. The bars show the mean slope of the IO curve for the Magstim pulses in blue and the mean slope for the pTMS pulses is in orange. The whiskers show the standard error and individual data points are overlaid in grey. The difference between the slopes for the pulses from the pTMS and Magstim device are shown in red for each participant with the group mean and 95% confidence interval overlaid in black.

3.3.3 Input-output curves

Fig. 3.4 shows the slopes of the input-output curves for both TMS devices and Fig. 3.5 shows the fitted IO curves of each participant. A paired t-test showed that the slopes were not significantly different between devices ($t(9) = 0.19, p = 0.85$), which is also evident from the distribution of the difference between the slopes shown on the right of Fig. 3.4. The mean difference was 0.007 and the standard deviation interval was ± 0.118.

3.3.4 Side effects

No adverse events occurred during or after the stimulation. After the experiment, participants were asked to verbally report any differences they noticed between stimulation with the two devices. Participants did not report any subjective difference in experience, apart from a difference in the sound during pulse firing that was reported by all participants, which is likely due to the high-frequency harmonics arising from the pulse-width modulation in the pTMS device. An output

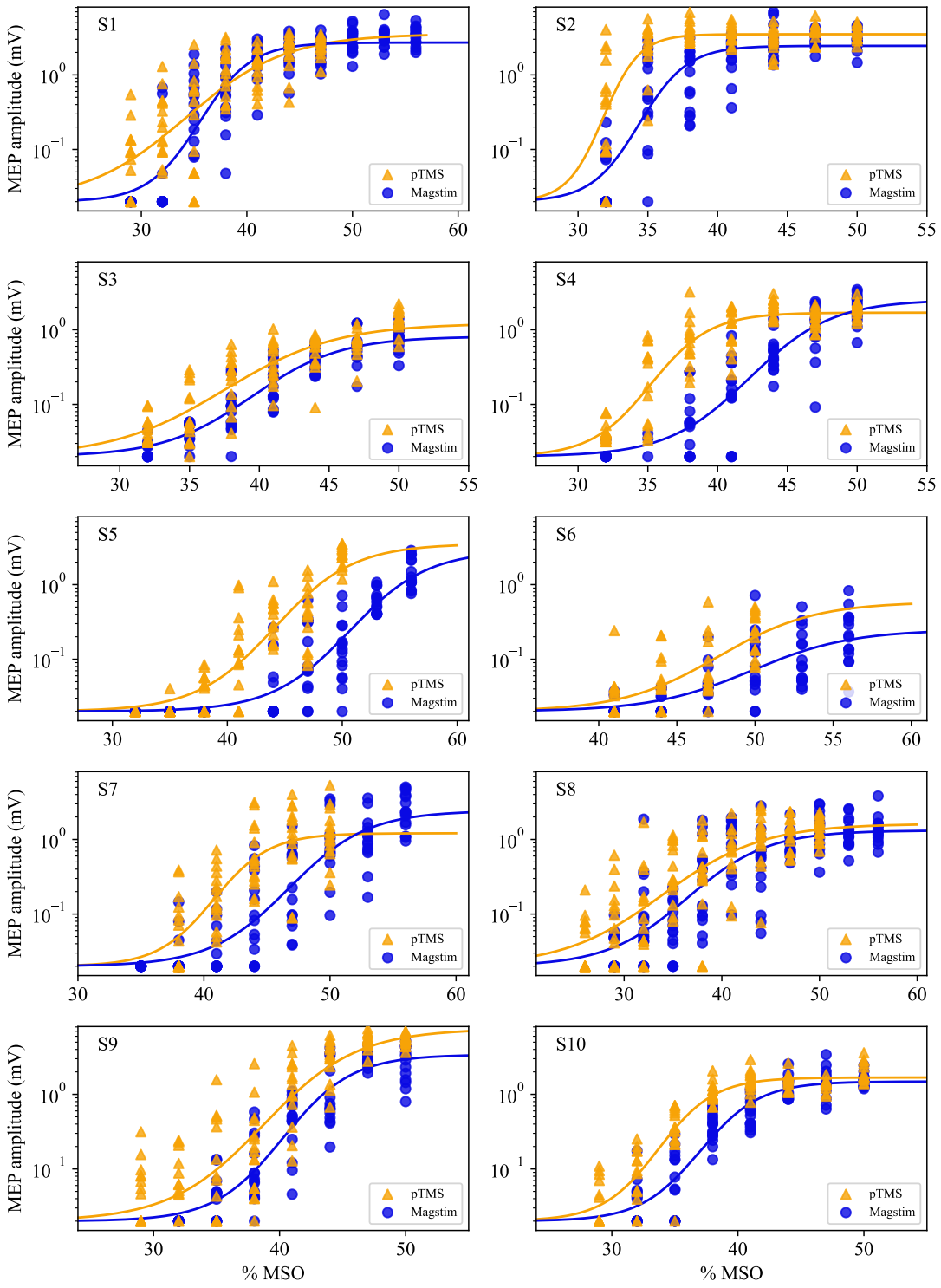

Figure 3.5: Individual input-output curves. The markers show the measured peak-to-peak amplitude of individual MEPs as a function of the TMS pulse intensity. The pTMS data is shown in orange triangles, and the Magstim data in blue circles. The lines show the best-fitting Boltzmann sigmoid function. MSO: Maximum stimulator output

filter which reduces the high-frequency components in the stimulation pulse may rectify this difference to some extent (see Section 6.3).

3.4 Discussion

In this study, both the computational model from Chapter 2 and the pTMS device itself were validated in comparison with a conventional stimulator in healthy human volunteers. The results showed a strong correlation between the motor thresholds of the two devices, suggesting that the peak coil voltage required to activate the neuron population responsible for the FDI movement is systematically lower for the pTMS device than for the Magstim 200. The observed difference in RMT may be related to the sharp edges and higher amplitude in the negative phase of the PWM pulses. Another study using rectangular pulses has reported a similar result of less energy being required to activate neurons (Goetz et al. 2016). In practice, this translates to lower peak intensities required to activate the same neuron population when using the pTMS device.

Consistent with the motor threshold results, the fitted curves for the pTMS pulses were shifted to the left, i.e. at lower stimulus intensities than for the Magstim pulses. No significant differences in input-output curve slopes or latencies were detected between the PWM and conventional stimuli which was confirmed by inspection of the distribution of the difference measured by the devices.

3.5 Limitations

PWM-based TMS pulses promise more flexibility in pulse generation but require further evaluation before routine use in research or clinical settings. Future studies should include additional physiological measurements such as electroencephalography or magnetic resonance imaging and larger sample sizes. The pTMS device is currently limited to lower stimulation amplitudes than the Magstim 200 for the pulse width used here, which precluded data collection from individuals with very high thresholds. The maximum pulse amplitude of the pTMS was 1600 V,

compared to the maximum outputs for the Magstim Rapid^2, MagVenture MagPro, and Magstim 200 which are approximately 1650, 1800 and 2800 V, respectively (Goetz et al. 2016). Furthermore, as the intensity of the pTMS device is adjusted manually, it is difficult to randomise stimulation intensities which may lead to hysteresis effects. To minimise this risk, stimuli were delivered in random intervals and participants had at least one-minute rest between each set of stimuli (Pearce et al. 2013). Additionally, measurements of the auditory signature are necessary for future comparison of residual artefacts.

3.6 Conclusions and contributions

In this chapter, the pTMS device was compared to a conventional stimulator and the computational model in the previous chapter was validated by applying TMS pulses to healthy participants. Similar to the results of the computational modelling study, the motor thresholds for the PWM stimuli were highly correlated to the thresholds for the Magstim device and consistently lower across participants. Additionally, the measured motor responses suggested no difference in MEP latencies or IO curve slopes between the devices. These results present the first-in-human tests of the pTMS device and give confidence that it can stimulate cortical neurons with similar effects to conventional stimulators, validating the low-pass filtering assumptions underlying the use of PWM in TMS. This allows us to move on to testing new stimulation parameters with the pTMS.

4

The effect of pulse shape in theta burst stimulation

Contents

The work presented in this chapter has been published in the following journal paper:

Wendt, K., *Sorkhabi, M. M., Stagg, C. J., Fleming, M. K., Denison, T., and O'Shea, J. (2023). "The effect of pulse shape in theta-burst stimulation: Monophasic vs biphasic TMS". Brain Stimulation 16.4, pp. 1178–1185.*

4.1 Introduction

The previous two chapters focussed on the validation of the pTMS device by comparing it to a conventional stimulator. The novelty of the pTMS, however, does not lie in its ability to imitate currently used pulses but in the ability to generate stimulation pulses and protocols that were not possible with conventional TMS devices. In our first research studies using the new pTMS device to stimulate human participants, we needed to use existing stimulation parameters to ensure safety and to obtain ethical approval for the studies, which could then be followed by the careful introduction of new parameters. Therefore, in this chapter, the focus was on using existing stimulation pulses (approximated conventional TMS pulses) and applying them in a repetitive protocol called theta burst stimulation (TBS), which conventional stimulators are not able to generate with monophasic pulses due to their limitations in energy recovery. This specific protocol was chosen due to the routine use of its implementation using biphasic pulses in clinical practice in the treatment of major depressive disorder. Despite its use in clinics, the response is variable with a remission rate of about 32% after daily treatment for $4-6$ weeks (Blumberger et al. 2018). While this is encouraging considering that these patients are classified as treatment-resistant (i.e. did not respond to one or two antidepressant medication trials), improvements in the protocol to make it more effective would be desirable.

The effects of the protocol on corticospinal excitability were assessed on healthy participants and compared to the conventional biphasic version of the protocol.

Different stimulation waveforms have been shown to recruit different neural populations, have different excitation thresholds, and have different effects on corticospinal excitability (Aberra et al. 2020) (Sommer et al. 2002) (Sommer et al. 2006) (Arai et al. 2007) (Hannah et al. 2017) (Taylor et al. 2007). However, the range of stimulation pulses and patterns that can be generated by conventional TMS devices is limited by the device hardware and is usually confined to either monophasic or biphasic damped cosine pulses, where the exact shape and length of the pulse is determined by the resonance between the device components (Sorkhabi et al. 2020). For monophasic pulses, the current flow is commonly dampened halfway through the cycle of the cosine pulse by letting the current flow through a shunting diode and dissipating the energy through a resistor. This restricts not only the choice of TMS pulse waveforms and widths but also the achievable repetition rates (Peterchev et al. 2023). For example, one class of repetitive TMS protocols, widely used for plasticity induction in fundamental research and clinical applications, that is constrained by these hardware limitations, is theta burst stimulation. During TBS, bursts of 3 pulses are applied at 50 Hz and repeated every 200 ms (Huang et al. 2005). In intermittent (i)TBS, a largely excitatory protocol, these triplets are applied for 2 s followed by an 8 s break and then repeated again, for 600 pulses in total (Huang et al. 2005). To sustain these repetition rates, large amounts of energy need to be recovered after each stimulation pulse, and so TBS can usually only be delivered via a conventional TMS device using biphasic stimulation pulses.

Monophasic pulses are thought to more selectively recruit cortical neurons and have been shown to modulate cortical excitability more strongly than biphasic pulses when used in other repetitive TMS protocols (Rossini et al. 2015) (Arai et al. 2007) (Taylor et al. 2007) (Huang et al. 2017) (Nakamura et al. 2016). For example, in quadripulse stimulation (QPS), bursts of four pulses are applied at inter-stimulus intervals of 1.5-1250 ms, repeated every 5s over 30 min (Hamada et al. 2008). A study comparing the after-effects of monophasic and biphasic QPS found that monophasic QPS induced stronger and longer-lasting after-effects compared with biphasic QPS (Nakamura et al. 2016). Such findings lead to the hypothesis that applying TBS

with monophasic pulses may be more effective than existing biphasic TBS, and thereby may improve therapy protocols such as in the treatment of depression.

The pTMS device recovers energy effectively after each pulse, including for monophasic pulses, making the generation of monophasic TBS possible. Thus, in this study, the pTMS device was used to generate both monophasic and biphasic iTBS and the effects on motor corticospinal excitability of healthy volunteers were compared. The hypothesis was that monophasic iTBS would produce a larger plasticity effect, indicated by higher motor evoked potential amplitudes after iTBS, than biphasic iTBS. To control for intra- and inter-individual variability, the same stimulation was also applied to the vertex in a control condition.

4.2 Methods

4.2.1 Ethical approval

This study and the use of the pTMS device in this study were approved by the local ethics committee at the University of Oxford (Central University Research Ethics Committee, R75180/RE008). All participants gave their written informed consent prior to participating and were compensated for their time with £10/hr.

4.2.2 Participants

30 healthy volunteers (mean age: 24.5 years, range: $19-33$ years, 16 females) participated in one familiarisation session followed by three data collection sessions for this single-blind, within-participants crossover study. The inclusion and exclusion criteria were identical to Chapter 3, with all participants being right-handed as assessed by the Edinburgh Handedness Inventory (Oldfield 1971) and screened to rule out any current significant medical condition and any contraindication to TMS in line with international safety guidelines (Rossi et al. 2009) (see Appendix A.2 and A.3 for detailed inclusion and exclusion criteria).

4.2.3 Transcranial magnetic stimulation protocol

The iTBS intervention protocols were applied using the pTMS stimulator. The pulse waveforms generated by the pTMS stimulator were designed to closely approximate the conventional biphasic and monophasic pulses generated by a Magstim Rapid^2 and a Magstim 200, respectively, as verified computationally in Chapter 2. To measure the motor corticospinal excitability before and after iTBS, a Magstim 200 stimulator was used to generate monophasic single-pulse TMS to induce MEPs. A 70 mm figure-of-8 coil (Magstim Co., P/N 9925−00) was used to deliver all stimulation. Owing to coil overheating, for participants with resting motor thresholds (RMTs) above 43% of the maximum stimulator output (MSO) of the Magstim 200 (N = 3), two figure-of-8 coils were used. To ensure that the use of two stimulation coils did not influence the study results, the electric field generated by each coil was measured using a pick-up coil and judged to be comparable. Furthermore, during the sessions, one coil was only connected to the Magstim 200, which was used to measure all MEPs during the data collection, and the second coil was only connected to the pTMS stimulator, which was used to apply the iTBS protocol. The motor thresholds used to titrate the stimulation intensity were measured for each stimulator with their individual coils, ensuring no effective differences in stimulation intensity due to the coils. For all participants with lower thresholds, one coil was used throughout.

Prior to the three test sessions, there was an initial familiarisation session for participants naïve to TMS, where TMS was introduced to the participant and the hotspot and thresholds for the different pulse shapes and devices were found. The pTMS stimulator's maximum pulse amplitude is 1600 V, compared to the maximum amplitude of the Magstim Rapid^2 and Magstim 200, which are approximately 1650 and 2800 V, respectively (Sorkhabi et al. 2022). Therefore, to ensure the pTMS stimulator could generate iTBS at 70% of the RMT for both monophasic and biphasic pulses, individuals with RMTs above 47% MSO of the Magstim 200 were excluded from any further participation in the study (N = 3).

During the familiarisation and test sessions, participants were seated in a chair with their arms resting on a pillow on top of a table in front of them (Fig. 3.1

(b)). The 'motor hotspot' of the left primary motor cortex was defined as the scalp location over which the lowest TMS pulse intensity elicited MEPs in the relaxed first dorsal interosseous (FDI) muscle of the right hand (Fig. 1.6). For all TMS pulses, the coil was held by the operator and oriented at 45° to the midline with the handle pointing posteriorly, which results in a posterior-anterior current flow in the brain for the monophasic pulse. The direction of the biphasic pulse was reversed via the software, such that the direction of the dominant second phase of the pulse matched the current flow of the monophasic pulse (Fig. 4.1) (Aberra et al. 2020) (Sommer et al. 2006). A Brainsight neuronavigation system (Rogue Research Inc., Montreal, Canada) was used to record the motor hotspot and for continuous tracking to maintain the position and orientation of the coil. Surface electromyography (EMG) of the right FDI was recorded using disposable neonatal ECG electrodes (Kendall, Cardinal Health, UK) in a belly-tendon montage with a ground electrode over the ulnar styloid process. EMG signals were sampled at 10 kHz, amplified with a gain of 1000, filtered (10 Hz - 1000 Hz) and recorded using a D440 Isolated Amplifier (Digitimer, Welwyn Garden City, UK), a Micro1401 (Cambridge Electronic Design, Cambridge, UK) and Signal software version 7.01 (Cambridge Electronic Design). The unwanted 50 Hz line noise was attenuated by subtracting a replica of the measured noise from the input signal using a HumBug Noise Eliminator (Digitimer).

The RMT, defined as the minimum intensity required to evoke an MEP of $\geq 50\mu$V peak-to-peak amplitude in 5 out of 10 consecutive trials, was determined by applying 10 pulses at each intensity and inspecting the EMG traces visually in real time for each device and pulse shape. To find the RMT, the pulses were triggered automatically via scripts in Signal version 7.01 (Magstim device) and Control desk (pTMS device) software at inter-pulse intervals of 5 seconds ($\pm$15%).

Corticospinal excitability before and after iTBS was quantified by blocks of 30 single TMS pulses at 120% of the RMT at inter-pulse intervals of 5 seconds ($\pm$15%). The TBS protocol consisted of 600 either monophasic or biphasic pulses applied at 70% of the RMT which is approximately equivalent to the original 80% of the active

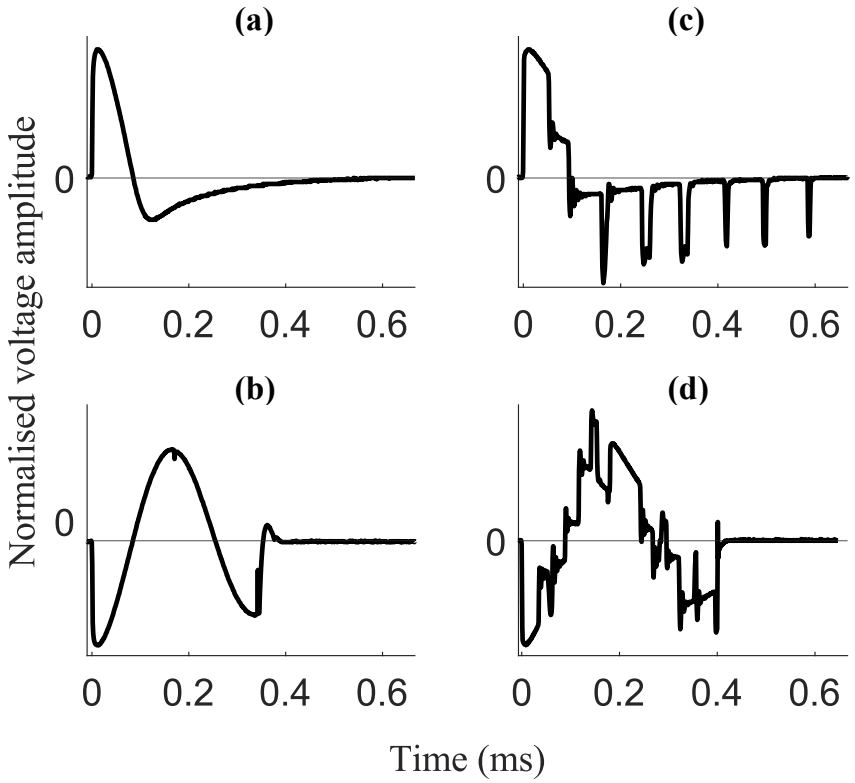

Figure 4.1: Recordings of the Magstim and pTMS pulse waveforms. Normalised voltage waveforms of **(a)** the Magstim 200 and **(b)** the Magstim Rapid^2 stimulators which were used as the reference pulses to generate **(c)** the monophasic pulses and **(d)** the biphasic pulses with the pTMS stimulator. The direction of the biphasic pulses in (b) and (d) was adjusted such that the dominant second phase of the pulse matched the direction of the monophasic pulse. All recordings were measured using a pick-up coil at a sampling rate of 1 MS/s.

motor threshold (Huang et al. 2005) but avoids voluntary contraction immediately before TBS which has been shown to influence plasticity effects (Gentner et al. 2008).

4.2.4 Procedure

The familiarisation and data collection sessions were at least one week apart, to avoid any carry-over effects from previous stimulation sessions. Each participant's total duration of participation did not exceed 10 hours. During each data collection session, the timeline was as shown in Fig. 4.2 (see Appendix A.1.2 for the step-by-step protocol). After confirmation of the hotspot and the motor threshold, two baseline blocks of MEPs were recorded 5 minutes apart (30 pulses per block). iTBS was applied 10 minutes after the start of the first baseline block and follow-up blocks

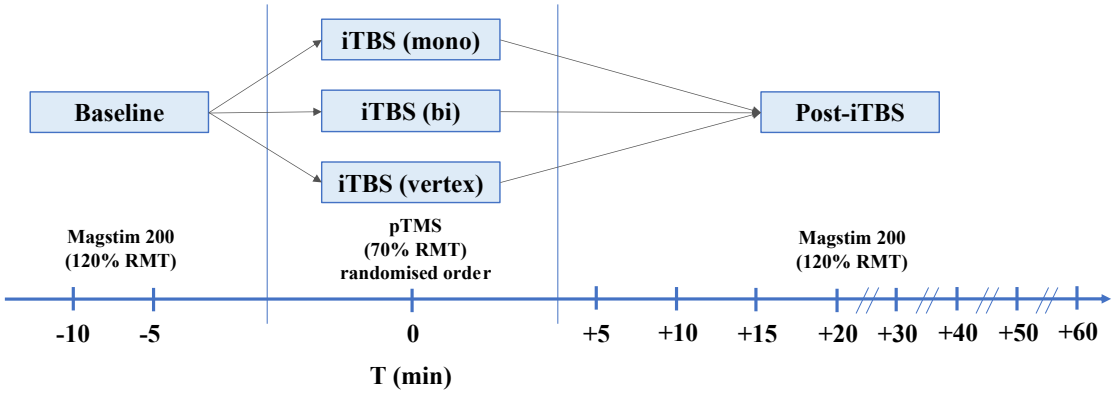

Figure 4.2: Overview of study design representing the flow of data collection at each visit. Each participant received each iTBS condition on separate days (at least one week apart) in counterbalanced order. Baseline MEPs in response to single-pulse TMS (30 pulses applied at 120% of the resting motor threshold) were collected in 2 separate blocks 10 and 5 min before the start of the iTBS administration. iTBS was applied to the primary motor cortex (M1 condition) or the vertex (control condition) using monophasic or biphasic pulses for 190 s. After iTBS, MEPs were collected every 5 min for the first 20 min and then at 10-min intervals up to 60 min post-iTBS.

were recorded every $5-10$ minutes after the start of the iTBS protocol over the following hour (at 5, 10, 15, 20, 30, 40, 50 and 60 min). The timings were chosen to allow enough sampling points during the expected 1h duration of the plasticity effects, while also giving the participants time to rest between stimulation blocks, similar to previous TBS studies (Schilberg et al. 2017) (Jannati et al. 2019). For each participant, two sessions were M1 conditions, where iTBS was applied to the motor hotspot, and one session was a control condition, where iTBS was applied to the vertex (similar to (Nettekoven et al. 2014)). In the control condition, participants were randomised to receive either monophasic iTBS (N = 14) or biphasic iTBS (N = 16). The coil was lifted from the participants' heads between each stimulation block and participants were instructed to keep their hands as relaxed as possible throughout. The three test sessions were performed at the same time of day for each participant and the session order was randomised and counterbalanced. The participants were blinded to the stimulation condition.

4.2.5 Data processing

The data were processed in Python using custom scripts which are available on the Open Science Framework (https://osf.io/9e62f/). Since muscle activation can influence MEP amplitude, trials were excluded if the root mean square (RMS) of the EMG trace in the 90ms before the TMS stimulus (excluding the 5 ms preceding the pulse to avoid contamination from the TMS artefact) exceeded 0.02 mV. The EMG recordings included burst noise, a type of electrical noise characterised by sudden transitions between discrete voltage levels, with a peak-to-peak amplitude of 0.039 mV. To distinguish between this noise and any muscle activation, the pre-stimulus RMS was compared to the RMS during the silent period after the MEP ($60-90$ ms after the TMS pulse), where no muscle activity is expected but electrical noise may be present. Any trials where the pre-stimulus RMS was 0.005 mV larger than the RMS of the silent period or where the MEP was indistinguishable from electrical noise (i.e. smaller than a peak-to-peak amplitude of 0.039 mV) were also excluded. The peak-to-peak MEP amplitude was calculated in the $15-60$ ms time window after the TMS pulse was applied. At the individual participant level, MEP amplitudes within each block were tested for normal distribution. Across participants, over 55% of the stimulation blocks were not normally distributed (Shapiro-Wilk < 0.05). This was not improved by log transformation of the data. Hence, the median (rather than the mean) MEP amplitude was calculated for each time point block per participant, as the median is a more appropriate measure of the central tendency of a non-normal distribution. In addition, it also helped reduce the effect of outliers without requiring outlier removal. On the group level, the data were not normally distributed (100% of the stimulation blocks). Log transformation helped render the MEP distribution more normal (only 0.03% of the stimulation blocks were not normally distributed after log transformation). Therefore, all MEP data were log-transformed using a logarithm with base 10, similar to previous studies (e.g. (Jannati et al. 2017)). The log-transformed medians from the two baseline blocks were averaged for each participant to give one baseline score per

session. Grand-average MEP data were calculated for each condition by averaging over all post-iTBS blocks ($5 - 60$ mins).

4.2.6 Data analysis

All analyses were performed on the log-transformed absolute MEP amplitudes, rather than on data transformed into post-iTBS ratio changes from baseline. Absolute values are preferable to ratios when analysing change, as ratios have been shown to misrepresent physiological processes and to lead to false inferences about group differences (Curran-Everett et al. 2015).

Since participants were randomised to receive either mono- or biphasic iTBS in the control vertex condition, analyses tested for any difference between the two. As there was no difference (see Section 4.3.5), the data were combined into a single control vertex condition for analysis.

To test for significant differences in pre-iTBS baseline excitability, repeated measures analysis of variance (rmANOVA) with factors Time (baseline blocks 1 and 2) and Condition (monophasic M1, biphasic M1, vertex) was used to compare the peak-to-peak MEP amplitudes of the two baseline blocks within and across conditions. Resting motor thresholds obtained using the Magstim 200 were also compared across testing sessions using rmANOVA with the factor Condition (monophasic M1, biphasic M1, vertex).

4.2.6.1 Grand-average MEP analysis

To test whether iTBS induced plasticity as predicted from previous studies (i.e. leading to an overall increase in MEP amplitude post-iTBS relative to pre-iTBS) (Huang et al. 2005), the block-wise log-transformed data of each participant were averaged over all post-iTBS time points to yield a single mean post-iTBS MEP score to contrast with each individual's baseline score pre-iTBS. Grubb's test on these data did not reveal any outliers on the group level. The grand-average MEP data were then compared within-condition against the baseline and across conditions using rmANOVA with factors Condition (monophasic M1, biphasic M1, vertex) and

Time (baseline, post-iTBS average). To compare relative plasticity induction across conditions, post hoc comparisons using pairwise t-tests were conducted. Holm-Bonferroni correction for multiple comparisons was applied. Greenhouse–Geisser correction was applied where necessary to correct for nonsphericity and effect sizes are reported using Cohen's dz for pairwise t-tests (Lakens 2013).

To test whether differences between conditions were driven by a small number of participants responding with very large MEP changes in the monophasic condition, a responder analysis of the grand average of the monophasic and biphasic M1 conditions was conducted, where responders were defined as having a grand average change from baseline (post-iTBS grand average – baseline) above zero and non-responders below zero, similar to the responder analysis in (Hamada et al. 2013).

4.2.6.2 Full MEP time-course analysis

To make use of the full MEP time-course data, complementary analyses were also run using linear mixed effects (LME) models. One advantage of this approach over rmANOVA is that it enables the inter- and intra-participant variability in the baseline data to be modelled in the analysis, as opposed to accounting for the baseline variability by calculating MEP percentage change scores, an approach which often fails to correctly model physiological processes (Curran-Everett et al. 2015). In contrast to the previous grand-average MEP analysis, the MEP amplitudes at each post-iTBS time point were used, without grand averaging over the time points. In the LME models, Baseline MEP amplitude, Time ($5-60$ min post-iTBS) and TBS condition (monophasic M1, biphasic M1, vertex) were modelled as fixed effects while participants were modelled as a random effect. This allowed model intercepts to differ for different participants. To test for an effect of iTBS condition, likelihood ratio testing was used to contrast two models – one that included the iTBS condition as a factor in the model versus a model without the iTBS condition. The χ^2 statistics representing the difference in deviance between the two models are reported, together with the p values calculated by the `anova` function using the Satterthwaite's method for denominator degrees-of-freedom and F-statistic (Kuznetsova et al. 2012). Post

hoc comparisons across conditions were used to test for differences between the monophasic and biphasic M1 conditions and the vertex condition.

A recent study investigated the reliability and sham effects of TBS and highlighted the need to account for placebo effects e.g. by subtracting the modulation of cortical excitability observed during sham TBS from the active TBS condition (Boucher et al. 2021). A similar analysis has been performed in previous studies such as (Schilberg et al. 2017). Thus, to account for the non-specific variability in cortical excitability observed across post-iTBS time points in this study, the LME model analysis on the active iTBS conditions was also repeated after subtracting the control condition. All linear mixed effects models were created and analysed using purpose-written R code using the `LME4` (Bates et al. 2010) and `lmerTest` packages (Kuznetsova et al. 2012). The post hoc comparisons were conducted using the `emmeans` package in R (Lenth 2023) using Holm-Bonferroni correction for multiple comparisons. The scripts are available on the Open Science Framework (`https://osf.io/9e62f/`). The significance level was set to 0.05 for all analyses.

4.3 Results

4.3.1 No differences in RMTs or MEP amplitude at baseline

Resting motor threshold intensities did not differ between conditions ($F(2, 58) = 0.43; p = 0.65$). Additionally, a two-way rmANOVA showed that within sessions, there were no significant differences between the first and second baseline measurements ($F(1, 29) = 0.004; p = 0.950$), nor did these differ across the iTBS conditions ($F(2, 58) = 1.774; p = 0.184$; Fig. 4.3). Thus, these analyses confirmed that participants were tested at comparable levels of motor corticospinal excitability prior to iTBS in all three conditions.

4.3.2 Both active iTBS conditions led to increased motor corticospinal excitability

Fig. 4.4 (a) shows the baseline and group mean average MEP amplitude over the follow-up period ($5-60$ min post-TBS) for each condition for the raw MEP data (in

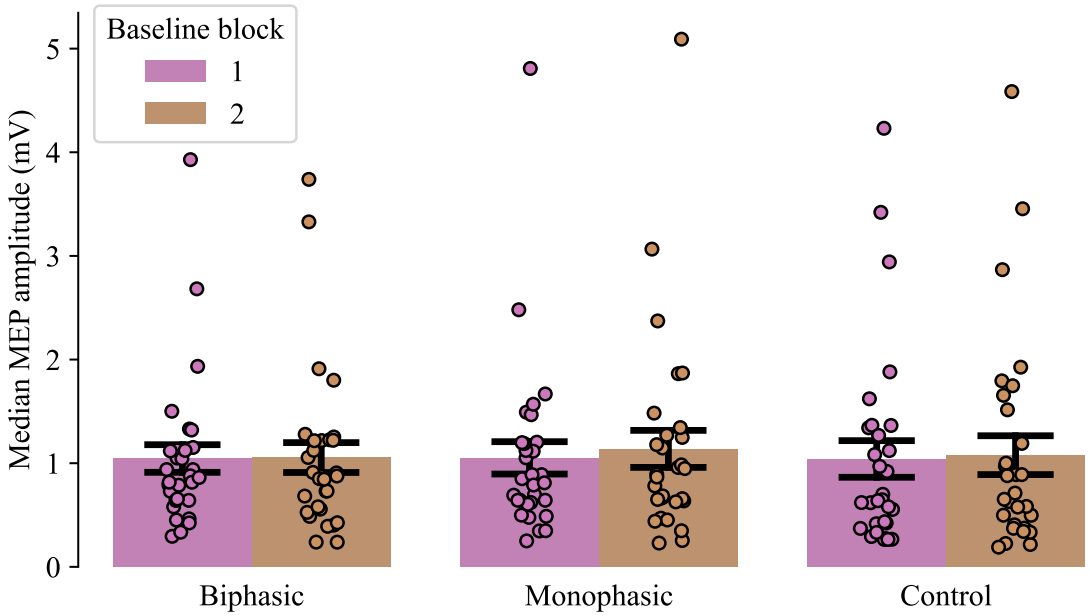

Figure 4.3: Group mean of the median peak-to-peak MEP amplitude for each of the two baseline blocks in each condition. Each baseline block consisted of MEPs elicited by 30 single TMS pulses at 120% of the resting motor threshold. The group mean MEP amplitude was close to 1 mV for each condition and block, but the median amplitudes of individual participants varied. Individual participants are indicated by dots, the bars indicate group means and the error bars represent ± standard error of the mean.

mV). Since the data were not normally distributed (note the positive skew), they were log-transformed, which resolved this problem. Fig. 4.4 (b) shows the log-transformed data that were entered into the analysis. RmANOVA revealed a significant effect of Time ($F(1, 29) = 23.738; p < 0.001$) and Condition ($F(2, 58) = 4.389; p = 0.023$) but no interaction of Time and Condition ($F(2, 58) = 1.686; p = 0.200$). To investigate the effect of time within each condition, Holm-Bonferroni corrected pairwise comparisons of baseline and post-iTBS averages were conducted for each condition. As predicted, biphasic iTBS induced a significant increase in MEP amplitude ($t(29) = 4.125, p < 0.001; \Delta M : 0.19mV, SEM : \pm 0.05mV; dz = 0.753$), confirming a plasticity effect. Monophasic iTBS also induced significant plasticity ($t(29) = 4.236, p < 0.001; \Delta M : 0.30mV, SEM : \pm 0.07mV; dz = 0.773$). In the control condition, iTBS over the vertex did not lead to a significant MEP increase ($t(29) = 1.604, p = 0.12; \Delta M : 0.06mV, SEM : \pm 0.05mV; dz = 0.293$). To contrast across conditions, Holm-Bonferroni corrected pairwise comparisons showed that only the monophasic plasticity effect was significantly larger than the control condition

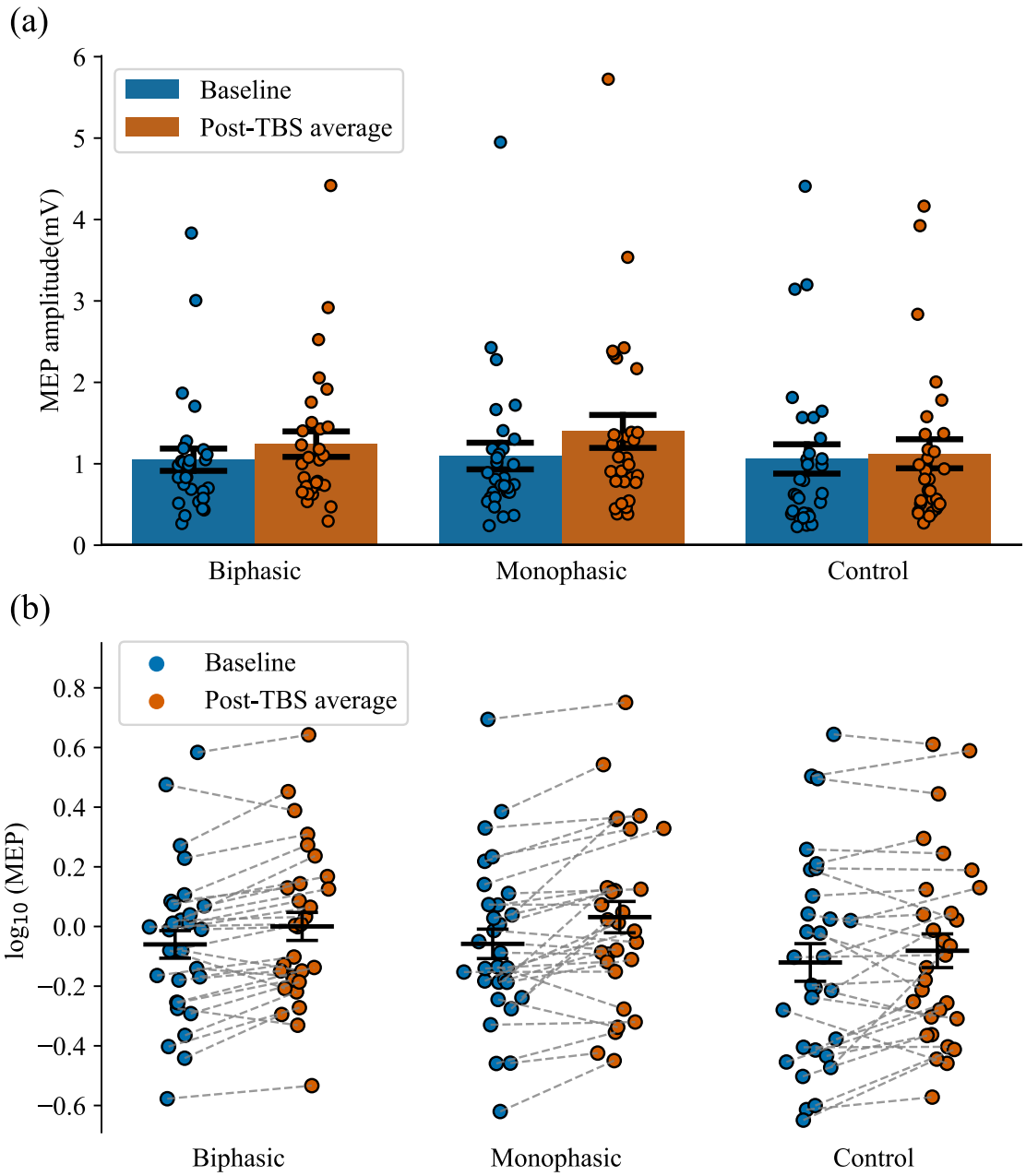

Figure 4.4: Group mean grand-average MEP amplitude compared to baseline, averaged across the 60-min post-iTBS time period for the M1 (monophasic and biphasic) and the control (vertex) conditions. **(a)** Absolute MEP values are shown in mV for ease of interpretation. As the data were not normally distributed, all analyses were performed on log-transformed data (which resolved the skew). Log-transformed data are visualised in **(b)**. Individual participants are indicated by dots, with grey lines in (b) connecting the Baseline and post-TBS average of each participant within conditions. The bars indicate group means and the error bars represent ± standard error of the mean.

($t(29) = 2.767; p = 0.029; dz = 0.505$), while no significant differences were found between monophasic and biphasic iTBS ($t(29) = 0.677; p = 0.504; dz = 0.124$) or

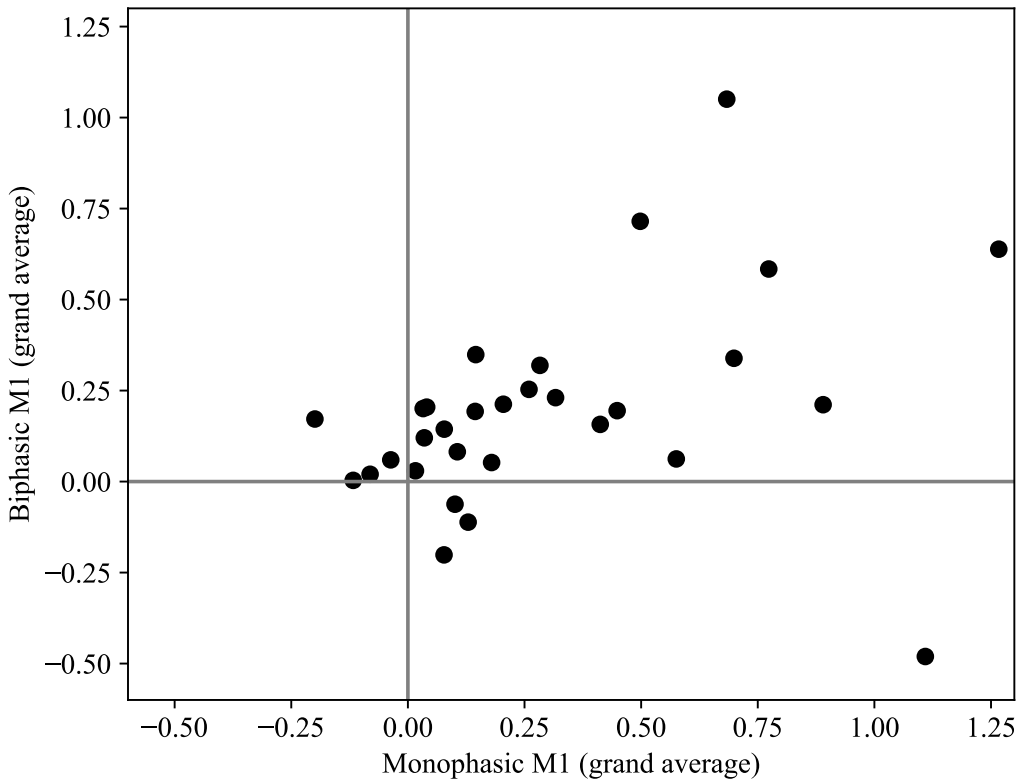

Figure 4.5: Group mean grand-average change in MEP amplitude compared to baseline across the 60-min post-iTBS time period for the biphasic M1 condition vs the monophasic M1 condition. Each participant is indicated by a dot. The non-responders in one condition are shown to not correspond to the non-responders in the other condition. For the majority of the data, participants responded in both conditions but overall, more strongly in the monophasic condition.

biphasic iTBS and the control condition ($t(29) = 1.927; p = 0.128; dz = 0.352$)).

The number of responders in both M1 conditions was 26, and the number of non-responders was 4. As shown in Fig. 4.5, the non-responders in the monophasic M1 condition did not correspond to the non-responders in the biphasic M1 condition and 73% of participants showed consistent responses (i.e. the predicted MEP increase) between the two conditions. In summary, this analysis indicates that both monophasic and biphasic M1 iTBS induced plasticity, with only the monophasic iTBS leading to larger plasticity induction than the control condition when averaging over post-iTBS time points. The responder analysis showed the effect was not driven by a small number of particularly strong responders in the monophasic condition.

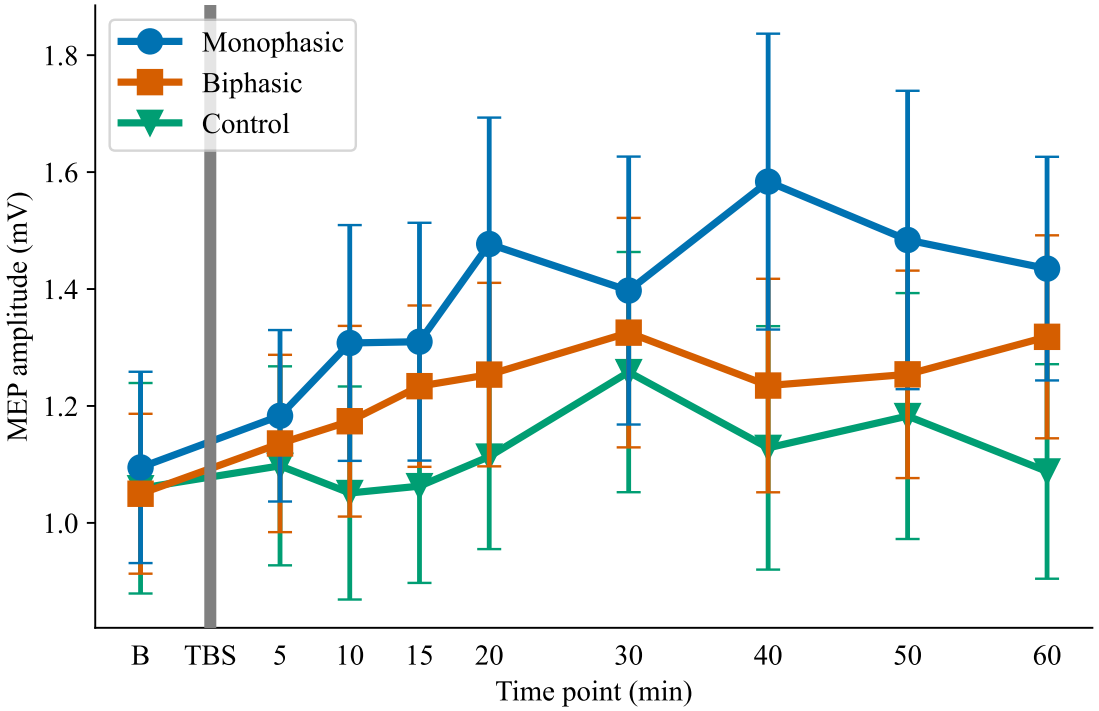

Figure 4.6: Group mean motor evoked potential amplitude over time for the different iTBS conditions. The mean MEP amplitude for the monophasic (blue) and biphasic (orange) M1 iTBS conditions and the control condition (green) are shown for the baseline and across the post-iTBS time points. Absolute MEP values are shown in mV for ease of interpretation. Error bars indicate the standard error of the mean.

4.3.3 TMS pulse shape affects the iTBS plasticity effect

Fig. 4.6 shows the full time-course MEP amplitudes (in mV) across the 60-minute follow-up period for each stimulation condition averaged across participants. As these were not normally distributed, they were log-transformed for the analysis, which resolved the positive skew. Fig. 4.7 shows individual plots of the full time-course data for each participant, time point and condition, highlighting the inter- and intra-individual variability of TMS effects similar to previous studies (Schilberg et al. 2017) (Boucher et al. 2021).

To take the full time-course data into account for the analysis, the LME models with and without the fixed effect of the iTBS condition were compared using likelihood ratio testing, which showed that the iTBS condition (monophasic M1, biphasic M1, vertex) had a significant effect on the MEP amplitude ($\chi^2(1) = 27.615, p < 0.001$). Fig. 4.8 (a) shows the log-transformed data which were passed

Figure 4.7: The median block-wise MEP amplitudes for each participant across all time points in all iTBS conditions are shown in mV. In blue: monophasic M1, in orange: biphasic M1, in green: control condition. The error bars represent the standard deviation. Note: the y-axis range has the same scale for S1-S9, and a different range for S10-S30.

into the LME models and Fig. 4.8 (b) shows the fit of the model that includes the fixed effect of iTBS condition for the different iTBS conditions. Although the difference between the log-transformed MEP amplitudes in the monophasic and biphasic conditions is modest and not visually clear in Fig. 4.8 (a), post-hoc comparisons revealed significant differences between the monophasic and biphasic M1 conditions ($t(693) = 2.311, p = 0.021$), as well as the M1 conditions and the vertex condition (biphasic vs vertex: $t(704) = 3.077, p = 0.004$, monophasic vs vertex: $t(704) = 5.345, p < 0.001$). This analysis confirms that when considering the full MEP time-course data, monophasic iTBS induced a stronger motor corticospinal excitability increase than biphasic iTBS, and both active conditions induced stronger increases than the control condition.

4.3.4 Supplementary analysis: control condition-subtracted monophasic iTBS shows trend-level improvement

The aim of this supplementary analysis was to account for the inter- and intra-individual variability in MEP amplitude across post-iTBS time points (Boucher et al. 2021). For this, the post-iTBS change in MEP amplitude was first calculated by subtracting the baseline for that condition from each post-iTBS time point block for each participant. Next, the vertex data of each individual were subtracted from the M1 iTBS conditions for each of the post-iTBS time point blocks.

The LME analysis was then repeated on the vertex control-subtracted data with Baseline MEP amplitude, Time ($5 - 60$ min post-iTBS) and iTBS condition (monophasic M1, biphasic M1) modelled as fixed effects while participants were modelled as a random effect. Two LME models, one that included iTBS condition as a factor in the model versus a model without the iTBS condition, were then contrasted using likelihood ratio testing. Fig. 4.9 shows the control-subtracted data for the monophasic and biphasic M1 conditions.

After subtracting the MEP values of the control condition from the M1 conditions, to control for the variability across the post-TBS time window, the likelihood ratio did not show a significant effect of the pulse shape on the change in MEP amplitude,

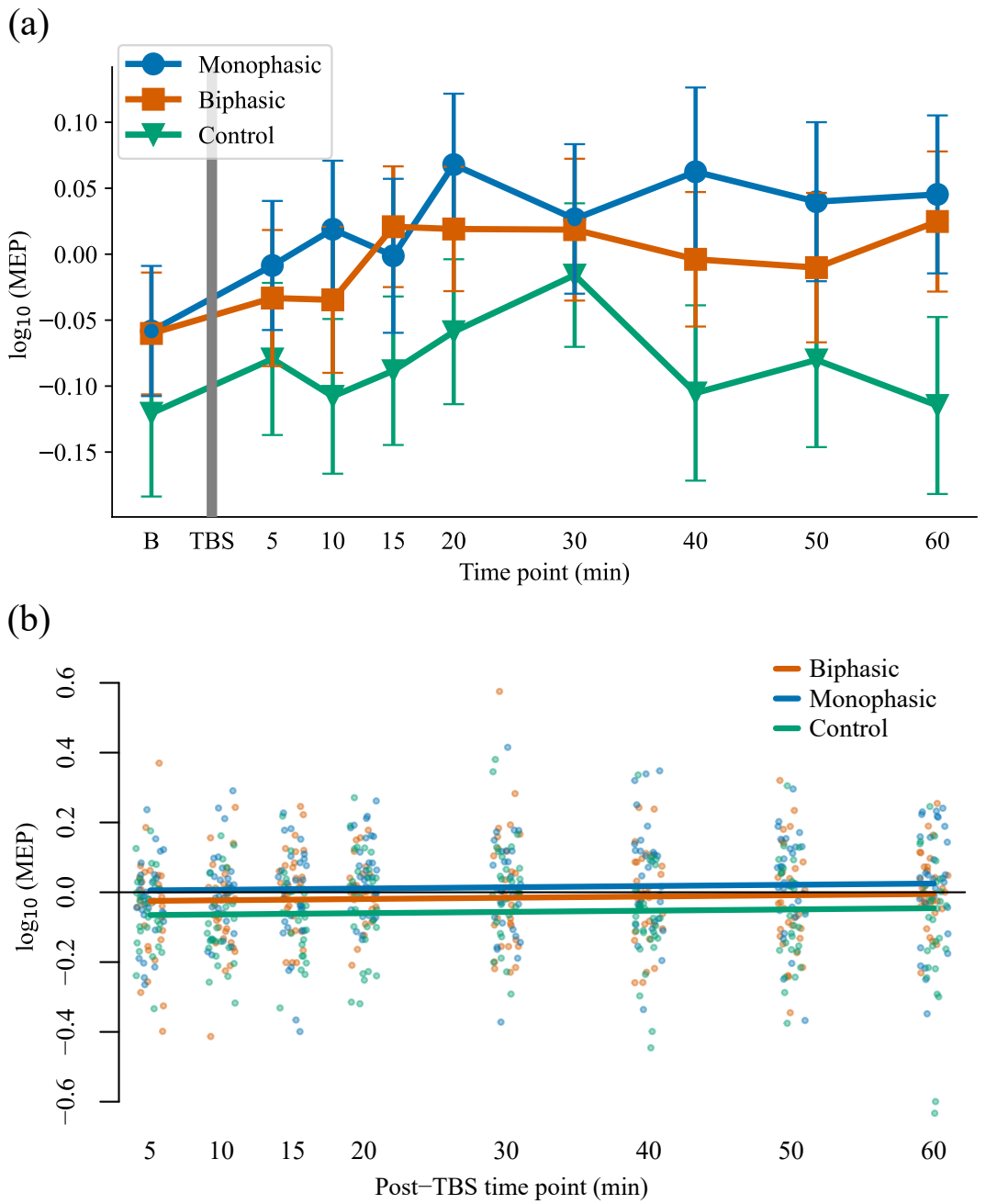

Figure 4.8: Analysed log-transformed motor evoked potential amplitude data and model fit. **(a)** The mean log-transformed MEP amplitude for the monophasic and biphasic M1 iTBS conditions and the control condition are shown for the baseline and across the post-iTBS time points, as passed into the analysis. Error bars indicate the standard error of the mean. **(b)** Visualisation of the fit of the linear mixed effects model (including the fixed effect of iTBS condition) to the data from the monophasic and biphasic M1 iTBS conditions and the vertex condition. The baseline data (not shown here) were modelled as a separate fixed effect. Solid lines show the model predictions, single dots show partial residuals as generated using the `visreg` function in R.

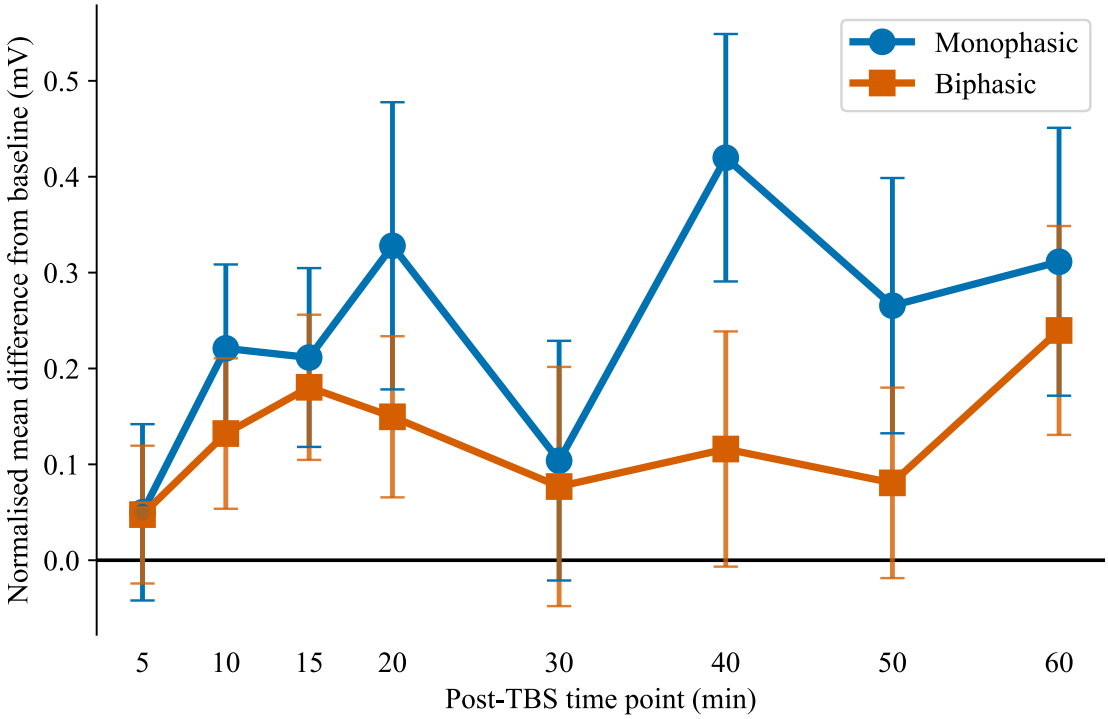

Figure 4.9: The group mean MEP change data over time for the monophasic and biphasic M1 TBS conditions, normalised by the control condition by subtracting the vertex change data for each participant across all post-TBS time points. Error bars indicate standard error of the mean.

but a trend in the same direction was visible ($\chi^2(1) = 3.675, p = 0.055$). This exploratory analysis highlights the variability observed in TMS protocols and how some of the variability captured in the control condition can account for stimulation effects. However, the trend-level difference between the monophasic and biphasic control-subtracted conditions indicates that the increased plasticity effect in the monophasic condition is likely still present.

4.3.5 Supplementary analysis: no difference between control conditions

In the control condition (iTBS applied to the vertex) participants were randomised 50 : 50 to receive either monophasic or biphasic pulses. Given the well-established spatial specificity of TMS, the prediction was that iTBS applied several centimetres ($5 - 7$cm) medial from M1 (i.e. over the vertex) would not induce a significant change in the excitability of the motor corticospinal tract. Thus, the participants

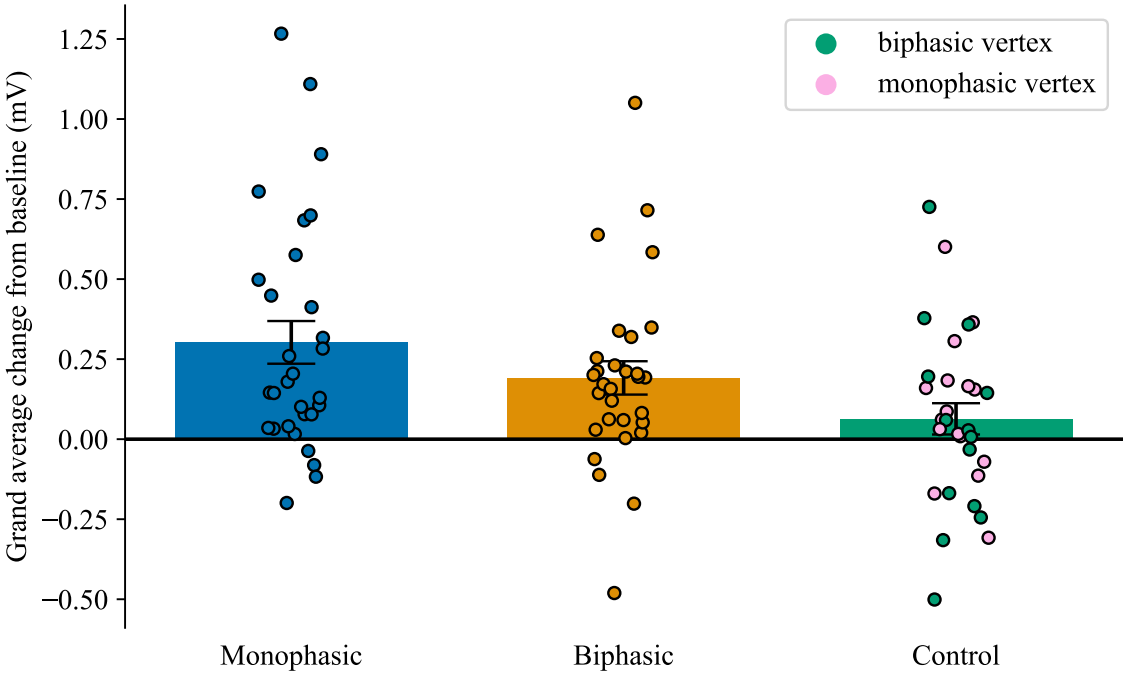

Figure 4.10: Group mean grand-average change in MEP amplitude compared to baseline across the 60-min post-iTBS time period for the M1 (monophasic and biphasic) condition and the control (vertex) condition. Individual participants are indicated by dots. Half of the participants received monophasic vertex stimulation (pink dots), and half biphasic (green). Note the overlapping distributions. The bars indicate group means and the error bars represent ±1 standard error of the mean.

were randomised to receive half monophasic and half biphasic iTBS to the vertex. Had they instead all received only monophasic or biphasic pulses in the control condition, one could wonder if the other untested control pulse shape might have induced different effects. To fully rule out a potential bias from one or the other pulse shape in the control condition, statistical analyses were conducted to test for any significant differences between these two halves of the control data set. Fig. 4.10 shows the grand-average change from baseline (post-iTBS grand average – baseline), with the control condition data split by pulse type. An independent two-sample t-test confirmed there was no significant difference between the two vertex conditions ($t(24.57) = 1.374, p = 0.182$), reflected in the overlapping distributions of individual data points across the two pulse types.

In addition, the full time-course data were tested for any differences between the monophasic and biphasic vertex control data sets. Fig. 4.11 shows the data for each participant. Two LME models were built and contrasted, one included the fixed effect

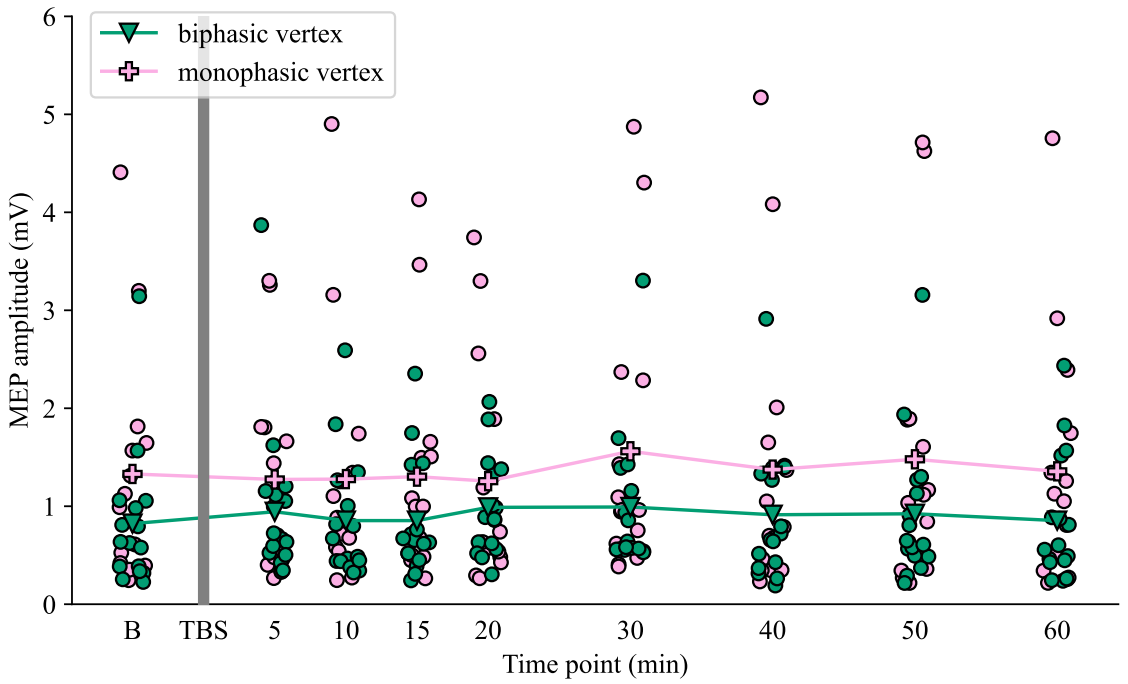

Figure 4.11: The group mean and individual participant MEP amplitudes over time for the control condition split for illustration into the two halves of the control data set, i.e. those who had monophasic versus those who had biphasic pulses in the control condition. Monophasic data are in pink and biphasic data are in green. The group means are indicated by the respective lines, and the individual participants by dots. Note the overlapping data distributions, reflecting no significant difference between the two halves of the control condition.

of pulse shape (mono- versus biphasic vertex iTBS) and the other did not. Likelihood ratio testing showed that the pulse shape in the control condition did not have a significant effect on the MEP amplitude ($\chi^2(1) = 0.76, p = 0.383$), further confirming no significant difference between the two halves of the vertex control data set.

In combination, both analyses (Fig. 4.10 and 4.11) demonstrated there was no difference between the mono- and biphasic halves of the control data set, hence confirming that it was acceptable to combine the vertex conditions into a single control condition for all analyses.

4.4 Discussion

In this study, both monophasic and biphasic iTBS applied to the primary motor cortex increased motor corticospinal excitability as measured using MEPs. The application of iTBS using the pulse-width modulation-based TMS device resulted

in excitability increases, as expected from studies applying iTBS using conventional resonance-based devices. On the group level, monophasic iTBS induced larger plasticity effects than conventional biphasic iTBS, confirming the importance of pulse shape in repetitive TMS protocols. Intermittent TBS applied to the vertex in the control condition did not lead to a change in MEPs. A responder analysis showed that for the majority of data, participants responded in both conditions but overall, more strongly in the monophasic condition. A supplementary analysis of the control-subtracted monophasic and biphasic M1 data showed a trend-level difference, highlighting the individual variability observed across time points.

4.4.1 Influence of high-frequency components in the stimulation pulses

In this study, iTBS was applied using PWM which includes more high-frequency components in the stimulation pulse than in conventional pulses. While Chapters 2 and 3 showed similar effects of PWM pulses compared to conventional single pulses, few studies have investigated the effects of PWM on plasticity induction via repetitive TMS. A study comparing the effects of 1Hz rTMS on cortical excitability using rectangular pulses applied using the cTMS device and conventional biphasic pulses found stronger effects with rectangular bidirectional and unidirectional pulses than with the conventional biphasic pulses (Goetz et al. 2016). The pulses applied using the pTMS device in this study approximate the conventional monophasic and biphasic pulses more closely than rectangular pulses do, however, the additional high-frequency components in the pTMS pulses may also contribute to the effects observed in this study. In particular, the current study did not track a return to baseline of the MEP amplitude at the end of the sampling interval at 60 minutes in the active iTBS conditions. For comparison, some previous studies applying conventional biphasic iTBS reported elevated MEP amplitudes up to 50 min after iTBS (e.g. (Gamboa et al. 2010), (Boucher et al. 2021)). A longer post-iTBS sampling window would be required in future studies to estimate how long the plasticity effect lasts with monophasic and PWM iTBS.

4.4.2 Choice of probing pulses

To measure the changes in motor corticospinal excitability, single pulses were applied at 120% of the RMT, similar to previous work such as (Jannati et al. 2017) (Schilberg et al. 2017). Other studies, including the early TBS studies (Huang et al. 2008), did not use % of RMT as a baseline/probe but instead used the individualised intensity of TMS needed to reliably elicit MEPs of 1mV on each trial. However, this approach can suffer from floor or ceiling effects across individuals (e.g. in some participants, TMS may not induce peak-to-peak amplitudes much higher than 1mV) which can contribute to the high variability across participants (Burke et al. 2010). Therefore, plasticity effects have been suggested to best be probed at a percentage of the resting motor threshold to take into account this difference in the input-output characteristics of the participants (Vallence et al. 2015). This reduces the risk of ceiling and flooring effects on plasticity but entails higher variability between participants at baseline. This was accounted for in the analysis of this study by including the baseline as a factor in the LME model.

Consistent with the literature, monophasic single pulses applied using a conventional Magstim 200 were used to measure MEPs pre/post-iTBS. While this allowed the direct comparison of effects across conditions, monophasic and biphasic pulses may activate different neural populations during TBS. Using monophasic pulses, therefore, limits the ability to probe the potentially different neural populations activated by biphasic TBS (Huang et al. 2017) (Tse et al. 2018). However, studies using both monophasic and biphasic single pulses to assess plasticity effects found the results of using either pulse shape to probe excitability highly comparable (Mastroeni et al. 2013) (Sasaki et al. 2018).

4.4.3 Directionality of pulse currents

The direction of the current induced in the brain affects which neuron populations are activated and influences the size of the motor threshold (Aberra et al. 2020) (Sommer et al. 2006). Early studies using epidural recordings in human participants have shown that anterior-posterior and posterior-anterior monophasic stimulation

likely activate different sites or different neuron populations, in particular at low intensities (Di Lazzaro et al. 2001b). Biphasic pulses with posterior-anterior current flow in their second phase have been shown to recruit descending volleys, similar to posterior-anterior monophasic pulses, however, cortical activation patterns depend on relative thresholds and intensities of the different pulse phases (Di Lazzaro et al. 2001a). In this study, the monophasic pulses were applied to induce currents in the posterior-anterior direction both for single pulses and for the iTBS protocol, as this has been shown to have the lowest thresholds (Sommer et al. 2006) and may therefore be the best current direction to use when the aim is to increase motor corticospinal excitability, as here. The biphasic pulses were applied to match this current direction in the second phase of the pulse, as this is thought to be the dominant activating phase of the biphasic pulse (Sommer et al. 2006). A previous study showed that the current direction of biphasic pulses had a significant effect on corticospinal excitability when using continuous TBS but not intermittent TBS (Talelli et al. 2007). However, another study found no difference in effects between different current directions in cTBS (Suppa et al. 2008). Another variable of potential interest is the current direction used in the probing pulses, although a previous study found no effect of current direction on MEP measures of cTBS response when using 1mV probing pulses (Sasaki et al. 2018). Future studies should explore the effects of different current directions of the different pulse shapes, both for single pulses and TBS protocols, to determine the optimal current direction for plasticity induction. As the current direction can be changed computationally in the pTMS device, rather than requiring the manual flipping of the coil as in conventional devices, protocols with interleaved pulses of different current directions could be used to investigate this further.

4.4.4 Further considerations to improve TBS

Monophasic pulses approximating the pulse shape of conventional stimulators were used in this study, but other pulse shapes or widths may cause larger effects in TBS and other repetitive TMS protocols. With the newer TMS devices such as the

pTMS device used in this study, researchers gain the ability to investigate more parameters to optimise the effects of TBS. Other studies looking at the number of pulses per burst (Meng et al. 2022), different stimulation intervals (Tse et al. 2018) (Abboud Chalhoub et al. 2020) as well as the total number of pulses (Gamboa et al. 2010) (McCalley et al. 2021) show further possible avenues to increase the plasticity effects induced by the stimulation.

4.4.5 Vertex stimulation as a control condition

In the control condition, iTBS was applied to the vertex, using the same parameters as in the M1 conditions. Real iTBS was applied to the vertex to achieve an active control condition in which the same stimulation is applied (but at an anatomical control site) and similar skin sensation and audio effects are experienced (Nettekoven et al. 2014) (Herwig et al. 2010). Supplementary analyses confirmed that applying monophasic and biphasic pulses in the control condition was comparable. The purpose of the vertex condition was to establish anatomical specificity (of M1 iTBS effects) and to quantify intrinsic intra- and inter-participant variability in MEP amplitude fluctuations over the same measurement time period as in the M1 conditions. While there were fluctuations in MEP amplitude over time in the post-iTBS blocks in the control condition, none of these were significant. At the individual level, such MEP fluctuations are likely due to non-specific psychological factors, such as attention and fatigue. In addition, as the brain was actively stimulated in the vertex condition, albeit in a different location, brain network effects may have also influenced the MEP results. However, the active control condition showed no systematic change post-iTBS, reflected in non-significant analyses, indicating that any apparent visual changes in Fig. 4.6 reflect weak and variable non-specific MEP fluctuations over time.

4.4.6 Analysis methods

It is worth noting, that there appears to be a lack of standardised methods to analyse changes in MEP amplitudes after TBS and other TMS protocols. Firstly, many

papers analyse post-TBS ratio changes from baseline rather than absolute amplitude values, although ratios have been shown to often misrepresent physiological processes and lead to false inferences about group differences (Curran-Everett et al. 2015). Furthermore, some studies average across time points while others consider the time points separately, some work with raw data while others log transform their data, sometimes without reporting if this helped make the data more normally distributed. Additionally, the control condition, if available, is often included in different ways in the analysis. While some analysis approaches may differ depending on the research question a study aims to answer, the publications in this research field would benefit from a standardisation of the analysis methods and fully transparent reporting of each analysis decision made. This would include a consensus on using MEP ratios versus using absolute amplitudes, the averaging across any time points and with this the use of statistical models such as ANOVAs or LME models, the use of log transformation to render non-normally distributed data more normal (with reports of normality tests before and after log transformation) and the use of control conditions and their inclusion in the analysis. While no such consensus exists at present, when analysing the data from this study, the aim was to report the analysis decisions in a transparent way.

4.5 Limitations

Due to the technical setup of the study, it was conducted in a single-blinded manner, where the participants were blinded to the condition and the study hypothesis, but the experimenters were aware of the stimulation condition. This was partially due to the online programming needed for the custom-made pTMS device to generate monophasic or biphasic pulses and the fact that the coil was placed in a different location during the control condition. Further, the pTMS stimulator's limit on its maximum pulse amplitude necessitated the exclusion of some participants with high thresholds. This is a limitation of the current prototype. However, the maximum output intensity of future generations of the device can be increased by cascading additional H-bridges (see Section 6.3).

The interval between probing pulses in this study was 5 seconds (±15%) which may lead to confounds due to anticipation or carry-over effects. However, as the same intervals were used in all conditions, these confounds are unlikely to account for differences between conditions. Additionally, the test sessions were $2-3$ hours long, during which experimenters interacted with the participants, albeit as little as possible, which may have had an influence on the results and the MEP variability, though the use of a within-participants crossover design should help to mitigate this potential issue to some extent.

4.6 Conclusions and contributions

This study confirms that the pulse shape affects the group-level plasticity effects induced after iTBS, with monophasic pulses leading to larger increases in MEP amplitude than conventional biphasic pulses. Although the difference between the MEP increases for monophasic and biphasic iTBS is modest and the inter-individual variability is large as is typical for these studies, it adds to the literature exploring improvements in the TBS protocol in the hope of enhancing plasticity induction. Additionally, it demonstrates the feasibility and importance of the increased flexibility achieved by the pTMS. As technology advances and the limitations of current devices are addressed, these findings hold promise for applications in basic neuroscience and medical practice as they may contribute to improving established therapies in disorders such as depression. Furthermore, the results of this study highlight the significant inter- and intra-individual variability observed in TMS protocols, warranting a closer investigation of potential sources of variance in TMS in the next chapter.

5

Investigating TMS variability in clinical practice

Contents

The work presented in this chapter has been published in the following publication:

***Wendt, K.**, Sorkhabi, M. M., O'Shea, J., Denison, T., and van Rheede, J. (2023). "Influence of time of day on resting motor threshold in clinical TMS practice". Clinical Neurophysiology 155, pp. 65–67, DOI: 10.1016/j.clinph.2023.08.017*

5.1 Introduction

The previous chapter investigating the effect of pulse shape in theta burst stimulation highlighted the large variability observed in plasticity induction between participants and sessions. In that study, iTBS was applied to the primary motor cortex of healthy participants and motor evoked potentials were used to assess the effects of the stimulation. Although MEPs are known to be a variable measure of TMS effects, they are commonly used to test the plasticity effects of stimulation protocols since they provide an objective measurement of the responses using electromyography. Clinical protocols, such as in the treatment of major depressive disorder (MDD), target areas outside the motor cortex but similar variability is observed in clinical outcomes. Identifying the sources of such variability is important to ensure consistency of treatment response. Recent papers from the 'Big TMS Data Collaboration' examined potential sources of variability in neural responses to TMS (Corp et al. 2020) (Corp et al. 2021), highlighting the effects of methodological differences between studies, such as the muscle being targeted, the stimulated hemisphere, the motor thresholds and TMS pulse parameters. Additionally, they identified time of day as an important factor. Indeed, cortical excitability has been shown to be influenced by various factors that vary systematically with time of day, such as time awake (Huber et al. 2013), circadian phase (Ly et al. 2016), and cortisol levels (Milani et al. 2010). On the other hand, studies looking at measures of the neural response to TMS in healthy participants, including resting motor threshold (RMT), motor evoked potentials and TMS evoked potentials, found no effect of time of day (ter Braack et al. 2019), (Doeltgen et al. 2010), (Koski et al. 2005), (Lang et al. 2011). However, these studies were conducted on healthy participants in a controlled laboratory environment, rather than on patients in clinical practice.

To reduce variability, one important step is to standardise methods. Before applying a TMS treatment protocol, common procedures include finding the resting motor threshold in the motor cortex to set the stimulation intensity of the treatment protocol to a percentage of this threshold. However, the primary motor cortex differs from other brain areas in terms of structure, myelination and cell density which

makes the motor threshold an inappropriate measure of cortical excitability in other brain areas (Siebner et al. 2022). Nonetheless, it is routinely used due to a lack of better alternatives although magnetic resonance imaging may at least be an option to adjust the stimulation intensity from the threshold to take into account individual anatomies. However, this is a costly option for clinics without a clear improvement. The resting motor threshold is broadly defined as the minimal intensity at which a TMS pulse above the motor hotspot elicits a motor response. Different methods can be used to determine the threshold, by targeting different muscles in the hand and by measuring the threshold either by using electromyography or by visual observation of finger twitching (McClintock et al. 2017). Further, if RMT is measured at one clock time while clinical TMS treatment is delivered at another, systematic time of day differences in cortical excitability could lead to discrepancies between the intended and achieved level of brain excitation and therefore treatment 'dose'. As clinical outcomes in TMS may be dose-dependent (Sackeim et al. 2020) (Tendler et al. 2023), this could have important implications.

The Magstim Horizon 3.0 system allows users to remotely manage patient protocols and analyse treatment outcomes. As my DPhil is in collaboration with Magstim, this gave me the opportunity to analyse a large proprietary data set of RMTs from TMS clinics across the United States. Using this data set, I investigated the sources of variability in clinical TMS practice to inform methods for more robust outcomes. In line with the available data, the analysis explored the relationship between time of day and resting motor thresholds in clinical practice and investigated the inter-clinic variability.

5.2 Methods

5.2.1 Data source

All data used in this study have been gathered in accordance with HIPAA guidelines and Magstim's Business Associate Agreement with each clinic, allowing the use of the pseudo-anonymised data for analysis purposes.

As all data were collected from Magstim Horizon 3.0 systems, all stimulators had the same specifications with a biphasic pulse waveform and a figure-of-8 stimulation coil. In total, the data set includes 2626 RMT measurements from 1550 patients collected between October 2021 and March 2023, encompassing 60 clinics in different states of the United States. All patients were undergoing TMS treatment for major depressive disorder.

5.2.2 Data pre-processing

The number of patients with multiple RMT measurements within the data set was insufficient to enable an analysis of repeated measures within patients (598 patient with more than one data point, few of which were at different times of day). Thus, duplicate RMT measurements from patients were removed, only keeping the data point with the last time stamp, as this was most likely the RMT measurement used for the treatment. The device time recorded in UTC was converted to local time according to the zip codes of the clinics using a US zip code database (simplemaps 2023).

Clinicians had the option to include metadata on patient gender, ethnicity, age and handedness, as well as motor thresholds, diagnosis and treatment results. However, the extent of the data entered into the system depends on the practitioner and varies across clinics. All data automatically includes the patient's resting motor threshold, the clinic ID and time stamp of the data collection. Table 5.1 shows the availability of patient metadata in the data set. Of the 1550 patients, only 189 included patient gender (53 males), and even less included handedness (28, only right-handers indicated) or ethnicity (30). No data on diagnosis or treatment results were included. For the statistical analysis, I therefore focussed on resting motor thresholds, together with the local time and clinic ID. Data points with RMTs more than 2.5 standard deviations away from the sample mean were removed, an empirically chosen threshold which ensured the removal of strong outliers which might not be meaningful physiological thresholds, while retaining around 98% of the data.

Table 5.1: Availability of RMT metadata in the data set

	Clinic ID	Time	RMTs	Gender	Handedness	Ethnicity
# data points	1550	1550	1550	205	28	32

The removed thresholds were confirmed to be threshold measurements of 100% of the machine output, where the clinician may not have found the threshold and simply set it to the highest possible value or very low thresholds that have likely arisen due to measurement errors. The resulting data set contained a total of 1514 RMT measurements.

5.2.3 Analysis of variance

5.2.3.1 Diurnal variations

To evaluate the influence of time of day on resting motor thresholds, a fit based on the average values for each time of day (TOD) was created and the variance explained by this fit (Var_{TOD}) was calculated, similar to the time of day analysis in (van Rheede et al. 2022). In brief, the method was implemented as follows. The fit was computed by sliding a 60-minute time window across the data from $8:00$ to $18:00$ in 6-minute steps. The mean of each window was computed and used as an estimate of the fit for the centre of the window. The resulting window centres ranged from $8:30 - 17:30$. The percentage of the variance explained by time of day was then calculated according to the following equation:

$$\%Var_{TOD} = (Var_{total} - Var_{remaining})/Var_{total} * 100 \tag{5.1}$$

Where Var_{total} is the total variance of the RMTs in the data set and $Var_{remaining}$ is the variance of the data set that remains after removing the variance captured by the time of day by subtracting the time of day fit estimate (van Rheede et al. 2022).

Finally, to establish a reference distribution for the variance explained by the time of day due to chance, the RMT data were shuffled and re-assigned to a random time stamp in the data set to generate $10,000$ shuffled versions of the data set. The value obtained for the percentage of variance explained by the time of day $\%Var_{TOD}$

in the original data set was then compared to this null distribution to determine the likelihood of observing the resulting value by chance (van Rheede et al. 2022).

5.2.3.2 Inter-clinic variability

Apparent effects of time of day could also arise from differences in average RMT, which may originate from methodological differences in the measurements, as well as different scheduling between clinics. To inspect this, the 10 largest clinics with at least 45 patient data points were selected. Analysis of variance (ANOVA) was used to estimate how much of the variance in the resting motor thresholds is accounted for by the clinics.

To control for the effect of clinic on Var_{TOD} in the time of day analysis, the RMTs of the largest clinics were then z-scored within each clinic. In addition to the outlier removal performed on the whole data set, the data points more than 2.5 standard deviations away from the mean of each clinic were removed, resulting in a total of 739 data points. The moving average analysis, including the $10,000$ shuffles, was then repeated for the z-scored data.

5.3 Results

The median resting motor threshold of the data set was 57.0% of the maximum stimulator output (MSO) of the Horizon 3.0 system. The distribution of the resting motor threshold values expressed in % MSO is shown in Fig. 5.1 (a). An independent two-sample t-test showed no effect of gender ($t(188) = 0.014, p = 0.988$) and a one-way analysis of variance with factor Ethnicity revealed no effect of ethnicity on the RMT ($F(10, 19) = 1.224; p = 0.337$). The analysis of both of these factors was limited by the small sample sizes for a between-subject analysis (Table 5.1), thus, these factors were excluded from the remainder of the analysis. Fig. 5.1 (b) shows the distribution of the measurement times, revealing a skew towards the morning in the measured time points.

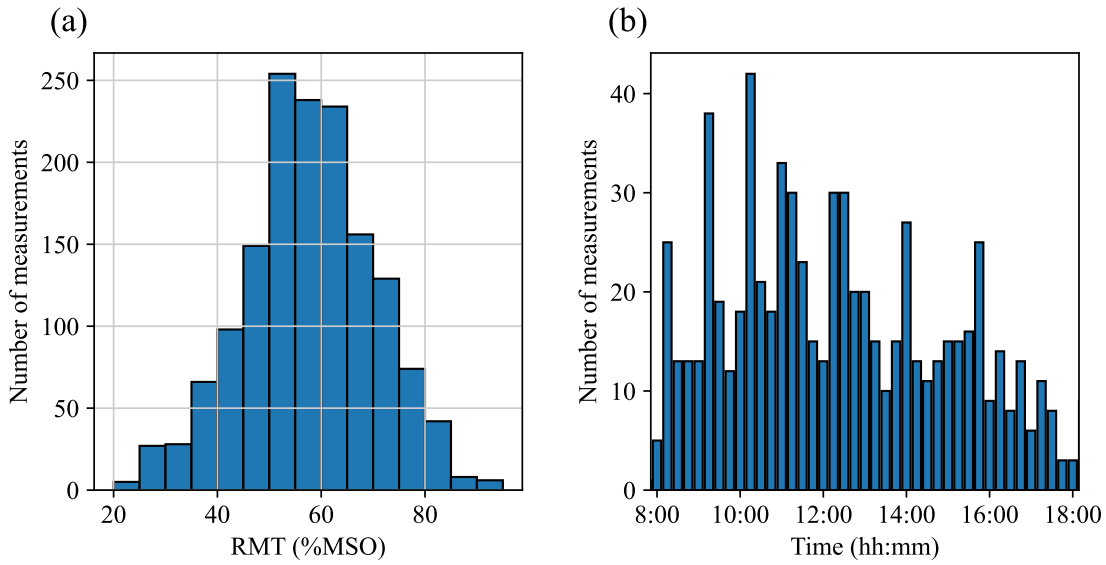

Figure 5.1: Data distribution of **(a)** resting motor thresholds (RMT) and of **(b)** measurement times for all patients in the data set.

5.3.1 Inter-clinic differences explain large proportion of RMT variability

Inspection of the time distribution of the measurements for each clinic (Fig. 5.2 (a)) revealed that clinics had different distributions of measurement times across the working day. For example, the clinic with the most patients in this data set (Clinic 1) scheduled the majority of their patients before noon. Fig. 5.2 (b) shows the RMT distributions of the 10 largest clinics. To quantify the variance in the RMTs which can be explained by differences between clinics, a one-way ANOVA with factor Clinic was conducted. The results indicate that resting motor thresholds differed significantly between the clinics ($F(9, 729) = 83.09; p < 0.001$) which explained 50.32% of the RMT variance. To ensure the ANOVA results were not merely driven by the evident outlier Clinic 1, the analysis was repeated when excluding this clinic, which still resulted in a significant explained RMT variance of 22.29% ($F(8, 552) = 5.68; p < 0.001$). Additionally, Fig. 5.2 (c) shows that the number of patients in each clinic did not seem to influence the average RMT of the respective clinic.

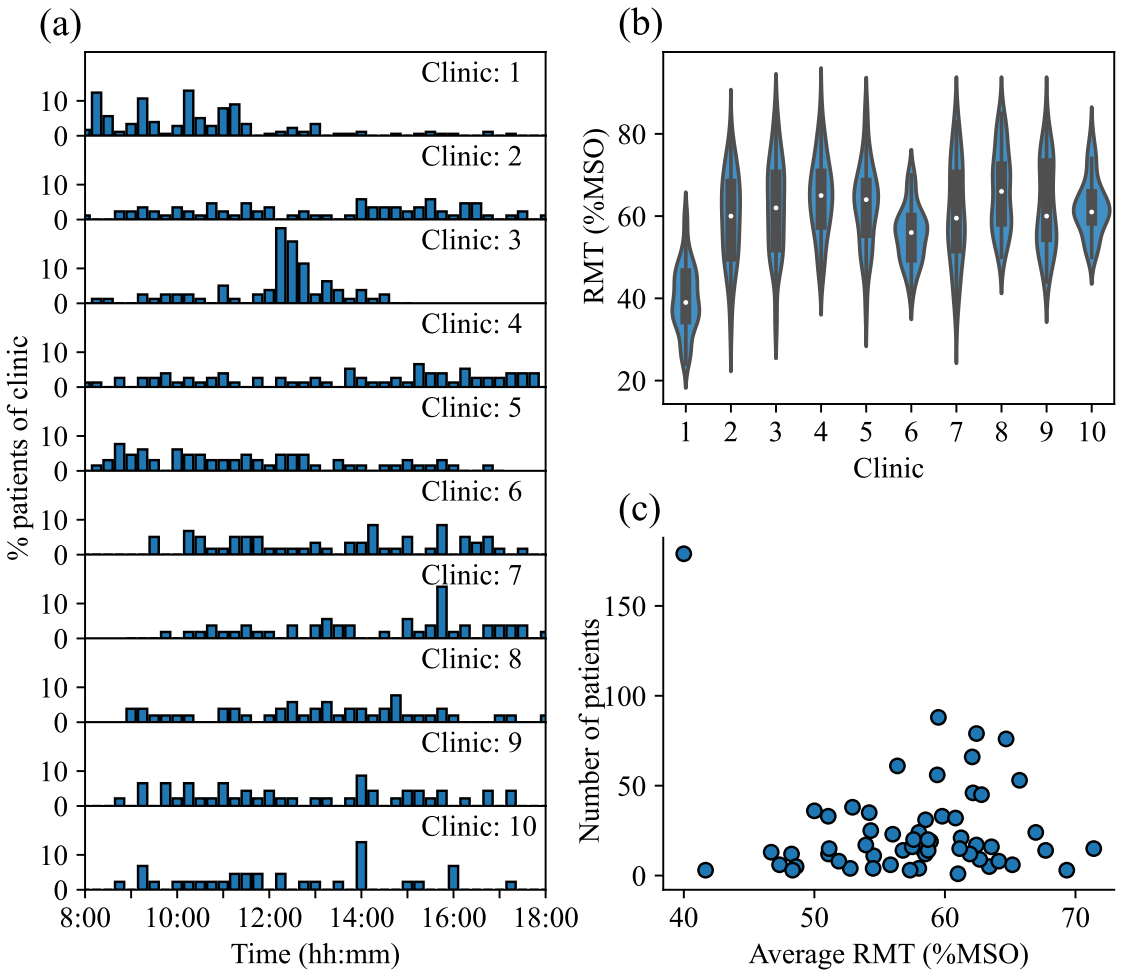

Figure 5.2: Data distributions and time of day fit for the 10 largest clinics. **(a)** The measurement time distributions across the day from 8 : 00 - 18 : 00 are shown for each clinic with at least 45 patients. The clinics are sorted by the number of patients they have in the data set. Of these 10 clinics, some tend to schedule their patients at particular times of day as indicated by the distributions that are skewed to a specific time of day, e.g. Clinic 1. **(b)** Distributions of resting motor thresholds (RMT) as a percentage of the maximum stimulator output (MSO) for each of the 10 largest clinics. **(c)** The number of patients in each clinic is plotted against the average RMT of the respective clinic, each indicated by a dot.

5.3.2 Statistically-significant diurnal variation effects disappear when controlling for clinics

Fig. 5.3 (a) shows the time of day fit obtained using a moving average of the raw RMT data of the 10 largest clinics between the times 8 : 00 and 18 : 00, including its standard error and the $5th$ and $95th$ percentile lines obtained by shuffling the data. The time of day fit explained a statistically significant percentage of the variance in the resting motor thresholds (11.07%, $p < 0.001$ vs. shuffled distribution).

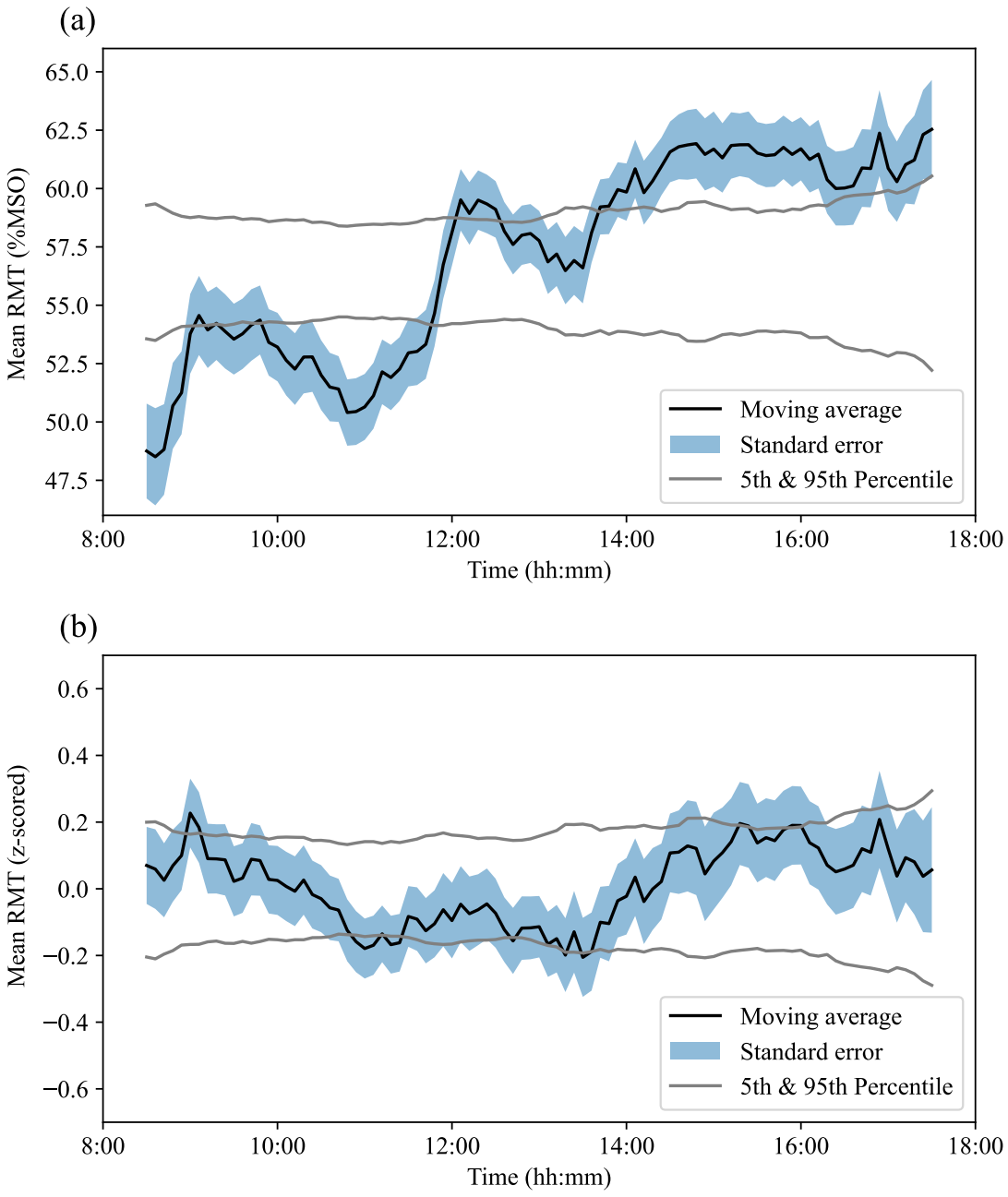

Figure 5.3: Moving average fit of the RMT values for the 10 largest clinics. Time of day fit of **(a)** the raw RMT values and of **(b)** the z-scored RMT values after controlling for clinic. The moving average time of day fit is shown in black with its standard error represented by the shaded region in blue. The grey lines indicate the $5th$ and $95th$ percentiles of the moving average fit, which represent the boundaries a moving average is likely to reach when no time of day effects are present. These were calculated using a reference distribution by shuffling the data $10,000$ times and computing the moving average of each shuffled data set.

Next, to control for the variance in RMTs by clinics, the resting motor thresholds of the 10 largest clinics were standardised using z-scoring. In contrast to the previous

results, the percentage of the variance explained by time of day after controlling for clinics by z-scoring the data was greatly reduced and not significant (1.19%, p = 0.498, vs. shuffled distribution). Fig. 5.3 (b) shows the time of day fit of the z-scored data together with its standard error and $5th$ and $95th$ percentiles obtained from temporal shuffling. While some variation in motor thresholds can be seen across the day, none of these showed a significant difference.

5.4 Discussion

In this study, the effect of time of day on the resting motor threshold was quantified in a data set across clinics. While at a first glance, the results show that the time of day may explain up to 11% of the RMT variability, which would be a small but statistically significant effect, the analysis of the variance by clinic revealed that around 50% of the variance could be explained by differences between RMTs across clinics. Analysis of the by-clinic z-scored data indicates that the apparent influence of time of day was due to the differences between clinics and their relative testing schedules.

5.4.1 Effects of time of day in the data set

While prior work on the effect of time awake (Huber et al. 2013) and circadian rhythm (Ly et al. 2016) on cortical excitability would predict a gradual *decrease* in RMT, in the analysis of the raw data set, the RMT levels appear to *increase* throughout the working day, indicating a decrease in excitability. The sharper fluctuations throughout the day could reflect for example cortisol spikes (Milani et al. 2010). However, after controlling for the variance across clinics by z-scoring the RMTs, there was no significant effect of time of day on individual RMTs measured in the clinic. On the one hand, this broadly agrees with the findings of previous studies in healthy volunteers which found no significant daytime changes in RMT (ter Braack et al. 2019), (Doeltgen et al. 2010), (Koski et al. 2005), (Lang et al. 2011). Findings from the Big TMS Data Collaboration, on the other hand, indicated that time of day significantly predicted iTBS-induced plasticity (Corp et al. 2020).

This may indicate that rather than showing different levels of excitability at certain times of day as measured using RMTs, the brain may have a greater plasticity response to the same level of excitation across the day.

5.4.2 Effect of inter-clinic differences

It is notable that our initial analysis, without accounting for inter-clinic variability, did suggest an effect of time of day which then disappeared after controlling for clinics. This highlights that it is important to control for possible methodological differences between clinics when pooling TMS data from multiple clinics. Some predictors of neural responses to TMS identified by the Big TMS Data Collaboration such as TMS machine and its pulse waveform (Corp et al. 2020) (Corp et al. 2021) were controlled for in this data set since all data were collected using the Magstim Horizon 3.0 system. However, the definition of motor threshold, i.e. which muscle is targeted (first dorsal interosseous vs abductor pollicis brevis) and which method is used to measure it (visible twitch, 5/10 MEPs etc.), may differ between clinics (McClintock et al. 2017). Visible twitch thresholds have been shown to be up to 25% higher than thresholds recorded using EMG (Westin et al. 2014), thus, these parameters need to be established to ensure comparability of motor thresholds across clinics. This can have important implications for TMS treatments since a difference of 25% in the estimation of thresholds could result in the application of much higher or lower intensities than intended. On one side, higher stimulation intensity relative to individual motor thresholds may lead to superior clinical outcomes (Tendler et al. 2023). On the other side, safety guidelines for TMS parameters have been established on the basis of resting motor thresholds that are measured using EMG (Rossi et al. 2021). Thus, applying stimulation based on visible twitch thresholds may result in intensities beyond the safety limits which could lead to accidental seizures (Westin et al. 2014). The lack of correlation between the number of patients in a clinic and their average motor thresholds suggests that the lower average RMT in Clinic 1 is not due to the clinic treating more patients and therefore being more 'experienced' in applying TMS than clinics with smaller numbers of patients.

5.4.3 Additional factors of variability

Compared to healthy participants, depression patients could have altered cortical excitability time courses due to the effects of antidepressant medication or disruption of sleep. Early morning awakening, later sleep times and daytime fatigue are frequently reported in depression (Vadnie et al. 2017). Further circadian factors such as the cortisol awakening response (Law et al. 2020) are known to be altered in depression (Dedovic et al. 2015), therefore likely contributing to the observed variance. To fully rule out any effects of time of day in clinical practice, future clinical studies should collect multiple RMT values per patient at time points spanning the working day to allow a within-participant analysis. Factoring in other variables, including age, gender, menstrual cycle and hormonal levels, will also be important to identify potential interactions with any effects of time of day on RMT. Nevertheless, the lack of a significant effect in this large data set suggests that any influence of time of day will be subtle and perhaps not clinically significant.

5.4.4 Limitations

While our study benefited from having a large number of individual data points collected in clinical practice and spread across the clinical working day, it is possible that the large inter-individual variability in RMTs masked more subtle effects of time of day in our analysis. Further, the distribution of the measurement times of the whole data set displays a skew towards the morning in the measured time points (Fig. 5.1 (b)). In the analysis, this skew is to some extent accounted for by comparing the time of day fit to a shuffled association between time stamps and RMTs, since the shuffled control data set retains the time stamps of the original data set.

5.5 Conclusions and contributions

In this study, I analysed a large data set of resting motor thresholds across the day collected from depression patients across different clinics. The findings showed that large differences between clinics and their testing schedules explained the

majority of the time of day effects on resting motor thresholds present in the data. Consistent methods across clinics and repeated measures for individual patients will be essential to investigate this further in future studies. The use of linked TMS devices could help monitor for systematic differences between clinics, allowing for actions to be taken to address these.

6 General discussion

Contents

6.1 Summary

Our group has introduced a new TMS device, called the programmable TMS or pTMS, which uses pulse-width modulation to rapidly switch between voltage levels. This allows the generation of stimulation pulses which can approximate any arbitrary shape with improved energy recovery, enabling higher repetition rates. This ability increases the flexibility of TMS parameters compared to conventional and other state-of-the-art devices. The stimulation pulses generated by the pTMS have a

high-frequency content (> 10 kHz) which conventional TMS stimuli do not have to the same extent. The targeted neurons are expected to filter out the high-frequency components due to their low-pass filtering properties (cut-off frequency of around 1 kHz) which would result in an equivalent effect of the PWM pulses on neurons as compared to conventional TMS pulses.

The aim of this thesis was (a) to validate this transcranial magnetic stimulation device using computational modelling and to substantiate the computational modelling in an in-human study, (b) to explore a novel stimulation protocol and (c) to address the variability observed in TMS by investigating its sources in clinics. In this section, I will summarise how these aims have been achieved.

In Chapter 2, I used computational modelling to compare the neuronal response to stimuli generated by the pTMS device and by a conventional transcranial magnetic stimulator. I first employed a simple linear model to approximate the subthreshold dynamics of a neuronal membrane to estimate how pulse-width modulated stimuli affect the membrane potential compared to conventional sinusoidal pulses. Next, I utilised a morphologically-realistic computational model incorporating the spatial and non-linear temporal dynamics of neurons to quantify the activation thresholds of different cortical neurons across the different layers of the primary motor cortex. For both monophasic and biphasic pulses, these models predicted highly correlated thresholds for conventional waveforms and their pulse-width modulation approximations, indicating that the PWM pulses approximate the neural activation by conventional pulses very closely. Additionally, the slope of the linear regression lines suggested that the energy required to stimulate a desired neuron population is lower for the PWM pulses than for the conventional pulses.

Next, in Chapter 3, I validated the pTMS and the computational modelling results in the human primary motor cortex. For this, I designed, applied for ethical approval and conducted a study comparing the effects of pulse-width modulated and conventional pulse forms on different physiological measures using motor evoked potentials. This formed the first in-human study of the pTMS device which was completed successfully without any adverse events and demonstrated the ability of

the pTMS device to stimulate the human nervous system. Comparing the resting motor thresholds of twelve healthy participants showed a strong correlation between the thresholds of the different TMS devices, with thresholds that were approximately 3% of the maximum stimulator output lower for the PWM pulses, consistent with the trend suggested by the modelling results in Chapter 2. Furthermore, the measured motor responses suggested no difference in MEP latencies or input-output curve slopes between the pulse types. Together, Chapter 2 and 3 gave confidence in the assumptions underlying the pTMS device and demonstrated that it can stimulate cortical neurons with similar effects to a conventional stimulator.

The successful completion and encouraging results from the validation studies thus allowed me to conduct a study using a so-far untested stimulation protocol, monophasic theta burst stimulation. Due to the high repetition rate of TBS, a large percentage of the energy needs to be recovered after each pulse which conventional stimulators can only achieve using a biphasic pulse shape. However, it has been hypothesised that monophasic pulse shapes may be superior at inducing plasticity since their single phase of stimulation may achieve a cleaner, more uniform activation of neuron populations. The pTMS device enables the generation of monophasic high-repetition protocols, as it allows the recovery of energy independent of the pulse shape. In Chapter 4, I tested the effects of monophasic intermittent theta burst stimulation on the corticospinal excitability of 30 healthy participants and compared the induced plasticity effects with the conventional biphasic stimulation protocol and an anatomical control condition. The results indicated that (a) both monophasic and biphasic intermittent theta burst stimulation increased motor corticospinal excitability as measured using MEPs, (b) the PWM pulses generated with the pTMS device enabled this plasticity induction and (c) monophasic induced larger plasticity effects than biphasic theta burst stimulation. These findings hold promise for improving the currently available stimulation protocols while also demonstrating the value of the increased parameter space enabled by the pTMS.

Finally, in Chapter 5, I explored the sources of variability of resting motor thresholds in a large data set collected from TMS clinics across the US with the

goal of addressing the variability observed in treatment outcomes. In accordance with some earlier studies identifying time of day as a potential source of variability in the neural response to TMS, I investigated the effects of time of day on resting motor thresholds collected from 1550 patients from 60 different clinics. The results indicated that the majority of the observed differences in thresholds across the day were due to differences between clinics and their treatment schedules. This highlights how variable measurements as simple as resting motor thresholds can be across clinics and underlines that methodological differences need to be considered when comparing TMS measures and effects across clinics. Since motor threshold measurements commonly determine the stimulation intensity for treatment protocols, differences in the measurements may influence treatment outcomes and impact the safety of the stimulation.

Taken together, this thesis describes the validation of the programmable TMS, a pulse-width modulation-based TMS device with an extended parameter set, and successfully demonstrates its enhanced capabilities. The results helped inform and guide the design of the xTMS, the final device prototype now licensed by Magstim and used by other researchers.

6.2 Generalisability and limitations of findings

6.2.1 pTMS limitations

The pTMS device used in this thesis was limited in its output power and required the exclusion of participants with high thresholds. Therefore, the generalisability of the results to higher threshold populations, in particular individuals of older age and patients, remains to be tested. However, the amplitude of the pTMS is not an in-principle limitation of the pTMS architecture but merely a technical feature of the current prototype. It could be increased by cascading additional H-bridges, although these come with the trade-off of increased complexity, size and cost of the device. For instance, a recent prototype from Duke University cascades ten H-bridge modules to generate high-amplitude ultra-brief pulses (from 8.25μs active electric field phase), reaching peak coil voltages and currents of 11 kV and 10 kA, respectively (Zeng et al.

2022). The high output power ensures the ability to stimulate populations with high motor thresholds. Additionally, applying ultra-brief pulses shifts the frequencies of the sound of the TMS pulse beyond the upper limit of human hearing (Zeng et al. 2022), a feature which may help control for the auditory confounds in TMS. However, the large number of H-bridges has practical implications by increasing the device cost and size which may make it difficult to use widely as a research tool. Thus, the value of increased output power needs to be weighed against its trade-offs depending on the application and any practical limitations.

Besides the temporal component of the stimulation which the pTMS device focusses on, another important factor in TMS is the spatial component, as this determines which brain areas can be stimulated. The spatial stimulation characteristics are largely determined by the stimulation coil and ongoing research is addressing this using innovative multi-locus stimulation coils, where multiple independently controlled H-bridge circuits connect to several overlapping coils (Koponen et al. 2018) (Nieminen et al. 2022). More control over the spatial characteristics of TMS pulses improves for example the ability to map structure-function relationships which can help answer fundamental neuroscientific questions as well as be used in clinics e.g. for surgical planning (Weise et al. 2020).

6.2.2 Value and limitations of validation studies

The validation of the pTMS device in Chapters 2 and 3 is an important first step towards using the device routinely in research which can also be translated to other state-of-the-art devices. In particular, devices that approximate conventional TMS pulses with fast switching circuits will encounter the same question of equivalent stimulation effects. Rectangular pulses as generated by the cTMS device (Peterchev et al. 2014) have already been used in several studies without adverse events, enabling explorations of the effects of different pulse widths and shapes (D'Ostilio et al. 2016) (Hannah et al. 2017) (Sommer et al. 2018). However, to date, the validations in this thesis have been the first to directly compare neural responses of conventional TMS pulses to their PWM approximations.

Nonetheless, while the modelling validation incorporated the latest available computational model combining morphologically-realistic neuron models with electric field estimations, it did not consider the effects of the stimulation pulses on non-neuronal elements. Glial cells, such as astrocytes and adult neural stem cells, also have the ability to respond to electrical activity but are rarely considered in the context of TMS, although the observed stimulation effects may arise at least partially from secondary activation of glial cells (Cullen et al. 2016). Thus, the high-frequency components of PWM pulses may affect glial cells differently from neurons which would not be evident from the computational modelling results. Yet, the in-human validation in Chapter 3, although conducted on a relatively small sample, did not show any effects that would suggest any differences. Further investigations into the effects of TMS pulses on glial cells are required to fully understand any differences between PWM and conventional pulses.

6.2.3 Limitations in study design

Ethical and safety considerations required the first in-human studies of the pTMS device to employ stimulation parameters that are routinely used in TMS such as the monophasic and biphasic stimulation pulses generated by conventional stimulators. This limited the risk of unexpected effects of the new device but also limited the possibilities in the study design in this thesis. Going forward, interesting research questions arise when changing the individual stimulation waveforms, for example by comparing the effects of different pulse widths and shapes (e.g. square pulses versus sinusoidal pulses) in both single and repetitive protocols. These parameters are being investigated in upcoming studies enabled by the pTMS principles as discussed in Section 6.3.1.

6.2.4 Generalisability of monophasic effects to other brain areas

The results in Chapter 4 expand the literature demonstrating larger plasticity effects in repetitive TMS when using monophasic pulses. In 1 Hz rTMS (Taylor

et al. 2007), 10 Hz rTMS (Arai et al. 2007) and QPS (Nakamura et al. 2016), monophasic pulses had already been shown to increase effects which raises the possibility that monophasic pulses should generally be used over biphasic pulses to induce plasticity. However, whether these effects translate to other brain areas that are of interest in treatments is currently unknown. Neuroanatomical and neurophysiological differences between the primary motor cortex and other cortical areas, such as the DLPFC, limit the generalisability of stimulation effects found in the motor cortex (Siebner et al. 2022). Therefore, future studies will be required to assess the effects of monophasic TBS on the DLPFC and clinical studies are needed to investigate the possibility of monophasic iTBS as a treatment protocol.

6.2.5 Challenges and possible methods to search for optimal stimulation parameters

The increased plasticity effect when using monophasic pulses also highlights that the currently used treatment protocols arose largely from what is technically feasible rather than what might be biologically optimal. Newer, more flexible TMS devices enable the possibility of finding more effective and efficient stimulation protocols. Yet, this increase in the number of possible parameter combinations also increases the complexity of finding suitable stimulation parameters, making manually searching the parameter space inefficient and not feasible. To utilise the full potential of the new devices, different methods may be used to help explore the parameter space efficiently. For single pulses, optimisation approaches such as Bayesian optimisation, which help sample the parameter space in a more efficient way (Lorenz et al. 2019), or control-theoretic system identification frameworks, which learn the input-output dynamics of the brain (Yang et al. 2018), may be possible ways forward. For this, parameters can be evaluated by combining TMS with sensors in an adaptive stimulation setting, providing a real-time readout. However, this approach is limited by the availability and often low signal-to-noise ratio of biomarkers that accurately indicate the effect of the stimulation. Additional help may come from computational models for example to estimate the effects of different parameters

in repetitive TMS protocols. Nevertheless, advancements in the fundamental understanding of the underlying mechanisms of TMS will be critical to discovering more optimal stimulation parameters.

6.2.6 Consistent methods may reduce variability

The findings in Chapter 5 highlight differences between clinics and underline the importance of standardisation of methods. International safety guidelines (Rossi et al. 2009) (Rossi et al. 2021) and clinical recommendations (Lefaucheur et al. 2014) (Lefaucheur et al. 2020) exist, but for some methods there is no clear consensus, or practical limitations result in deviations from the established methods. Internet-connected TMS stimulators, which allow automated data collection such as the data explored in Chapter 5, can be used by manufacturers to engage with the clinics, e.g. to identify good and suboptimal practices. For example, leveraging additional data, such as records of the localisation of the stimulation coil during pulse firing, could provide information on the targeting accuracy of a clinic which could then be followed up with further training if needed. This could help improve clinical practice and thus might even improve treatment efficacy across clinics.

6.3 Next-generation device: xTMS

The work in this thesis guided and supported the development of the next-generation device, the xTMS, which was developed in collaboration with the Power Electronics Group in Oxford, led by Prof. Dan Rogers.

The xTMS was built on the same concepts as the pTMS but was optimised further to address some drawbacks that emerged from the pTMS design. First, the xTMS was built using a fully modular design, cascading three H-bridge modules to generate stimulation pulses with seven voltage levels, improving the approximation of the reference pulses. Yet, even with more voltage levels, carrier-based pulse-width modulation suffers from large deviations from the pulse reference due to limitations on the switching frequency of commercial IGBTs and large DC-link voltage drops in TMS pulse generation (Ali et al. 2023). Thus, to improve the approximation

of reference pulses compared to the pTMS, the xTMS device is controlled by an offline model predictive control (MPC) algorithm, which is an optimisation approach that automatically determines the switching sequence to generate the target pulses, subject to the constraints of the system. For this, a state-space model of the system is built, incorporating the circuit elements including the stimulation coil, and the desired coil current is fed in as a reference. The MPC algorithm takes in the states of the system and calculates the optimal switching states at each time step up to a pre-defined horizon (Ali et al. 2023). This is done in an offline fashion and the switching sequence for the output pulse is stored in a library which can then be retrieved quickly to generate the pulse when needed. The algorithm takes a maximum number of IGBT switching events into account and does not allow the DC-link capacitors to become too unbalanced (Ali et al. 2023). As a result, the stimulation pulse approximates the reference waveform as closely as possible while adhering to the switching and capacitor voltage balance constraints. Additionally, the xTMS includes an output filter before the stimulation coil which helps attenuate the high-frequency components of the stimulation pulse introduced by the fast switching between voltage levels. Fig. 6.1 (a) shows the final xTMS prototype.

The MPC and the control of the xTMS device are implemented on a field-programmable gate array (FPGA) which can be interfaced with through Python via a Secure Shell (ssh), a network communication protocol. To address the limitation of the pTMS where the intensity needed to be adjusted manually, all stimulation parameters, including the intensity, of the xTMS are fully controlled using the software interface. To simplify the control of the xTMS for our first lead users, I built a graphical user interface (GUI) in Python that allows the operator to set the relevant stimulation parameters by clicking a range of buttons, similar to existing TMS devices (Fig. 6.1 (b)). The GUI allows the selection of different pulse shapes and widths with different polarities and generates all commonly used stimulation protocols, including single pulses, paired pulses, rTMS at different frequencies, theta burst stimulation and quadripulse stimulation. Fig. 6.2 shows recordings of a set of pulses generated by the xTMS device. Compared to the pulses generated by the

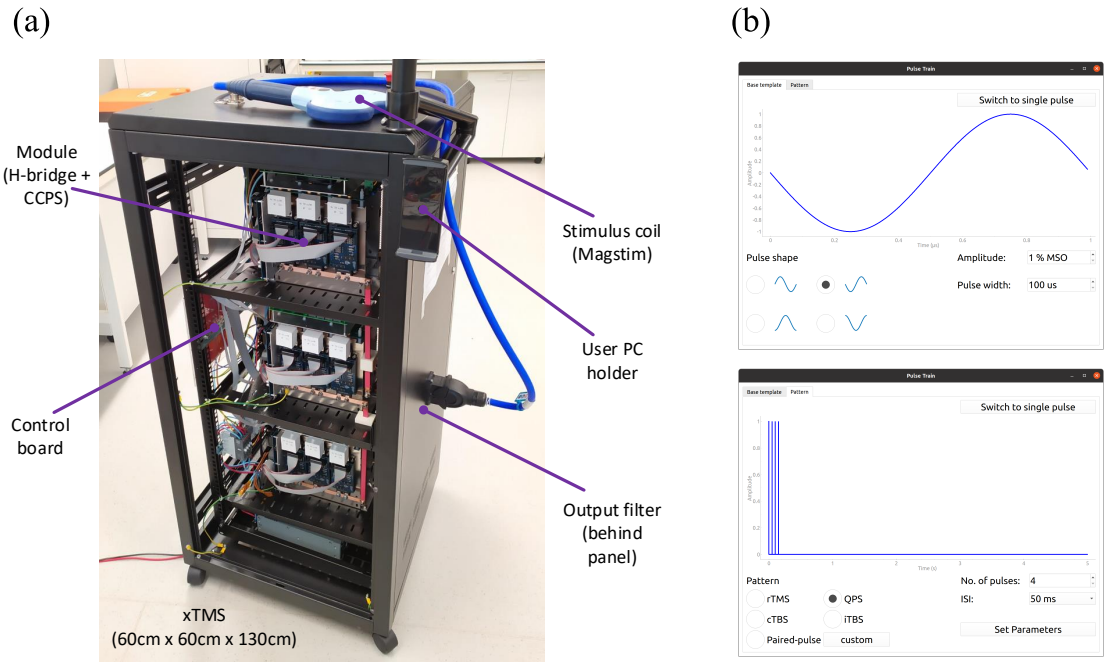

Figure 6.1: Overview of the xTMS device and the graphical user interface. **(a)** The xTMS device was built with a modular design consisting of three H-bridge modules and an output filter. The stimulation coil connected to the xTMS is a figure-of-8 coil from Magstim. Reproduced from (Ali et al. 2023) ©2023 IEEE. **(b)** The graphical user interface is used to control the xTMS from a user tablet. In the first window, the user can select different pulse shapes, their polarity, width and amplitude. The second window allows the selection of all commonly used stimulation protocols, including single pulses, rTMS at different frequencies, quadripulse stimulation (QPS), theta burst stimulation (TBS) and paired pulses, together with their relevant parameters such as the number of pulses and inter-stimulus intervals (ISI).

pTMS (Fig. 1.15), the coil voltage of the xTMS shows seven voltage levels which have been smoothed out to some extent by the output filter. The recorded coil currents show close approximations of the reference waveforms.

To summarise, the xTMS achieves a high degree of flexibility in generating TMS pulses and patterns. It can approximate any arbitrary pulse shape and width and repeat them at high frequencies in arbitrary patterns, as long as it is within the electrical limits of the device, which is restricted by the capacitor energy, peak current and peak voltage (Ali et al. 2023). It can deliver up to 1.5 kV pulses, which currently limits its ability to stimulate participants with high thresholds and with short stimulation pulses but this is not a fundamental limitation as it could be increased by adding further H-bridge modules. Additionally, the xTMS has

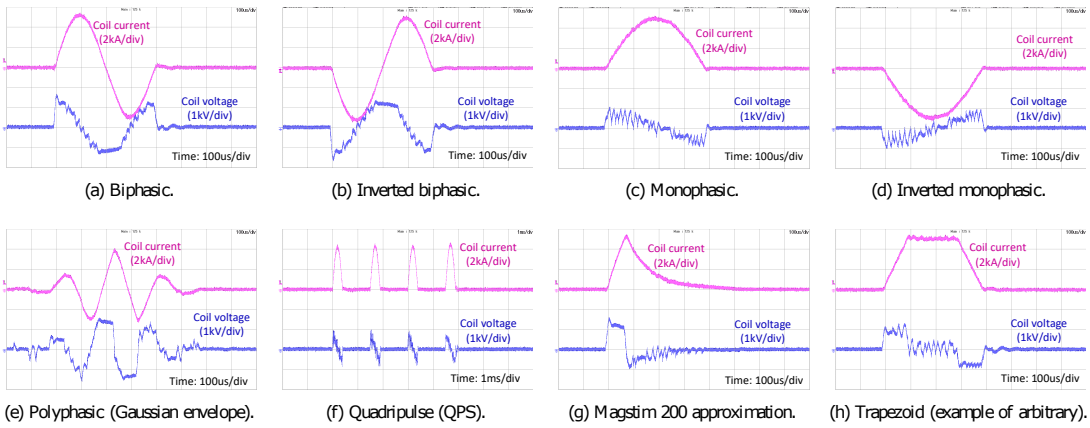

Figure 6.2: Recordings of example pulses generated by the xTMS, showing its capability of generating arbitrary pulse shapes. **(a)** and **(b)** show biphasic sinusoidal pulses with opposite polarities, **(c)** and **(d)** show monophasic pulses with opposite polarities, **(e)** shows a polyphasic pulse, **(f)** shows four monophasic pulses as used in quadripulse stimulation, **(g)** shows the approximation of a monophasic pulse generated by a Magstim 200 and **(h)** shows a trapezoidal pulse. For each pulse, the coil voltage is shown in blue and the coil current is shown in pink. Reproduced from (Ali et al. 2023) ©2023 IEEE.

full software control over the stimulation parameters, including over the direction of the current induced in the brain.

6.3.1 Research enabled by the xTMS

As part of my DPhil, I supported the testing of the xTMS device and worked with our lead users in Oxford, Cambridge and London to generate and test new protocols of interest. With the results of the modelling validation and in-human validation of the pTMS and the theta burst stimulation study presented in this thesis, the pTMS and the xTMS were approved for use in other studies in healthy participants and a study in patients in Oxford. This section outlines the currently implemented and planned protocols.

6.3.1.1 Validation of monophasic iTBS results

As part of the MRC Networking call, our group collaborates with researchers at the MRC Cognition and Brain Sciences Unit (MRC CBU) at the University of Cambridge and the MRC Centre for Neurodevelopmental Disorders (MRC CNDD) at King's College London. Within this collaboration, the MRC CBU plan to evaluate the effect of different stimulation protocols generated by the xTMS using magnetic

resonance imaging (MRI) and EEG measures. Since motor evoked potentials only serve as a readout of stimulation effects in the motor cortex, EEG and MRI will be instrumental in assessing the effects of xTMS pulses and especially of monophasic TBS in other brain areas. In particular, the interest lies in using TMS-evoked potentials, an EEG measure that can be used to assess excitability, to validate the increased plasticity effects of monophasic iTBS over biphasic iTBS that I demonstrated in Chapter 4. Additionally, magnetic resonance spectroscopy can be used to investigate the effects of TMS protocols on the level of neurotransmitters such as gamma-aminobutyric acid (Cuypers et al. 2021). Using this to compare the effects of monophasic and biphasic TBS with sham stimulation will give further insights into the mechanisms of action underlying the pulse shapes and protocols.

6.3.1.2 Cognitive effects of monophasic iTBS

Building on the results of the monophasic iTBS study in Chapter 4, another study has been approved by Oxford's local ethics committee and will be conducted in Prof. Jacinta O'Shea's lab. In this study, monophasic and biphasic iTBS will be applied to the left DLPFC (active condition) in participants with low mood and its effects on task performance in a facial expression recognition task will be evaluated and compared to the performance after a sham TBS condition. The task assesses participants' ability to distinguish between negative and positive emotions which has been shown to be biased towards negative emotions in depression. A reduction in the negative bias would indicate a positive effect of iTBS on emotional face processing. This study therefore aims to test whether the increased plasticity effects of monophasic iTBS observed in the motor cortex translate to cognitive effects when stimulating the DLPFC.

6.3.1.3 Effects of pulse shapes and widths in rTMS

A first study using the xTMS has already been completed in Prof. Charlotte Stagg's lab, leveraging the xTMS's flexibility in generating pulses of different widths and repeating them at high frequencies. The aim of the study was to find stimulation pulses that more optimally engage the frontal-vagal pathway. For this, the study

used heart-rate monitoring to measure target engagement when stimulating the DLPFC since accurately targeting the subgenual anterior cingulate cortex (indirectly through the DLPFC) leads to activation of the vagus nerve, modulating heart rate (Iseger et al. 2020). 10 Hz rTMS protocols with monophasic and biphasic pulses of different widths were generated using the xTMS and the level of heart-brain coupling was compared across protocols. In this study, the xTMS approximated the stimulation pulses of several different conventional stimulators, including the Mag&More Apollo, the Deymed XT35, the Magstim Rapid^2, the MagVenture MagPro and the Magstim 200, allowing the direct comparison of their pulse shapes while keeping the other parameters and the stimulation coil constant.

6.3.1.4 Effects of pulse shapes and widths using single pulses

On a single-pulse level, the increased control over TMS pulse shapes allows the investigation of strength-duration curves of cortical neurons, similar to what has been studied using electrical stimulation in the peripheral nervous system (D'Ostilio et al. 2016). Studies using the cTMS device have revealed physiological insights into the properties of distinct cortical neuronal populations (D'Ostilio et al. 2016) (Sommer et al. 2018), however, the pulse widths have so far been limited to 0.03 to 0.12 ms for TMS. The xTMS offers the opportunity to increase this range to enable direct comparisons with electrical stimulation measurements of the peripheral nervous system, which use pulses with widths of up to 1 ms (Siebner et al. 2022). Our collaboration partners at the MRC CNDD are planning future studies using the xTMS to investigate this.

6.3.1.5 Responsive stimulation in patient population

Finally, a study investigating the effects of TMS pulses synchronised to the frequency of hand tremors in Parkinson's Disease and Essential Tremor patients has been approved under the supervision of Dr Ashwini Oswal. In this study, the tremor of the patient's hand is measured using an accelerometer in real time and the stimulation pulses are triggered at different phases of the tremor oscillation with the aim of finding the phase that maximally suppresses the amplitude of the tremor.

The study therefore follows a responsive stimulation approach, optimising the timing of the stimulation. For this, the tremor oscillation is used as a biomarker, which is classified into its different phases and then used to try to stimulate the brain at potentially more optimal time points. Once implemented, this concept will be applicable to other applications using different sensors such as EMG and EEG which can be used to classify biomarkers and inform the timing of the stimulation.

6.4 Concluding remarks

In this thesis, I demonstrated and validated the capabilities of a next-generation TMS device, to firstly mimic the stimulation effects of conventional stimulators and secondly to expand the parameter set to new stimulation protocols with the potential to have stronger effects on the stimulated neurons. Additionally, I discussed the variability observed in TMS measures and explored their sources in a clinical data set. The pTMS and the next-generation xTMS devices will provide researchers with an enhanced tool to probe and perturb the nervous system. My contributions help to make this tool accessible to other researchers by demonstrating its validity and value in going beyond the limits of conventional stimulators, as indicated by the list of ongoing and planned studies using the xTMS. Together with the continuous research in other groups on stimulator design, including on spatial aspects of TMS, these enhanced stimulators offer the opportunity to characterise currently unexplored dynamics of the brain as well as improve clinical protocols in the future.

Appendices

A

TMS study documents

Contents

A.1 Step-by-step study procedures

A.1.1 In-human validation study

Participant ID: RMT Magstim:
Date: pTMS mono:
Session no:

Lab Setup	*Turn on PCs* Signal PC Neuronav Mac computer Switch on Magstim machine – plugs at wall
	Check connections Check machine plugged in and coils appropriately plugged in. Check appropriate connections for trigger at 1401 machine
	Start software Signal PC – D440 monitoring software, Signal 7.0, load first configuration Neuronav mac – Brainsight
Meet Participant	Meet participant at door and screen for Covid symptoms – Covid sheet
	Give participant mask, Sanitise hands
NIBS LAB	Keep window and door open
	Ask participant to enter the lab and sit down on chair closest to window; researchers sit on other 2 chairs and need to make sure these are at 2m distance
	Sanitise hands (researchers and participant)
	Ask participant to complete **symptom checklist**
	Ask for **contact details** for contact tracing
	Explain study and take **consent**
	Go through TMS **safety questionnaire**
	Study questionnaires: **Handedness**
	Payment Details
	Ask if participant needs comfort break
	Sanitise hands, put on PPE
Measure head	Measure head, mark left M1
EMG setup	Clean hand with abrasive tape and alcohol wipes
	Surface EMG electrodes • ground – styloid process of ulna ↔ black port • tendon – medial aspect of index finger↔ red port • muscle belly – on bulk of FDI↔ blue port
Neuronav setup	Put head tracker on participant
	Configure Neuronavigation
Run study	Hotspot determination by moving coil around marked M1 spot, observing MEP trace – using Magstim, save in Neuronav
	RMT measurement – Magstim or pTMS first, then repeat with other Start at previous intensity, reduce until intensity which elicits 5/10 MEPs
	IO curve measurement – Magstim or pTMS first, then repeat with other Starting low, apply 15 pulses, then increase by 3% until MSO
	Ensure participant comfortable, check if needs break
Save data	Sanitise hands
	Bring participant to exit, person closest to door leaves first to maintain 2m
Cleaning	Wipe down all surfaces and the TMS machines – Cleaning sheet
	Store forms in cabinet

A.1.2 Effect of pulse shape in TBS study

Participant ID: TBS type: RMT Magstim:
Date: pTMS:
Session no:

Previous RMT	*Magstim:* *pTMS:* *120% RMT:*
Lab Setup	*Turn on PCs* Signal PC Neuronav Mac computer Switch on Magstim machine – plugs at wall
	Check connections Check machine plugged in and coils appropriately plugged in. Check appropriate connections for trigger at 1401 machine
	Start software Signal PC – D440 monitoring software, Signal 7.0, load first configuration Neuronav mac – Brainsight
Meet Participant	Meet participant at door and screen for Covid symptoms – Covid sheet
	Give participant mask, Sanitise hands
NIBS LAB	Keep window and door open
	Sanitise hands (researchers and participant)
	Explain study and take **consent**
	Go through TMS **safety questionnaire**
	Study questionnaires: **Handedness**
	Ask if participant needs comfort break
	Sanitise hands, put on PPE
Measure head	Measure head, mark left M1
EMG setup	Clean hand with abrasive tape and alcohol wipes
	Surface EMG electrodes • ground – styloid process of ulna ↔ black port • tendon – medial aspect of index finger↔ red port • muscle belly – on bulk of FDI↔ blue port
Neuronav setup	Put head tracker on participant
	Configure Neuronavigation, save vertex hotspot
Run study	**Hotspot** determination by moving coil around marked M1 spot, observing MEP trace – using Magstim, save in Neuronav
	RMT measurement – Magstim & pTMS first Start at previous intensity, reduce until intensity which elicits 5/10 MEPs
Timings	Baselines at -5, -10, TBS at 0, post-TBS at 5, 10, 15, 20, 30, 40, 50, 60 mins
	Baseline: apply 30 pulses at 120% RMT - Magstim
	TBS: monophasic: adjust to 70% of RMT - pTMS biphasic: same as RMT (configured in software)
	Post-TBS: apply 30 pulses at 120% RMT - Magstim
	Ensure participant comfortable, check if needs break
Save data	Sanitise hands
	Bring participant to exit, person closest to door leaves first to maintain 2m
Cleaning	Wipe down all surfaces and the TMS machines – Cleaning sheet
	Store forms in cabinet

A.2 TMS safety screening

Department of Psychiatry
Warneford Hospital
Oxford OX3 7JX

Brain Stimulation Safety Screening Form (Confidential)

If you agree to take part in this study, please answer the following questions. The information you provide is for screening purposes only and will be kept completely confidential

1.	Do you have epilepsy, or have you ever had a convulsion or a seizure (fit)?	YES	NO
2.	Has anyone in your wider family suffered from seizures?	YES	NO
	If YES please state your relationship to the affected family member _____		
3.	Have you ever had a fainting spell or syncope?	YES	NO
	If YES please describe on which occasion(s) _____		
4.	Have you ever had a head trauma that was diagnosed as a concussion or was associated with loss of consciousness?	YES	NO
5.	Do you have any hearing problems or ringing in your ears?	YES	NO
6.	Do you have cochlear implants?	YES	NO
7.	Are you pregnant, or is there any chance that you might be?	YES	NO
8.	Do you have metal in the brain, skull or elsewhere in your body (e.g., splinters, fragments, clips, etc.)?	YES	NO
	If YES, specify the type of metal and where it is located _____		
9.	Do you have an implanted neurostimulator (e.g. DBS, epidural/subdural, VNS)?	YES	NO
10.	Do you have a cardiac pacemaker or intracardiac lines?	YES	NO
11.	Do you have a medication infusion device?	YES	NO
12.	Are you taking any prescribed or unprescribed medications (or herbal remedies)?	YES	NO
	If YES, please list _____		
13.	Did you ever undergo TCS or TMS in the past?	YES	NO
	If YES, please state if there were any problems and describe them _____		
	_____		

(Based on Screening13-item Questionnaire for rTMS Candidates recommended by Rossi, Hallett, Rossini and Pascual-Leone 2011; updated 15 Dec 2015)

Department of Psychiatry
Warneford Hospital
Oxford OX3 7JX

When was your last TMS/TCS session? _____

How many TMS/TCS sessions have you had in the past month? _____

How many TMS/TCS sessions have you had in the past 12 months? _____

1. Did you ever undergo MRI in the past? YES NO
   If YES, please state if there were any problems and describe them _____
   _____

2. Have you ever undergone a neurosurgical procedure (including eye surgery)? YES NO
   If YES, please give details _____
3. Are you currently undergoing anti-malarial treatment? YES NO
4. Have you drunk more than 3 units of alcohol in the last 24 hours? YES NO
5. Have you drunk alcohol already today? YES NO
6. Have you had more than one cup of coffee, or other sources of caffeine, in the last hour? YES NO

20. How much liquid in total have you drunk already today?_____ ml
21. When was your last meal? _____ hours ago
22. Have you used recreational drugs in the last 24 hours? YES NO
23. How many hours sleep did you have last night? _____

I (please give full name in CAPITALS) _____ confirm that I have personally completed the above questionnaire.

Signature _____ Date _____

Please note: All data arising from this study will be held and used in accordance with the Data Protection Act (2018). The results of the study will not be made available in a way that could reveal the identity of individuals.

(Based on Screening13-item Questionnaire for rTMS Candidates recommended by Rossi, Hallett, Rossini and Pascual-Leone 2011; updated 15 Dec 2015)

A.3 Study participant information sheet

Department of Psychiatry
Warneford Hospital
Oxford OX3 7JX

Principal investigator: Dr Jacinta O'Shea
E-mail: jacinta.oshea@psych.ox.ac.uk
Primary researcher: Karen Wendt, DPhil student
E-mail: karen.wendt@some.ox.ac.uk

In-human validation of a novel non-invasive brain stimulation device in healthy adults

A transcranial magnetic stimulation (TMS) study

PARTICIPANT INFORMATION SHEET

Ethics Approval Reference: R75180/RE006

We would like to invite you to take part in a research project. This sheet provides some information to help you decide whether to do so. Please take time to read this carefully and discuss it with friends, family or your GP if you wish. If there is anything that you do not understand, or if you would like more information, please ask us. Please take time to consider whether you wish to take part.

What is the purpose of the research?

We are interested in comparing our new brain stimulator to a commonly used stimulator. The stimulation we use is called Transcranial Magnetic Stimulation (TMS) which can stimulate the brain by placing a stimulation coil over the head which generates a magnetic field. TMS is an approved treatment for depression and has the potential to treat a range of other diseases.

We are interested in demonstrating that our new TMS device can trigger muscle responses, such as a finger twitch, that are equivalent to muscle responses triggered by a conventional stimulator. We will use both devices to stimulate an area of the brain that is involved in muscle movement and measure the effects of these stimulations by recording the activity of muscles. These measurements will allow us to draw a comparison between the two stimulators and help us explore new stimulation treatments for depression and other neurological and psychiatric disorders in the future.

Why have I been invited?

You have been invited to take part in this research because you are healthy, between 18 and 45 years of age, right-handed and speak fluent English. For safety reasons we can only include volunteers without a family history of epilepsy and who are not currently taking any medication. We will be recruiting up to 60 participants in this research.

Do I have to take part?

No. It is up to you to decide if you want to take part in this research. We will describe the research, go through this information sheet with you, and answer any questions you may have. If you agree to take part, we will ask you to sign a consent form and will give you a copy for you to keep. However, you would still be free to withdraw at any time, without needing to give a reason. This would not affect

legal rights you would receive. If you are a student at the University of Oxford or Oxford Brookes, there would be absolutely no academic penalty if you decide you do not want to take part, or if you decide to withdraw at any point.

What will happen to me if I take part?

A researcher will contact you or meet you to go over the information sheet, safety screening, and explain the procedures. The researcher will go through a screening form with you to make sure that it is safe for you to participate in the research. If you are happy to continue they will then ask you to sign a consent form. This research includes a familiarisation session and 3 study visits (at least one week apart) to the Oxford Centre for Human Brain Activity at the Department of Psychiatry in Oxford. The familiarisation session takes no more than 1.5 hours and each study visit takes no more than 3 hours and follows the same structure of three blocks of stimulation. The stimulation protocols applied at each visit will be very similar.

During your visit we will use TMS to stimulate your brain by rapid switching of a magnetic field in a coil placed over the head. We will measure the effects of this stimulation by recording the activity of muscles (electromyography; EMG). EMG activity of the muscle is measured at the surface of the skin by attaching an electrode (small silver disc). Several electrodes will be taped on the skin over muscles on your hands. During TMS, a coil is positioned over the scalp and single pulses are used to stimulate the brain. In the first block, the intensity of stimulation is varied until the EMG recording consistently shows activity in the muscle in response to the stimulation. We will repeat this procedure with two different stimulation devices. Once we have determined the minimum intensity at which this muscle activity is observed, we proceed with the research.

In the next block, you will be asked to contract or relax your hand muscles while we will use TMS to stimulate your brain by applying single pulses and pairs of pulses (separated by less than a second) over the scalp. At the same time, the activity will be measured in your muscles using EMG.
In the third block of the session, we will use a patterned repetitive stimulation protocol called theta-burst stimulation which involves bursts of high-frequency (50 Hz) triplets applied every 200ms for 2 s periods, separated by 8 s of rest. The total stimulation time using this protocol will be 190 seconds (a total of 600 pulses). This stimulation could be in active or sham (i.e. no stimulation or stimulation of the top of the head) form. After this, we will apply single-pulse stimulation and measure the muscle responses for up to 60 minutes.
The total stimulation and recording time will be around 2 hours and the researcher will explain to you what to do before each measurement starts. We will take 5-minute breaks between stimulation blocks and any additional breaks within blocks as needed.

We will be using two stimulation devices for this research. One of the devices is CE marked (i.e. it has been assessed to ensure it meets EU safety, health and environmental protection requirements) and is routinely used in research studies. The other device has been developed in our research lab and is not CE marked, however it has been developed and undergone electrical safety testing according to the relevant standards for electrical medical devices. We expect both devices to have the same effect on the brain. This study will be the first time the second device will be tested on the human brain.

Participants may experience some discomfort during TMS. In susceptible individuals, TMS may cause headache, which usually responds well to over-the-counter painkillers (e.g. paracetamol) but remember you can always ask the researcher to stop the stimulation at any point if you become uncomfortable.

Before you take part in our research, we ask that you get a good night's sleep the night before, so that you are alert. Also, we ask you to refrain from excessive alcohol consumption (more than 3 units) the day before each visit and not to drink any alcohol on the day. We also ask that you refrain from use of recreational drugs before the visit. You may drink coffee or tea as normal but we ask that you do not

have a coffee for one hour before the visit. If you are unsure about any of the above, please discuss these with the researcher before taking part.

Are there any risks in taking part in this research?

TMS carries a risk of causing seizures (fits) in susceptible individuals. Seizures were reported in approximately 20 individuals worldwide between 1994 and 2009. This was across more than 6000 research studies and over 60,000 participants. In most cases the seizure was associated with a family history of epilepsy, existing neurological disease (e.g. multiple sclerosis) or medication (anti-depressant or dopamine medication). The risk of a provoked seizure occurring in healthy individuals due to TMS is extremely small. As a precaution, it may not be possible to give TMS to someone with a personal or close family (first-degree relative e.g. parent, sibling, child) history of epilepsy, another significant neurological or psychiatric disorder, or extreme mood fluctuations. If you are taking any medication, you should discuss this with the researcher beforehand. If you suffer with migraine headaches, you should not take part in this research.
Other possible side effects include discomfort underneath the stimulation coil, transient hearing changes or syncope. The table below summarises the relevant potential side effects of TMS according to an international safety study led by Rossi and colleagues in 2009. We will be taking measures to reduce these risks by screening participants, by providing ear plugs during the stimulation sessions and by adapting the coil position to minimise discomfort. To reduce the risk of a syncope, we will ensure that participants are feeling well and comfortable on the day and otherwise reschedule the session.

Side effect	**Single-pulse TMS**	**Paired-pulse TMS**	**Theta burst**
Seizure induction	Rare	Not reported	Possible
Syncope (fainting due to a decrease in blood flow to the brain)	Possible (not caused by the brain stimulation)	Possible (not caused by the brain stimulation)	Possible
Transient headache, discomfort under the coil, neck pain, toothache, prickling sensation	Possible	Likely possible	Possible
Transient hearing changes	Possible	Likely possible	Not reported
Transient cognitive/ neuropsychological changes	Not reported	Not reported	Transient impairment of working memory

How often an individual can safely participate in non-invasive brain stimulation research is unclear. Many studies use non-invasive brain stimulation to treat disorders (e.g. depression) and administer stimulation daily, as the therapeutic effects are thought to accumulate across periods of stimulation. Sessions separated by 48h do not show cumulative effects, however. To minimise the possibility of cumulative effects of brain stimulation for healthy participants not enrolled in treatment studies, we recommend that volunteers receive brain stimulation on a maximum of two consecutive days and four sessions in one month. While no guideline has been provided for “cooling-off” between stimulation periods, some have suggested it to be between 48 hours and one week after stimulation. Therefore, we recommend that you should not take part in another study using brain stimulation for at least one week after completing this study.

It is our policy not to give TMS to someone who is pregnant. If there is a possibility that you are pregnant, you must not take part in this research.

Are there any benefits from taking part in this research?

No. There will be no direct benefit to you from taking part in this research. It is hoped that the results from this research will help us to identify better treatments for future studies in patients with medical conditions such as depression and epilepsy.

Will my time/travel costs be reimbursed?

Yes. We will compensate you £10 per hour for your time plus reasonable travel costs for every session.

What will happen to the data provided?

The information you provide during the study is the **research data**. Any research data from which you can be identified is known as **personal data**. This includes more sensitive categories of personal data such as your racial or ethnic origin or data concerning your health. This study involves the collection of contact details, consent forms, screening forms and health information.

Your contact details will be stored in paper format in lockable file cabinets and in digital format on a secure password-protected firewall-protected university server. They will be deleted once all data has been analysed, unless you agree for your contact details to be kept by us for the purpose of contacting you for future studies.

Consent and screening forms will be stored on a password-protected firewall-protected university server for 5 years after final publication of the research. Signed paper consent forms will be stored for 5 years. Where possible, research data will be pseudonymised as soon as possible using an ID number. Only the DPhil student conducting the study (Karen Wendt) and the principal investigator (Dr Jacinta O'Shea) will have access to the code break. The code break will be destroyed after final analysis of the data.

The research team will have access to the research data. Responsible members of the University of Oxford may be given access to data for monitoring and/or audit of the research.

With your consent, we will keep your contact details on a secure database in order to contact you for future studies.

Will the research be published?

The University of Oxford is committed to the dissemination of its research for the benefit of society and the economy and, in support of this commitment, has established an online archive of research materials. This archive includes digital copies of student theses successfully submitted as part of a University of Oxford postgraduate degree programme. Holding the archive online gives easy access for researchers to the full text of freely available theses, thereby increasing the likely impact and use of that research.

The research will be written up as a thesis. On successful submission of the thesis, it will be deposited both in print and online in the University archives, to facilitate its use in future research. The thesis will be openly accessible.

We hope to publish the results of this study in a scientific journal. We may also present the results at a scientific conference or a seminar in a university. We may also publish results on our website. We would

be happy to discuss the results of the study with you and to send you a copy of the published results. It will not be possible to identify you in any report or publication.

Who has reviewed this research?

All research studies are checked by an ethics committee to ensure the research is conducted safely and to the best standards. This research has been reviewed by, and received favourable opinion from, the University of Oxford Central University Research Ethics Committee.

Who is organising and funding the research?

This research is led by Dr Jacinta O'Shea at the Department of Psychiatry and Karen Wendt, a PhD student. The research is funded by the Medical Research Council and the Wellcome Trust.

Who do I contact if I have a concern about the research or I wish to complain?

If you have a concern about any aspect of this research, please contact Karen Wendt (karen.wendt@some.ox.ac.uk) or Dr Jacinta O'Shea (jacinta.oshea@psych.ox.ac.uk), and we will do our best to answer your query. I/we will acknowledge your concern within 10 working days and give you an indication of how it will be dealt with. If you remain unhappy or wish to make a formal complaint, please contact the Chair of the Medical Sciences Interdivisional Research Ethics Committee (MS IDREC) at the University of Oxford who will seek to resolve the matter as soon as possible - Email: ethics@medsci.ox.ac.uk; Address: Research Services, University of Oxford, Wellington Square, Oxford OX1 2JD.

Data Protection

The University of Oxford is the data controller with respect to your personal data, and as such will determine how your personal data is used in the research.

The University will process your personal data for the purpose of the research outlined above. Research is a task that we perform in the public interest.

Further information about your rights with respect to your personal data is available from https://compliance.web.ox.ac.uk/individual-rights.

Further Information and Contact Details

If you would like to discuss the research with someone beforehand, or if you have any questions afterwards, please contact Karen Wendt on karen.wendt@some.ox.ac.uk.

References

Abboud Chalhoub, C., Awasthi, S., et al. (May 2020). "Optimizing the Effects of Theta-Burst Stimulation (TBS)". In: *Biological Psychiatry* 87.9, Supplement, S317. DOI: 10.1016/j.biopsych.2020.02.816.

Aberra, A. S. (2019). *TMSsim_Aberra2019*. Github. DOI: 10.5281/zenodo.3475608.

Aberra, A. S., Peterchev, A. V., and Grill, W. M. (Oct. 2018). "Biophysically realistic neuron models for simulation of cortical stimulation". In: *J Neural Eng* 15.6, p. 066023. DOI: 10.1088/1741-2552/aadbb1.

Aberra, A. S., Wang, B., et al. (2020). "Simulation of transcranial magnetic stimulation in head model with morphologically-realistic cortical neurons". In: *Brain Stimulation* 13.1, pp. 175–189. DOI: 10.1016/j.brs.2019.10.002.

Ali, K., Wendt, K., et al. (May 2023). "xTMS: A Pulse Generator for Exploring Transcranial Magnetic Stimulation Therapies". eng. In: *Conf Proc (IEEE Appl Power Electron Conf Expo)* 2023, pp. 1875–1880. DOI: 10.1109/apec43580.2023.10131554.

Amassian, V. E., Cracco, R. Q., et al. (Nov. 1989). "Suppression of visual perception by magnetic coil stimulation of human occipital cortex". In: *Electroencephalography and Clinical Neurophysiology/Evoked Potentials Section* 74.6, pp. 458–462. DOI: 10.1016/0168-5597(89)90036-1.

Arai, N., Okabe, S., et al. (Oct. 2007). "Differences in after-effect between monophasic and biphasic high-frequency rTMS of the human motor cortex". In: *Clinical Neurophysiology* 118.10, pp. 2227–2233. DOI: 10.1016/j.clinph.2007.07.006.

Arns, M., Drinkenburg, W. H., et al. (Oct. 2012). "Neurophysiological predictors of non-response to rTMS in depression". In: *Brain Stimulation* 5.4, pp. 569–576. DOI: 10.1016/j.brs.2011.12.003.

Awiszus, F. (Jan. 2003). "Chapter 2 TMS and threshold hunting". In: *Supplements to Clinical Neurophysiology*. Ed. by W. Paulus, F. Tergau, et al. Vol. 56. Elsevier, pp. 13–23. DOI: 10.1016/S1567-424X(09)70205-3.

Barker, A. T., Garnham, C. W., and Freeston, I. L. (1991). "Magnetic nerve stimulation: the effect of waveform on efficiency, determination of neural membrane time constants and the measurement of stimulator output". eng. In: *Electroencephalogr Clin Neurophysiol Suppl* 43. Edition: 1991/01/01, pp. 227–37.

Barker, A. T., Jalinous, R., and Freeston, I. L. (May 1985). "Non-invasive magnetic stimulation of human motor cortex". In: *The Lancet* 325.8437, pp. 1106–1107. DOI: 10.1016/S0140-6736(85)92413-4.

Bates, D., Mächler, M., et al. (July 2010). "Fitting Linear Mixed-Effects Models Using lme4". In: *Journal of Statistical Software* 67.1. Section: Articles, pp. 1–48. DOI: 10.18637/jss.v067.i01.

Berlim, M. T., van den Eynde, F., et al. (Jan. 2014). "Response, remission and drop-out rates following high-frequency repetitive transcranial magnetic stimulation (rTMS) for treating major depression: a systematic review and meta-analysis of randomized,

double-blind and sham-controlled trials." eng. In: *Psychological medicine* 44.2. Place: England, pp. 225–239. DOI: 10.1017/S0033291713000512.

Blumberger, D. M., Vila-Rodriguez, F., et al. (Apr. 2018). "Effectiveness of theta burst versus high-frequency repetitive transcranial magnetic stimulation in patients with depression (THREE-D): a randomised non-inferiority trial". In: *The Lancet* 391.10131, pp. 1683–1692. DOI: 10.1016/S0140-6736(18)30295-2.

Bossetti, C. A., Birdno, M. J., and Grill, W. M. (Dec. 2007). "Analysis of the quasi-static approximation for calculating potentials generated by neural stimulation". In: *J Neural Eng* 5.1, pp. 44–53. DOI: 10.1088/1741-2560/5/1/005.

Boucher, P. O., Ozdemir, R. A., et al. (Oct. 2021). "Sham-derived effects and the minimal reliability of theta burst stimulation." eng. In: *Scientific reports* 11.1. Place: England, p. 21170. DOI: 10.1038/s41598-021-98751-w.

Brunoni, A. R., Moffa, A. H., et al. (2016). "Transcranial direct current stimulation for acute major depressive episodes: meta-analysis of individual patient data". eng. In: *The British journal of psychiatry : the journal of mental science* 208.6. Edition: 2016/04/07, pp. 522–531. DOI: 10.1192/bjp.bp.115.164715.

Burke, D. and Pierrot-Deseilligny, E. (Feb. 2010). "Caveats when studying motor cortex excitability and the cortical control of movement using transcranial magnetic stimulation". In: *Clinical Neurophysiology* 121.2, pp. 121–123. DOI: 10.1016/j.clinph.2009.10.009.

Casali, A. G., Gosseries, O., et al. (Aug. 2013). "A theoretically based index of consciousness independent of sensory processing and behavior." eng. In: *Science translational medicine* 5.198. Place: United States, 198ra105. DOI: 10.1126/scitranslmed.3006294.

Cheeran, B., Talelli, P., et al. (Dec. 2008). "A common polymorphism in the brain-derived neurotrophic factor gene (BDNF) modulates human cortical plasticity and the response to rTMS". In: *The Journal of Physiology* 586.23. Publisher: John Wiley & Sons, Ltd, pp. 5717–5725. DOI: 10.1113/jphysiol.2008.159905.

Cohen, S. L., Bikson, M., et al. (Feb. 2022). "A visual and narrative timeline of US FDA milestones for Transcranial Magnetic Stimulation (TMS) devices." eng. In: *Brain stimulation* 15.1. Place: United States, pp. 73–75. DOI: 10.1016/j.brs.2021.11.010.

Cole, E. J., Phillips, A. L., et al. (Feb. 2022). "Stanford Neuromodulation Therapy (SNT): A Double-Blind Randomized Controlled Trial". In: *American Journal of Psychiatry* 179.2. Publisher: American Psychiatric Publishing, pp. 132–141. DOI: 10.1176/appi.ajp.2021.20101429.

Cole, E. J., Stimpson, K. H., et al. (Aug. 2020). "Stanford Accelerated Intelligent Neuromodulation Therapy for Treatment-Resistant Depression". In: *American Journal of Psychiatry* 177.8, pp. 716–726. DOI: 10.1176/appi.ajp.2019.19070720.

Conte, A., Gilio, F., et al. (Sept. 2007). "Attention influences the excitability of cortical motor areas in healthy humans." eng. In: *Experimental brain research* 182.1. Place: Germany, pp. 109–117. DOI: 10.1007/s00221-007-0975-3.

Corlier, J., Carpenter, L. L., et al. (Nov. 2019). "The relationship between individual alpha peak frequency and clinical outcome with repetitive Transcranial Magnetic Stimulation (rTMS) treatment of Major Depressive Disorder (MDD)". In: *Brain Stimulation* 12.6, pp. 1572–1578. DOI: 10.1016/j.brs.2019.07.018.

Corp, D. T., Bereznicki, H. G., et al. (Sept. 2020). "Large-scale analysis of interindividual variability in theta-burst stimulation data: Results from the 'Big TMS Data Collaboration'". In: *Brain Stimulation: Basic, Translational, and Clinical Research in*

Neuromodulation 13.5. Publisher: Elsevier, pp. 1476–1488. DOI: 10.1016/j.brs.2020.07.018.

Corp, D. T., Bereznicki, H. G., et al. (Oct. 2021). "Large-scale analysis of interindividual variability in single and paired-pulse TMS data". In: *Clinical Neurophysiology* 132.10, pp. 2639–2653. DOI: 10.1016/j.clinph.2021.06.014.

Cotovio, G., Ventura, F., et al. (2023). "Regulatory Clearance and Approval of Therapeutic Protocols of Transcranial Magnetic Stimulation for Psychiatric Disorders". In: *Brain Sciences* 13.7. DOI: 10.3390/brainsci13071029.

Cullen, C. L. and Young, K. M. (2016). "How Does Transcranial Magnetic Stimulation Influence Glial Cells in the Central Nervous System?" eng. In: *Frontiers in neural circuits* 10. Place: Switzerland, p. 26. DOI: 10.3389/fncir.2016.00026.

Curran-Everett, D. and Williams, C. L. (June 2015). "Explorations in statistics: the analysis of change". In: *Advances in Physiology Education* 39.2, pp. 49–54. DOI: 10.1152/advan.00018.2015.

Cuypers, K. and Marsman, A. (Jan. 2021). "Transcranial magnetic stimulation and magnetic resonance spectroscopy: Opportunities for a bimodal approach in human neuroscience". In: *NeuroImage* 224, p. 117394. DOI: 10.1016/j.neuroimage.2020.117394.

D'Ostilio, K., Goetz, S. M., et al. (Jan. 2016). "Effect of coil orientation on strength–duration time constant and I-wave activation with controllable pulse parameter transcranial magnetic stimulation". In: *Clinical Neurophysiology* 127.1, pp. 675–683. DOI: 10.1016/j.clinph.2015.05.017.

Dedovic, K. and Ngiam, J. (2015). "The cortisol awakening response and major depression: examining the evidence." eng. In: *Neuropsychiatric disease and treatment* 11. Place: New Zealand, pp. 1181–1189. DOI: 10.2147/NDT.S62289.

Deng, Z.-D., Lisanby, S. H., and Peterchev, A. V. (Jan. 2011). "Electric field strength and focality in electroconvulsive therapy and magnetic seizure therapy: a finite element simulation study". In: *Journal of Neural Engineering* 8.1, p. 016007. DOI: 10.1088/1741-2560/8/1/016007.

— (Jan. 2013). "Electric field depth–focality tradeoff in transcranial magnetic stimulation: Simulation comparison of 50 coil designs". In: *Brain Stim* 6.1, pp. 1–13. DOI: 10.1016/j.brs.2012.02.005.

Devanne, H., Lavoie, B. A., and Capaday, C. (Apr. 1997). "Input-output properties and gain changes in the human corticospinal pathway". In: *Experimental Brain Research* 114.2, pp. 329–338. DOI: 10.1007/PL00005641.

Di Lazzaro, V., Oliviero, A., et al. (Nov. 2001a). "Comparison of descending volleys evoked by monophasic and biphasic magnetic stimulation of the motor cortex in conscious humans". In: *Experimental Brain Research* 141.1, pp. 121–127. DOI: 10.1007/s002210100863.

Di Lazzaro, V., Oliviero, A., et al. (May 2001b). "The effect on corticospinal volleys of reversing the direction of current induced in the motor cortex by transcranial magnetic stimulation". In: *Experimental Brain Research* 138.2, pp. 268–273. DOI: 10.1007/s002210100722.

Di Lazzaro, V., Profice, P., et al. (Apr. 2010). "The effects of motor cortex rTMS on corticospinal descending activity". In: *Clinical Neurophysiology* 121.4, pp. 464–473. DOI: 10.1016/j.clinph.2009.11.007.

Di Lazzaro, V. and Rothwell, J. C. (Oct. 2014). "Corticospinal activity evoked and modulated by non-invasive stimulation of the intact human motor cortex". In: *The*

Journal of Physiology 592.19. Publisher: John Wiley & Sons, Ltd, pp. 4115–4128. DOI: 10.1113/jphysiol.2014.274316.

Doeltgen, S. H. and Ridding, M. C. (Mar. 2010). "Behavioural exposure and sleep do not modify corticospinal and intracortical excitability in the human motor system". In: *Clinical Neurophysiology* 121.3, pp. 448–452. DOI: 10.1016/j.clinph.2009.11.085.

Epstein, C. M. (2008). "Electromagnetism". In: *The Oxford Handbook of Transcranial Stimulation*. Ed. by E. Wassermann, C. Epstein, et al. Oxford: Oxford Universtiy Press, pp. 3–5.

Ermentrout, G. B. and Terman, D. H. (2010). "The Hodgkin–Huxley Equations". In: *Mathematical Foundations of Neuroscience*. Ed. by G. B. Ermentrout and D. H. Terman. New York, NY: Springer New York, pp. 1–28. DOI: 10.1007/978-0-387-87708-2_1.

Farzan, F. (2014). "Single-Pulse Transcranial Magnetic Stimulation (TMS) Protocols and Outcome Measures". In: *Transcranial Magnetic Stimulation*. Ed. by A. Rotenberg, J. C. Horvath, and A. Pascual-Leone. New York, NY: Springer New York : Imprint: Humana Press.

Feng, W., Bowden, M. G., and Kautz, S. (Jan. 2013). "Review of Transcranial Direct Current Stimulation in Poststroke Recovery". In: *Topics in Stroke Rehabilitation* 20.1, pp. 68–77. DOI: 10.1310/tsr2001-68.

Fitzgerald, P. B., Fountain, S., and Daskalakis, Z. J. (Dec. 2006). "A comprehensive review of the effects of rTMS on motor cortical excitability and inhibition". In: *Clinical Neurophysiology* 117.12, pp. 2584–2596. DOI: 10.1016/j.clinph.2006.06.712.

Fox, M. D., Buckner, R. L., et al. (Oct. 2012). "Efficacy of Transcranial Magnetic Stimulation Targets for Depression Is Related to Intrinsic Functional Connectivity with the Subgenual Cingulate". In: *Biological Psychiatry* 72.7. Publisher: Elsevier, pp. 595–603. DOI: 10.1016/j.biopsych.2012.04.028.

Gamboa, O. L., Antal, A., et al. (July 2010). "Simply longer is not better: reversal of theta burst after-effect with prolonged stimulation". In: *Experimental Brain Research* 204.2, pp. 181–187. DOI: 10.1007/s00221-010-2293-4.

Gattinger, N., Moßnang, G., and Gleich, B. (2012). "flexTMS—A Novel Repetitive Transcranial Magnetic Stimulation Device With Freely Programmable Stimulus Currents". In: *IEEE Transactions on Biomedical Engineering* 59.7, pp. 1962–1970.

Gentner, R., Wankerl, K., et al. (2008). "Depression of Human Corticospinal Excitability Induced by Magnetic Theta-burst Stimulation: Evidence of Rapid Polarity-Reversing Metaplasticity". In: *Cerebral Cortex* 18.9, pp. 2046–2053. DOI: 10.1093/cercor/bhm239.

Gerstner, W., Kistler, W. M., et al. (2014). *Neuronal Dynamics: From Single Neurons to Networks and Models of Cognition*. Cambridge: Cambridge University Press. DOI: 10.1017/CBO9781107447615.

Goetz, S. M., Luber, B., et al. (Jan. 2016). "Enhancement of Neuromodulation with Novel Pulse Shapes Generated by Controllable Pulse Parameter Transcranial Magnetic Stimulation". In: *Brain Stimulation: Basic, Translational, and Clinical Research in Neuromodulation* 9.1. Publisher: Elsevier, pp. 39–47. DOI: 10.1016/j.brs.2015.08.013.

Goldsworthy, M. R., Pitcher, J. B., and Ridding, M. C. (Jan. 2012). "The application of spaced theta burst protocols induces long-lasting neuroplastic changes in the human

motor cortex". In: *European Journal of Neuroscience* 35.1. Publisher: John Wiley & Sons, Ltd, pp. 125–134. DOI: 10.1111/j.1460-9568.2011.07924.x.

Grandy, T. H., Werkle-Bergner, M., et al. (June 2013). "Peak individual alpha frequency qualifies as a stable neurophysiological trait marker in healthy younger and older adults". In: *Psychophysiology* 50.6. Publisher: John Wiley & Sons, Ltd, pp. 570–582. DOI: 10.1111/psyp.12043.

Groppa, S., Oliviero, A., et al. (May 2012). "A practical guide to diagnostic transcranial magnetic stimulation: Report of an IFCN committee". In: *Clinical Neurophysiology* 123.5, pp. 858–882. DOI: 10.1016/j.clinph.2012.01.010.

Halawa, I., Shirota, Y., et al. (Sept. 2019). "Neuronal tuning: Selective targeting of neuronal populations via manipulation of pulse width and directionality". In: *Brain Stimulation: Basic, Translational, and Clinical Research in Neuromodulation* 12.5. Publisher: Elsevier, pp. 1244–1252. DOI: 10.1016/j.brs.2019.04.012.

Hamada, M., Hanajima, R., et al. (Dec. 2007). "Quadro-pulse stimulation is more effective than paired-pulse stimulation for plasticity induction of the human motor cortex". In: *Clinical Neurophysiology* 118.12, pp. 2672–2682. DOI: 10.1016/j.clinph.2007.09.062.

Hamada, M., Murase, N., et al. (July 2013). "The Role of Interneuron Networks in Driving Human Motor Cortical Plasticity". In: *Cerebral Cortex* 23.7, pp. 1593–1605. DOI: 10.1093/cercor/bhs147.

Hamada, M., Terao, Y., et al. (Aug. 2008). "Bidirectional long-term motor cortical plasticity and metaplasticity induced by quadripulse transcranial magnetic stimulation". In: *The Journal of Physiology* 586.16, pp. 3927–3947. DOI: 10.1113/jphysiol.2008.152793.

Hannah, R. and Rothwell, J. C. (Jan. 2017). "Pulse Duration as Well as Current Direction Determines the Specificity of Transcranial Magnetic Stimulation of Motor Cortex during Contraction". eng. In: *Brain Stimul* 10.1. Edition: 2016/12/29, pp. 106–115. DOI: 10.1016/j.brs.2016.09.008.

Heller, L. and van Hulsteyn, D. B. (July 1992). "Brain stimulation using electromagnetic sources: theoretical aspects." eng. In: *Biophysical journal* 63.1. Place: United States, pp. 129–138. DOI: 10.1016/S0006-3495(92)81587-4.

Herwig, U., Cardenas-Morales, L., et al. (Feb. 2010). "Sham or real—Post hoc estimation of stimulation condition in a randomized transcranial magnetic stimulation trial". In: *Neuroscience Letters* 471.1, pp. 30–33. DOI: 10.1016/j.neulet.2010.01.003.

Hess, G., Aizenman, C. D., and Donoghue, J. P. (May 1996). "Conditions for the induction of long-term potentiation in layer II/III horizontal connections of the rat motor cortex". In: *Journal of Neurophysiology* 75.5. Publisher: American Physiological Society, pp. 1765–1778. DOI: 10.1152/jn.1996.75.5.1765.

Hines, M. L. and Carnevale, N. T. (Aug. 1997). "The NEURON Simulation Environment". In: *Neural Computation* 9.6, pp. 1179–1209. DOI: 10.1162/neco.1997.9.6.1179.

Hodgkin, A. and Huxley, A. (1952). "A quantitative description of membrane current and its application to conduction and excitation in nerve". In: *Bull Math Biol* 52.

Hsu, Y.-F., Liao, K.-K., et al. (Nov. 2011). "Intermittent theta burst stimulation over primary motor cortex enhances movement-related beta synchronisation". In: *Clinical Neurophysiology* 122.11, pp. 2260–2267. DOI: 10.1016/j.clinph.2011.03.027.

Huang, Y.-Z., Edwards, M. J., et al. (Jan. 2005). "Theta Burst Stimulation of the Human Motor Cortex". In: *Neuron* 45.2, pp. 201–206. DOI: 10.1016/j.neuron.2004.12.033.

Huang, Y.-Z., Lu, M.-K., et al. (Nov. 2017). "Plasticity induced by non-invasive transcranial brain stimulation: A position paper". In: *Clinical Neurophysiology* 128.11, pp. 2318–2329. DOI: 10.1016/j.clinph.2017.09.007.

Huang, Y.-Z., Rothwell, J. C., et al. (2008). "Effect of Physiological Activity on an NMDA-Dependent Form of Cortical Plasticity in Human". In: *Cerebral Cortex* 18.3, pp. 563–570. DOI: 10.1093/cercor/bhm087.

Huang, Y.-Z., Rothwell, J. C., et al. (May 2011). "The theoretical model of theta burst form of repetitive transcranial magnetic stimulation". In: *Clinical Neurophysiology* 122.5, pp. 1011–1018. DOI: 10.1016/j.clinph.2010.08.016.

Huber, R., Mäki, H., et al. (Feb. 2013). "Human cortical excitability increases with time awake." eng. In: *Cerebral cortex (New York, N.Y. : 1991)* 23.2. Place: United States, pp. 332–338. DOI: 10.1093/cercor/bhs014.

Hutcheon, B. and Yarom, Y. (May 2000). "Resonance, oscillation and the intrinsic frequency preferences of neurons". In: *Trends in Neurosciences* 23.5, pp. 216–222. DOI: 10.1016/S0166-2236(00)01547-2.

Ilmoniemi, R. J., Deng, Z.-D., et al. (2023). "Transcranial magnetic stimulation coils". In: *The Oxford Handbook of Transcranial Stimulation*. Ed. by E. M. Wassermann, A. V. Peterchev, et al. Oxford University Press, p. 0. DOI: 10.1093/oxfordhb/9780198832256.013.4.

Iseger, T. A., van Bueren, N. E., et al. (Jan. 2020). "A frontal-vagal network theory for Major Depressive Disorder: Implications for optimizing neuromodulation techniques". In: *Brain Stimulation* 13.1, pp. 1–9. DOI: 10.1016/j.brs.2019.10.006.

Jannati, A., Block, G., et al. (Nov. 2017). "Interindividual variability in response to continuous theta-burst stimulation in healthy adults". In: *Clinical Neurophysiology* 128.11, pp. 2268–2278. DOI: 10.1016/j.clinph.2017.08.023.

Jannati, A., Fried, P. J., et al. (2019). "Test–Retest Reliability of the Effects of Continuous Theta-Burst Stimulation". In: *Frontiers in Neuroscience* 13.

Jezernik, S., Sinkjaer, T., and Morari, M. (June 2010). "Charge and energy minimization in electrical/magnetic stimulation of nervous tissue". In: *Journal of Neural Engineering* 7.4, p. 046004. DOI: 10.1088/1741-2560/7/4/046004.

Jin, Y., Kemp, A. S., et al. (Oct. 2012). "Alpha EEG guided TMS in schizophrenia". In: *Brain Stimulation* 5.4, pp. 560–568. DOI: 10.1016/j.brs.2011.09.005.

Jin, Y., Potkin, S. G., et al. (2006). "Therapeutic Effects of Individualized Alpha Frequency Transcranial Magnetic Stimulation (αTMS) on the Negative Symptoms of Schizophrenia". In: *Schizophrenia Bulletin* 32.3, pp. 556–561. DOI: 10.1093/schbul/sbj020.

Kammer, T. (Feb. 1999). "Phosphenes and transient scotomas induced by magnetic stimulation of the occipital lobe: their topographic relationship." eng. In: *Neuropsychologia* 37.2. Place: England, pp. 191–198. DOI: 10.1016/s0028-3932(98)00093-1.

Kammer, T., Beck, S., et al. (Feb. 2001). "Motor thresholds in humans: a transcranial magnetic stimulation study comparing different pulse waveforms, current directions and stimulator types". In: *Clinical Neurophysiology* 112.2, pp. 250–258. DOI: 10.1016/S1388-2457(00)00513-7.

Kemlin, C., Moulton, E., et al. (2019). "Redundancy Among Parameters Describing the Input-Output Relation of Motor Evoked Potentials in Healthy Subjects and Stroke Patients". In: *Frontiers in Neurology* 10.

Kiers, L., Cros, D., et al. (Dec. 1993). "Variability of motor potentials evoked by transcranial magnetic stimulation". In: *Electroencephalography and Clinical Neurophysiology/Evoked Potentials Section* 89.6, pp. 415–423. DOI: 10.1016/0168-5597(93)90115-6.

Kocabicak, E., Temel, Y., et al. (2015). "Current perspectives on deep brain stimulation for severe neurological and psychiatric disorders." eng. In: *Neuropsychiatric disease and treatment* 11. Place: New Zealand, pp. 1051–1066. DOI: 10.2147/NDT.S46583.

Kondacs, A. and Szabó, M. (Oct. 1999). "Long-term intra-individual variability of the background EEG in normals". In: *Clinical Neurophysiology* 110.10, pp. 1708–1716. DOI: 10.1016/S1388-2457(99)00122-4.

Koponen, L. M., Nieminen, J. O., and Ilmoniemi, R. J. (2018). "Multi-locus transcranial magnetic stimulation—theory and implementation". In: *Brain Stimulation* 11.4, pp. 849–855. DOI: https://doi.org/10.1016/j.brs.2018.03.014.

Koski, L., Schrader, L. M., et al. (Sept. 2005). "Normative data on changes in transcranial magnetic stimulation measures over a ten hour period". In: *Clinical Neurophysiology* 116.9, pp. 2099–2109. DOI: 10.1016/j.clinph.2005.06.006.

Krepel, N., Sack, A. T., et al. (May 2018). "Non-replication of neurophysiological predictors of non-response to rTMS in depression and neurophysiological data-sharing proposal". In: *Brain Stimulation* 11.3, pp. 639–641. DOI: 10.1016/j.brs.2018.01.032.

Kuznetsova, A., Brockhoff, P. B., and Christensen, R. H. B. (June 2012). "lmerTest Package: Tests in Linear Mixed Effects Models". In: *Journal of Statistical Software* 82.13. Section: Articles, pp. 1–26. DOI: 10.18637/jss.v082.i13.

Lakens, D. (2013). "Calculating and reporting effect sizes to facilitate cumulative science: a practical primer for t-tests and ANOVAs". In: *Frontiers in Psychology* 4.

Lang, N., Rothkegel, H., et al. (Oct. 2011). "Circadian Modulation of GABA-Mediated Cortical Inhibition". In: *Cerebral Cortex* 21.10, pp. 2299–2306. DOI: 10.1093/cercor/bhr003.

Larson, J. and Lynch, G. (June 1989). "Theta pattern stimulation and the induction of LTP: the sequence in which synapses are stimulated determines the degree to which they potentiate". In: *Brain Research* 489.1, pp. 49–58. DOI: 10.1016/0006-8993(89)90007-3.

Larson, J., Wong, D., and Lynch, G. (Mar. 1986). "Patterned stimulation at the theta frequency is optimal for the induction of hippocampal long-term potentiation". In: *Brain Research* 368.2, pp. 347–350. DOI: 10.1016/0006-8993(86)90579-2.

Law, R. and Clow, A. (Jan. 2020). "Chapter Eight - Stress, the cortisol awakening response and cognitive function". In: *International Review of Neurobiology*. Ed. by A. Clow and N. Smyth. Vol. 150. Academic Press, pp. 187–217. DOI: 10.1016/bs.irn.2020.01.001.

Lefaucheur, J.-P., Aleman, A., et al. (Feb. 2020). "Evidence-based guidelines on the therapeutic use of repetitive transcranial magnetic stimulation (rTMS): An update (2014–2018)". In: *Clinical Neurophysiology* 131.2, pp. 474–528. DOI: 10.1016/j.clinph.2019.11.002.

Lefaucheur, J.-P., André-Obadia, N., et al. (Nov. 2014). "Evidence-based guidelines on the therapeutic use of repetitive transcranial magnetic stimulation (rTMS)". In:

Clinical Neurophysiology 125.11, pp. 2150–2206. DOI: 10.1016/j.clinph.2014.05.021.

Lenth, R. V. (2023). *emmeans: Estimated Marginal Means, aka Least-Squares Means.*

Leuchter, A., Cook, I., et al. (Feb. 2013). "The relationship between brain oscillatory activity and therapeutic effectiveness of transcranial magnetic stimulation in the treatment of major depressive disorder". English. In: *Frontiers in Human Neuroscience* 7.37. DOI: 10.3389/fnhum.2013.00037.

Li, Z., Zhang, J., et al. (Nov. 2022). "Modular pulse synthesizer for transcranial magnetic stimulation with fully adjustable pulse shape and sequence". In: *Journal of Neural Engineering* 19.6. Publisher: IOP Publishing, p. 066015. DOI: 10.1088/1741-2552/ac9d65.

Liebetanz, D., Nitsche, M. A., et al. (Oct. 2002). "Pharmacological approach to the mechanisms of transcranial DC-stimulation-induced after-effects of human motor cortex excitability." eng. In: *Brain : a journal of neurology* 125.Pt 10. Place: England, pp. 2238–2247. DOI: 10.1093/brain/awf238.

Lorenz, R., Simmons, L. E., et al. (Nov. 2019). "Efficiently searching through large tACS parameter spaces using closed-loop Bayesian optimization". In: *Brain Stimulation* 12.6, pp. 1484–1489. DOI: 10.1016/j.brs.2019.07.003.

Ly, J. Q. M., Gaggioni, G., et al. (June 2016). "Circadian regulation of human cortical excitability". In: *Nature Communications* 7.1, p. 11828. DOI: 10.1038/ncomms11828.

Markram, H., Muller, E., et al. (Oct. 2015). "Reconstruction and Simulation of Neocortical Microcircuitry". In: *Cell* 163.2. Publisher: Elsevier, pp. 456–492. DOI: 10.1016/j.cell.2015.09.029.

Mastroeni, C., Bergmann, T. O., et al. (2013). "Brain-derived neurotrophic factor–a major player in stimulation-induced homeostatic metaplasticity of human motor cortex?" eng. In: *PloS one* 8.2. Place: United States, e57957. DOI: 10.1371/journal.pone.0057957.

Matsumoto, H. and Ugawa, Y. (Aug. 2020). "Quadripulse stimulation (QPS)". In: *Experimental Brain Research* 238.7, pp. 1619–1625. DOI: 10.1007/s00221-020-05788-w.

Mayberg, H. S., Lozano, A. M., et al. (Mar. 2005). "Deep Brain Stimulation for Treatment-Resistant Depression". In: *Neuron* 45.5. Publisher: Elsevier, pp. 651–660. DOI: 10.1016/j.neuron.2005.02.014.

McCalley, D. M., Lench, D. H., et al. (Apr. 2021). "Determining the optimal pulse number for theta burst induced change in cortical excitability". In: *Scientific Reports* 11.1, p. 8726. DOI: 10.1038/s41598-021-87916-2.

McClintock, S. M., Reti, I. M., et al. (2017). "Consensus recommendations for the clinical application of repetitive transcranial magnetic stimulation (rTMS) in the treatment of depression". In: *The Journal of clinical psychiatry* 79.1. ISBN: 0160-6689 Publisher: Physicians Postgraduate Press, Inc., p. 3651.

Meng, Q., Nguyen, H., et al. (2022). "A high-density theta burst paradigm enhances the aftereffects of transcranial magnetic stimulation: Evidence from focal stimulation of rat motor cortex". In: *Brain Stimulation: Basic, Translational, and Clinical Research in Neuromodulation* 15.3, pp. 833–842. DOI: 10.1016/j.brs.2022.05.017.

Milani, P., Piu, P., et al. (2010). "Cortisol-induced effects on human cortical excitability". In: *Brain Stimulation* 3.3, pp. 131–139. DOI: https://doi.org/10.1016/j.brs.2009.07.004.

Möller, C., Arai, N., et al. (May 2009). "Hysteresis effects on the input–output curve of motor evoked potentials". In: *Clinical Neurophysiology* 120.5, pp. 1003–1008. DOI: 10.1016/j.clinph.2009.03.001.

Nagarajan, S. S. and Durand, D. M. (Mar. 1996). "A generalized cable equation for magnetic stimulation of axons." eng. In: *IEEE transactions on bio-medical engineering* 43.3. Place: United States, pp. 304–312. DOI: 10.1109/10.486288.

Nakamura, K., Groiss, S. J., et al. (2016). "Variability in Response to Quadripulse Stimulation of the Motor Cortex". In: *Brain Stimulation: Basic, Translational, and Clinical Research in Neuromodulation* 9.6, pp. 859–866. DOI: 10.1016/j.brs.2016.01.008.

Nettekoven, C., Volz, L. J., et al. (May 2014). "Dose-dependent effects of theta burst rTMS on cortical excitability and resting-state connectivity of the human motor system". eng. In: *J Neurosci* 34.20. Edition: 2014/05/16, pp. 6849–59. DOI: 10.1523/jneurosci.4993-13.2014.

Nieminen, J. O., Sinisalo, H., et al. (Jan. 2022). "Multi-locus transcranial magnetic stimulation system for electronically targeted brain stimulation". In: *Brain Stimulation* 15.1, pp. 116–124. DOI: 10.1016/j.brs.2021.11.014.

O'Reardon, J. P., Solvason, H. B., et al. (Dec. 2007). "Efficacy and safety of transcranial magnetic stimulation in the acute treatment of major depression: a multisite randomized controlled trial." eng. In: *Biological psychiatry* 62.11. Place: United States, pp. 1208–1216. DOI: 10.1016/j.biopsych.2007.01.018.

Oldfield, R. C. (Mar. 1971). "The assessment and analysis of handedness: the Edinburgh inventory". eng. In: *Neuropsychologia* 9.1. Edition: 1971/03/01, pp. 97–113. DOI: 10.1016/0028-3932(71)90067-4.

Pascual-Leone, A., Valls-Solé, J., et al. (1994). "Responses to rapid-rate transcranial magnetic stimulation of the human motor cortex". In: *Brain* 117.4, pp. 847–858. DOI: 10.1093/brain/117.4.847.

Pasqualetti, P. and Ferreri, F. (June 2011). "W14.4 Amplitude values of motor evoked potentials: statistical properties and neurophysiological implications". In: *Abstracts of the 14 European Congress of Clinical Neurophysiology and the 4 International Conference on Transcranial Magnetic and Direct Current Stimulation.* 122, S44–S45. DOI: 10.1016/S1388-2457(11)60148-X.

Pearce, A. J., Clark, R. A., and Kidgell, D. J. (May 2013). "A Comparison of Two Methods in Acquiring Stimulus–Response Curves with Transcranial Magnetic Stimulation". In: *Brain Stimulation* 6.3, pp. 306–309. DOI: 10.1016/j.brs.2012.05.010.

Perera, T., George, M. S., et al. (May 2016). "The Clinical TMS Society Consensus Review and Treatment Recommendations for TMS Therapy for Major Depressive Disorder". In: *Brain Stimulation: Basic, Translational, and Clinical Research in Neuromodulation* 9.3. Publisher: Elsevier, pp. 336–346. DOI: 10.1016/j.brs.2016.03.010.

Peterchev, A. V., D'Ostilio, K., et al. (Sept. 2014). "Controllable pulse parameter transcranial magnetic stimulator with enhanced circuit topology and pulse shaping". In: *Journal of Neural Engineering* 11.5. Publisher: IOP Publishing, p. 056023. DOI: 10.1088/1741-2560/11/5/056023.

Peterchev, A. V., Jalinous, R., and Lisanby, S. H. (2008). "A Transcranial Magnetic Stimulator Inducing Near-Rectangular Pulses With Controllable Pulse Width

(cTMS)". In: *IEEE Transactions on Biomedical Engineering* 55.1, pp. 257–266. DOI: 10.1109/TBME.2007.900540.

Peterchev, A. V., Murphy, D. L., and Lisanby, S. H. (May 2011). "Repetitive transcranial magnetic stimulator with controllable pulse parameters". In: *Journal of Neural Engineering* 8.3, p. 036016. DOI: 10.1088/1741-2560/8/3/036016.

Peterchev, A. V. and Riehl, M. E. (2023). "Transcranial Magnetic Stimulators". In: *The Oxford Handbook of Transcranial Stimulation*. Ed. by E. M. Wassermann, A. V. Peterchev, et al. Oxford University Press, p. 0. DOI: 10.1093/oxfordhb/9780198832256.013.3.

Philiastides, M. G., Auksztulewicz, R., et al. (June 2011). "Causal Role of Dorsolateral Prefrontal Cortex in Human Perceptual Decision Making". In: *Current Biology* 21.11, pp. 980–983. DOI: 10.1016/j.cub.2011.04.034.

Pitcher, D., Walsh, V., et al. (Sept. 2007). "TMS Evidence for the Involvement of the Right Occipital Face Area in Early Face Processing". In: *Current Biology* 17.18, pp. 1568–1573. DOI: 10.1016/j.cub.2007.07.063.

Plonsey, R. and Heppner, D. B. (Dec. 1967). "Considerations of quasi-stationarity in electrophysiological systems". In: *The bulletin of mathematical biophysics* 29.4, pp. 657–664. DOI: 10.1007/BF02476917.

Pospischil, M., Toledo-Rodriguez, M., et al. (Nov. 2008). "Minimal Hodgkin-Huxley type models for different classes of cortical and thalamic neurons". In: *Biol Cybern* 99.4-5. Edition: 2008/11/18, pp. 427–41. DOI: 10.1007/s00422-008-0263-8.

Raggi, A. and Leonardi, M. (Jan. 2020). "Burden of brain disorders in Europe in 2017 and comparison with other non-communicable disease groups." eng. In: *Journal of neurology, neurosurgery, and psychiatry* 91.1. Place: England, pp. 104–105. DOI: 10.1136/jnnp-2019-320466.

Rattay, F. (June 1998). "Analysis of the electrical excitation of CNS neurons." eng. In: *IEEE transactions on bio-medical engineering* 45.6. Place: United States, pp. 766–772. DOI: 10.1109/10.678611.

Ridding, M. C. and Rothwell, J. C. (July 2007). "Is there a future for therapeutic use of transcranial magnetic stimulation?" In: *Nature Reviews Neuroscience* 8.7, pp. 559–567. DOI: 10.1038/nrn2169.

Ridding, M. C. and Ziemann, U. (July 2010). "Determinants of the induction of cortical plasticity by non-invasive brain stimulation in healthy subjects". In: *The Journal of Physiology* 588.13. Publisher: John Wiley & Sons, Ltd, pp. 2291–2304. DOI: 10.1113/jphysiol.2010.190314.

Roesler, K. M. and Magistris, M. R. (2008). "The size of motor-evoked potentials: influencing parameters and quantification". English. In: *Oxford Handbook of Transcranial Stimulation*. Ed. by C. M. Epstein, E. M. Wassermann, and U. Ziemann. Oxford University Press, pp. 77–89. DOI: 10.1093/oxfordhb/9780198568926.001.0001.

Rossi, S., Antal, A., et al. (Jan. 2021). "Safety and recommendations for TMS use in healthy subjects and patient populations, with updates on training, ethical and regulatory issues: Expert Guidelines". In: *Clinical Neurophysiology* 132.1, pp. 269–306. DOI: 10.1016/j.clinph.2020.10.003.

Rossi, S., Hallett, M., et al. (Dec. 2009). "Safety, ethical considerations, and application guidelines for the use of transcranial magnetic stimulation in clinical practice and research". In: *Clinical Neurophysiology* 120.12, pp. 2008–2039. DOI: 10.1016/j.clinph.2009.08.016.

Rossini, P. M., Barker, A., et al. (Aug. 1994). "Non-invasive electrical and magnetic stimulation of the brain, spinal cord and roots: basic principles and procedures for routine clinical application. Report of an IFCN committee". In: *Electroencephalography and Clinical Neurophysiology* 91.2, pp. 79–92. DOI: 10.1016/0013-4694(94)90029-9.

Rossini, P. M., Burke, D., et al. (June 2015). "Non-invasive electrical and magnetic stimulation of the brain, spinal cord, roots and peripheral nerves: Basic principles and procedures for routine clinical and research application. An updated report from an I.F.C.N. Committee". In: *Clin Neurophysiol* 126.6. Edition: 2015/03/24, pp. 1071–1107. DOI: 10.1016/j.clinph.2015.02.001.

Rotenberg, A., Horvath, J. C., and Pascual-Leone, A. (2014). *Transcranial Magnetic Stimulation*. eng. Neuromethods, 89. New York, NY: Springer New York : Imprint: Humana Press.

Sackeim, H. A., Aaronson, S. T., et al. (Dec. 2020). "Clinical outcomes in a large registry of patients with major depressive disorder treated with Transcranial Magnetic Stimulation". In: *Journal of Affective Disorders* 277, pp. 65–74. DOI: 10.1016/j.jad.2020.08.005.

Sasaki, T., Kodama, S., et al. (Mar. 2018). "The intensity of continuous theta burst stimulation, but not the waveform used to elicit motor evoked potentials, influences its outcome in the human motor cortex". In: *Brain Stimulation* 11.2, pp. 400–410. DOI: 10.1016/j.brs.2017.12.003.

Saturnino, G. B., Thielscher, A., et al. (Mar. 2019). "A principled approach to conductivity uncertainty analysis in electric field calculations". In: *NeuroImage* 188, pp. 821–834. DOI: 10.1016/j.neuroimage.2018.12.053.

Schilberg, L., Schuhmann, T., and Sack, A. T. (2017). "Interindividual Variability and Intraindividual Reliability of Intermittent Theta Burst Stimulation-induced Neuroplasticity Mechanisms in the Healthy Brain". In: *Journal of Cognitive Neuroscience* 29.6, pp. 1022–1032. DOI: 10.1162/jocn_a_01100.

Schmidt, S. L., Iyengar, A. K., et al. (Nov. 2014). "Endogenous Cortical Oscillations Constrain Neuromodulation by Weak Electric Fields". In: *Special Issue: NYC Neuromodulation 2015 Conference* 7.6, pp. 878–889. DOI: 10.1016/j.brs.2014.07.033.

Siebner, H. R., Dressnandt, J., et al. (Sept. 1998). "Continuous intrathecal baclofen infusions induced a marked increase of the transcranially evoked silent period in a patient with generalized dystonia". In: *Muscle & Nerve* 21.9, pp. 1209–1212. DOI: 10.1002/(SICI)1097-4598(199809)21:9<1209::AID-MUS15>3.0.CO;2-M.

Siebner, H. R., Funke, K., et al. (Aug. 2022). "Transcranial magnetic stimulation of the brain: What is stimulated? – A consensus and critical position paper". In: *Clinical Neurophysiology* 140, pp. 59–97. DOI: 10.1016/j.clinph.2022.04.022.

simplemaps (Feb. 2023). *US Zip Codes Database*.

Sommer, M., Alfaro, A., et al. (Apr. 2006). "Half sine, monophasic and biphasic transcranial magnetic stimulation of the human motor cortex". In: *Clin Neurophysiol* 117.4, pp. 838–844. DOI: 10.1016/j.clinph.2005.10.029.

Sommer, M., Ciocca, M., et al. (May 2018). "TMS of primary motor cortex with a biphasic pulse activates two independent sets of excitable neurones". In: *Brain Stimulation* 11.3, pp. 558–565. DOI: 10.1016/j.brs.2018.01.001.

Sommer, M., Lang, N., et al. (2002). "Neuronal tissue polarization induced by repetitive transcranial magnetic stimulation?" eng. In: *Neuroreport* 13.6, p. 809. DOI: 10.1097/00001756-200205070-00015.

Sorkhabi, M. M., Benjaber, M., et al. (2020). "Programmable Transcranial Magnetic Stimulation- A Modulation Approach for the Generation of Controllable Magnetic Stimuli". In: *IEEE Transactions on Biomedical Engineering*, pp. 1–1. DOI: 10.1109/TBME.2020.3024902.

Sorkhabi, M. M., Gingell, F., et al. (2021). "Design Analysis and Circuit Topology Optimization for Programmable Magnetic Neurostimulator". In: *2021 43rd Annual International Conference of the IEEE Engineering in Medicine & Biology Society (EMBC)*, pp. 6384–6389. DOI: 10.1109/EMBC46164.2021.9630915.

Sorkhabi, M. M., Wendt, K., et al. (Aug. 2022). "Pulse width modulation-based TMS: Primary motor cortex responses compared to conventional monophasic stimuli." eng. In: *Brain stimulation* 15.4. Place: United States, pp. 980–983. DOI: 10.1016/j.brs.2022.06.013.

Suppa, A., Asci, F., and Guerra, A. (Jan. 2022). "Chapter 5 - Transcranial magnetic stimulation as a tool to induce and explore plasticity in humans". In: *Handbook of Clinical Neurology*. Ed. by A. Quartarone, M. F. Ghilardi, and F. Boller. Vol. 184. Elsevier, pp. 73–89. DOI: 10.1016/B978-0-12-819410-2.00005-9.

Suppa, A., Huang, Y.-Z., et al. (May 2016). "Ten Years of Theta Burst Stimulation in Humans: Established Knowledge, Unknowns and Prospects". In: *Brain Stimulation* 9.3, pp. 323–335. DOI: 10.1016/j.brs.2016.01.006.

Suppa, A., Ortu, E., et al. (Sept. 2008). "Theta burst stimulation induces after-effects on contralateral primary motor cortex excitability in humans". In: *The Journal of Physiology* 586.18. Publisher: John Wiley & Sons, Ltd, pp. 4489–4500. DOI: 10.1113/jphysiol.2008.156596.

Talelli, P., Cheeran, B., et al. (Aug. 2007). "Pattern-specific role of the current orientation used to deliver Theta Burst Stimulation". In: *Clinical Neurophysiology* 118.8, pp. 1815–1823. DOI: 10.1016/j.clinph.2007.05.062.

Taylor, J. L. and Loo, C. K. (Jan. 2007). "Stimulus waveform influences the efficacy of repetitive transcranial magnetic stimulation". In: *Journal of Affective Disorders* 97.1, pp. 271–276. DOI: 10.1016/j.jad.2006.06.027.

Tendler, A., Goerigk, S., et al. (June 2023). "Deep TMS H1 Coil treatment for depression: Results from a large post marketing data analysis". In: *Psychiatry Research* 324, p. 115179. DOI: 10.1016/j.psychres.2023.115179.

Ter Braack, E. M., de Goede, A. A., and van Putten, M. J. A. M. (Jan. 2019). "Resting Motor Threshold, MEP and TEP Variability During Daytime". In: *Brain Topography* 32.1, pp. 17–27. DOI: 10.1007/s10548-018-0662-7.

Thielscher, A., Antunes, A., and Saturnino, G. B. (Aug. 2015). "Field modeling for transcranial magnetic stimulation: A useful tool to understand the physiological effects of TMS?" In: pp. 222–225. DOI: 10.1109/EMBC.2015.7318340.

Thut, G., Bergmann, T. O., et al. (May 2017). "Guiding transcranial brain stimulation by EEG/MEG to interact with ongoing brain activity and associated functions: A position paper". In: *Clinical Neurophysiology* 128.5, pp. 843–857. DOI: 10.1016/j.clinph.2017.01.003.

Tse, N. Y., Goldsworthy, M. R., et al. (June 2018). "The effect of stimulation interval on plasticity following repeated blocks of intermittent theta burst stimulation". In: *Scientific Reports* 8.1, p. 8526. DOI: 10.1038/s41598-018-26791-w.

Vadnie, C. A. and McClung, C. A. (Nov. 2017). "Circadian Rhythm Disturbances in Mood Disorders: Insights into the Role of the Suprachiasmatic Nucleus". In: *Neural Plasticity* 2017. Ed. by H. Pantazopoulos. Publisher: Hindawi, p. 1504507. DOI: 10.1155/2017/1504507.

Vallence, A. M., Goldsworthy, M. R., et al. (Sept. 2015). "Inter- and intra-subject variability of motor cortex plasticity following continuous theta-burst stimulation". In: *Neuroscience* 304, pp. 266–278. DOI: 10.1016/j.neuroscience.2015.07.043.

Vallence, A. M., Rurak, B. K., et al. (Mar. 2023). "Covariation of the amplitude and latency of motor evoked potentials elicited by transcranial magnetic stimulation in a resting hand muscle". In: *Experimental Brain Research* 241.3, pp. 927–936. DOI: 10.1007/s00221-023-06575-z.

Van Rheede, J. J., Feldmann, L. K., et al. (July 2022). "Diurnal modulation of subthalamic beta oscillatory power in Parkinson's disease patients during deep brain stimulation". In: *npj Parkinson's Disease* 8.1, p. 88. DOI: 10.1038/s41531-022-00350-7.

Wagner, T. A., M. Zahn, et al. (Sept. 2004). "Three-dimensional head model Simulation of transcranial magnetic stimulation". In: *IEEE Transactions on Biomedical Engineering* 51.9, pp. 1586–1598. DOI: 10.1109/TBME.2004.827925.

Wang, B., Aberra, A. S., et al. (2023). "Physics and biophysics fundamentals of transcranial stimulation". In: *The Oxford Handbook of Transcranial Stimulation*. Ed. by E. M. Wassermann, A. V. Peterchev, et al. Oxford University Press, p. 0. DOI: 10.1093/oxfordhb/9780198832256.013.1.

Wang, B., Grill, W. M., and Peterchev, A. V. (July 2018). "Coupling Magnetically Induced Electric Fields to Neurons: Longitudinal and Transverse Activation". In: *Biophysical Journal* 115.1, pp. 95–107. DOI: 10.1016/j.bpj.2018.06.004.

Weise, K., Numssen, O., et al. (Apr. 2020). "A novel approach to localize cortical TMS effects". In: *NeuroImage* 209, p. 116486. DOI: 10.1016/j.neuroimage.2019.116486.

Wendt, K., Denison, T., et al. (2022). "Physiologically informed neuromodulation". In: *Journal of the Neurological Sciences* 434. DOI: 10.1016/j.jns.2021.120121.

Wendt, K., Sorkhabi, M. M., et al. (Nov. 2021). "Comparison between the modelled response of primary motor cortex neurons to pulse-width modulated and conventional TMS stimuli". eng. In: *Annu Int Conf IEEE Eng Med Biol Soc* 2021. Edition: 2021/12/12, pp. 6058–6061. DOI: 10.1109/embc46164.2021.9629605.

Wendt, K., Sorkhabi, M. M., et al. (Nov. 2023a). "Influence of time of day on resting motor threshold in clinical TMS practice". In: *Clinical Neurophysiology* 155, pp. 65–67. DOI: 10.1016/j.clinph.2023.08.017.

Wendt, K., Sorkhabi, M. M., et al. (July 2023b). "The effect of pulse shape in theta-burst stimulation: Monophasic vs biphasic TMS". In: *Brain Stimulation* 16.4, pp. 1178–1185. DOI: 10.1016/j.brs.2023.08.001.

Westin, G. G., Bassi, B. D., et al. (Jan. 2014). "Determination of motor threshold using visual observation overestimates transcranial magnetic stimulation dosage: Safety implications". In: *Clinical Neurophysiology* 125.1, pp. 142–147. DOI: 10.1016/j.clinph.2013.06.187.

Wischnewski, M., Haigh, Z. J., et al. (Sept. 2022). "The phase of sensorimotor mu and beta oscillations has the opposite effect on corticospinal excitability". In: *Brain Stimulation* 15.5, pp. 1093–1100. DOI: 10.1016/j.brs.2022.08.005.

Yang, Y., Connolly, A. T., and Shanechi, M. M. (Sept. 2018). "A control-theoretic system identification framework and a real-time closed-loop clinical simulation testbed for

electrical brain stimulation". In: *Journal of Neural Engineering* 15.6, p. 066007. DOI: 10.1088/1741-2552/aad1a8.

Zeng, Z., Koponen, L. M., et al. (Mar. 2022). "Modular multilevel TMS device with wide output range and ultrabrief pulse capability for sound reduction". In: *Journal of Neural Engineering* 19.2, p. 026008. DOI: 10.1088/1741-2552/ac572c.

Zrenner, B., Zrenner, C., et al. (Jan. 2020). "Brain oscillation-synchronized stimulation of the left dorsolateral prefrontal cortex in depression using real-time EEG-triggered TMS". In: *Brain Stimulation: Basic, Translational, and Clinical Research in Neuromodulation* 13.1. Publisher: Elsevier, pp. 197–205. DOI: 10.1016/j.brs.2019.10.007.

Zrenner, C., Desideri, D., et al. (Mar. 2018). "Real-time EEG-defined excitability states determine efficacy of TMS-induced plasticity in human motor cortex". In: *Brain Stimulation* 11.2, pp. 374–389. DOI: 10.1016/j.brs.2017.11.016.